# AD-A141 826

AFWAL-TR-84-4029

STRENGTH OF BOLTED JOINTS IN
LAMINATED COMPOSITES

Fu-Kuo Chang
Richard A. Scott
George S. Springer

Department of Mechanical Engineering and Applied Mechanics
The University of Michigan
Ann Arbor, MI  48109

March 1984

Final Report for Period June 1983-December 1983
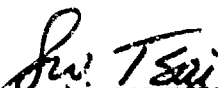
DTIC
ELECTE
JUN 5 1984
B

DTIC FILE COPY

84  06  04  044

# NOTICE

When Government drawings, specifications, or other data are used for any purpose other than in connection with a definitely related Government procurement operation, the United States Government thereby incurs no responsibility nor any obligation whatsoever; and the fact that the Government may have formulated, furnished, or in any way supplied the said drawings, specifications, or other data, is not to be regarded by implication or otherwise as in any manner licensing the holder or any other person or corporation, or conveying any rights or permission to manufacture, use, or sell any patented invention that may in any way be related thereto.

This report has been reviewed by the Office of Public Affairs (ASD/PA) and is releasable to the National Technical Information Service (NTIS). At NTIS, it will be available to the general public, including foreign nations.

This technical report has been reviewed and is approved for publication.

S.W. Tsai, Project Engineer & Chief
Mechanics and Surface Interactions Branch
Nonmetallic Materials Division

FOR THE COMMANDER

F.D. CHERRY, Chief
Nonmetallic Materials Division

| REPORT DOCUMENTATION PAGE | | READ INSTRUCTIONS BEFORE COMPLETING FORM |
|---|---|---|
| 1. REPORT NUMBER<br>AFWAL-TR-84-4029 | 2. GOVT ACCESSION NO.<br>AD A141 876 | 3. RECIPIENT'S CATALOG NUMBER |
| 4. TITLE (and Subtitle)<br><br>STRENGTH OF BOLTED JOINTS IN LAMINATED COMPOSITES | | 5. TYPE OF REPORT & PERIOD COVERED<br>Final Report<br>June, 1983-December 1983 |
| | | 6. PERFORMING ORG. REPORT NUMBER |
| 7. AUTHOR(s)<br><br>Fu-kuo Chang<br>Richard A. Scott<br>George S. Springer | | 8. CONTRACT OR GRANT NUMBER(s)<br><br>F33615-81-C-5050 |
| 9. PERFORMING ORGANIZATION NAME AND ADDRESS<br><br>Department of Mechanical Engineering and Applied Mechanics, The University of Michigan, Ann Arbor, Michigan 48109 | | 10. PROGRAM ELEMENT, PROJECT, TASK AREA & WORK UNIT NUMBERS<br><br>FY1457-81-02013 |
| 11. CONTROLLING OFFICE NAME AND ADDRESS<br>Materials Laboratory (AFWAL/MLBM)<br>Air Force Wright Aeronautical Laboratories (AFSC)<br>Wright-Patterson, AFB, OH 45433 | | 12. REPORT DATE<br>March 1984 |
| | | 13. NUMBER OF PAGES<br>175 |
| 14. MONITORING AGENCY NAME & ADDRESS(if different from Controlling Office) | | 15. SECURITY CLASS. (of this report)<br><br>Unclassified |
| | | 15a. DECLASSIFICATION/DOWNGRADING SCHEDULE |

16. DISTRIBUTION STATEMENT (of this Report)

Approved for public release, distribution unlimited

17. DISTRIBUTION STATEMENT (of the abstract entered in Block 20, if different from Report)

18. SUPPLEMENTARY NOTES

19. KEY WORDS (Continue on reverse side if necessary and identify by block number)

Composite Materials
Failure Hypothesis
Joints
Bolted Joints

20. ABSTRACT (Continue on reverse side if necessary and identify by block number)

A method is presented for predicting the failure strength and failure mode of pin-loaded holes in fiberite reinforced composite laminates. The method includes two steps. First, the stress distribution in the laminate is calculated by the use of a finite element method. Second, the failure load and failure mode are predicted by means of a proposed failure hypothesis together with the Yamada-Sun failure criterion. A computer code was developed, which can be used to calculate the maximum load and the mode of failure of joints involving laminates with different ply orientations, different material

DD FORM 1473
1 JAN 73

properties, and different geometries.

Tests were performed, measuring the rail-shear strength and the characteristic lengths for Fiberite T300/1034-C composites. Tests were also conducted, measuring the failure strengths and failure modes of Fiberite T300/1034-C laminates containing a pin-loaded hole or two pin-loaded holes in parallel or in series.

Comparisons were made between the data and the results of the model. Good agreement was found between the analytical and the experimental results.

Using the computer code, parametric studies were performed, illustrating the procedures which can be used to size composites containing pin-loaded holes.

# FOREWORD

This report was prepared by Fu-Kuo Chang, Richard A. Scott, and George S. Springer, Department of Mechanical Engineering and Applied Mechanics, The University of Michigan for the Mechanics and Surface Interactions Branch (AFWAL/MLBM), Nonmetallic Materials Division, Materials Laboratory, Air Force Wright Aeronautical Laboratories, Wright-Patterson AFB, Ohio. The work was performed under Contract Number F 33615-81-C5050, Project number FY1457-81-02013.

This report covers work accomplished during the period June 1983-December 1983.

# TABLE OF CONTENTS

TABLE OF CONTENTS (Concluded)

## LIST OF ILLUSTRATIONS

LIST OF ILLUSTRATIONS (Cont'd)

x

# LIST OF TABLES

LIST OF TABLES (Cont'd)

# LIST OF SYMBOLS

| | |
|---|---|
| A | Total Surface Area of Laminate |
| $A_L$ | Stress Prescribed Area |
| $A_F$ | Stress Free Area |
| $A_R$ | Displacement Prescribed Area |
| $A_{RS}$ | Surface Along Symmetric Axis |
| $A_{RC}$ | Total Contact Surfaces Inside Upper and Lower Holes |
| $A_{Lg}$ | Surface Area of an Element g on Which Surface Tractions are Applied |
| B | Bearing Stress |
| D | Diameter of Hole |
| E | Edge Distance |
| $E_{ijkl}$ | Elastic Moduli |
| $E_{mn}$ | Reduced Elastic Moduli |
| e | Failure Indicator ($e<1$ Non-Failure, $e \geq 1$ Failure) |
| $e_o$ | Maximum Value of e on Characteristic Curve |
| f | Fraction of By-Pass Load over Total Load |
| $\bar{F}_{i\beta}$ | Assembled Load Vector |
| $G_H$ | Distance Between Two Holes in Parallel |
| $G_V$ | Distance Between Two Holes in Series |
| $g_E$ | Edge Distance Coefficient |
| $g_H$ | Parallel Hole Interaction Coefficient |
| $g_S$ | Side Interaction Coefficient |
| $g_V$ | Series Hole Interaction Coefficient |
| H | Thickness of Laminate |
| $h^p$ | Thickness of p-th Ply |

LIST OF SYMBOLS (Cont'd)

| | |
|---|---|
| $K^g_{i\beta k\alpha}$ | Stiffness Matrix of g-th Element |
| $\bar{K}_{i\beta k\alpha}$ | Assembled Stiffness Matrix |
| $L$ | Plate Length |
| $L_s$ | Total Length of Steel Pin |
| $M$ | Number of Element |
| $N$ | Number of Plies in Laminate |
| $N_o$ | Number of Holes in a Row |
| $N_\alpha$ | Shape Function |
| $n_j$ | Unit Vector Normal to Surface |
| $P$ | Applied Load |
| $P_1$ | Load Carried by Pin (Pins) |
| $P_2$ | By-pass Load |
| $P_{r1}$ | Failure Load of Laminate Containing One Row of Holes |
| $P_{r2}$ | Failure Load of Laminate Containing Two Row of Holes |
| $P_c$ | Failure Load of Laminate (Width W) Containing Single Hole at the Center of Laminate |
| $P_G$ | Failure Load of Laminate (Width 2W) Containing Two Holes Separated by Distance $G_H$ ($G_H \geq W$) |
| $P_H$ | Failure Load of Laminate (Width 2W) Containing Two Holes Separated by Distance W |
| $P_S$ | Failure Load of Laminate (Width W) Containing Single Hole at Distance E from the Edge |
| $P_T$ | Failure Load of Laminate (Width W) Containing Two Holes; One Located at Distance E from the Edge, the Other Located at the Center of the Laminate |
| $P_V$ | Failure Load of Laminate (Width W) Containing Two Holes in Series |
| $P_M$ | Maximum Failure Load of a Laminate Containing Pin-Loaded Holes |
| $P^*$ | Failure Load Per Unit Weight |

$P^*_M$ — Maximum Failure Load Per Unit Weight of a Laminate Containing Pin-Loaded Holes

$P^*_{r1}$ — Failure Load Per Unit Weight of a Laminate Containing one Row of Holes

$P^*_{r2}$ — Failure Load Per Unit Weight of a Laminate Containing Two Rows of Holes

$P_{N_o-2}$ — Failure Load Carried by Second Through Next to Last Pins in Laminate Containing One Row or Two Rows of Holes

$P_{side}$ — Failure Load Carried by the Two Pins Next to the Sides in a Laminate Containing One Row or Two Rows of Holes

$Q$ — The Distance Between the Side and the Adjacent Hole

$\bar{Q}^p_{ij}$ — Transformed Reduced Stiffness Matrix of p-th Ply

$q_{i\alpha}$ — Nodal Displacement

. — Radial Distance

$r_c$ — Radial Distance to the Characteristic Curve

$R_t$ — Characteristic Length for Tension

$R_c$ — Characteristic Length for Compression

$S$ — Laminate Shear Strength

$S_{50}$ — Laminate Shear Strength of $[0/90]_s$ Laminate With 50 Percent Volume Fraction of 0 Degree Fibers.

$s$ — Total Surface Area of Two-Dimensional Laminate

$s_g$ — Area of Element g

$T_i$ — Surface Traction Component

$T_i^*$ — Surface Traction Component on $A_{L1}$ Surface

$T_i^{**}$ — Surface Traction Component on $A_{L2}$ Surface

$T_{x_2}$ — Normal Stress on Hole Surface at $\theta = 0$

$u_i$ — Displacements

| | |
|---|---|
| $\bar{u}_i$ | Arbitrary Displacement Functions |
| $V_o$ | Total Volume of Laminate |
| $v_g$ | Volume of Element g |
| $W$ | Width of Plate |
| $w$ | The Combined Weight of Laminate and Pins |
| $w_c$ | The Weight of the Laminate |
| $w_s$ | The Weight of the Pins |
| $X_t$ | Ply Tensile Strength |
| $X_c$ | Ply Compressive Strength |
| $x$ | Coordinate Along Fiber Direction in Each Ply |
| $x_1$ | Coordinate Perpendicular to the Loading Direction in Laminate Plane |
| $x_2$ | Coordinate Opposed to the Loading Direction and Perpendicular to the $x_1$ Direction |
| $x_3$ | Coordinate Perpendicular to the $x_1$ and $x_2$ Axes |
| $y$ | Coordinate Perpendicular to the Fiber Direction in Each Ply |
| $\Gamma_L$ | Boundary Curve of Hole on Which Surface Traction is Applied |
| $\Gamma_{cg}$ | Boundary of Element Along Contact Regions |
| $\Gamma_{Lg}$ | Boundary Curve of Element g on Which Surface Traction is Applied |
| $\epsilon_{ij}$ | Strain Components in $x_1$-$x_2$ Coordinate System |
| $\eta$ | Angle Measured Counterclockwise from $x_1$-axis |
| $\theta_f$ | Angle at which Failure Occurs |
| $\theta_U$ | The Contact Angle on the Upper Hole |
| $\theta_L$ | The Contact Angle on the Lower Hole |
| $\rho_c$ | Density of the Laminate |
| $\rho_s$ | Density of the pin |
| $\nu_o$ | Volume Fraction of Plies With 0 Degree Fibers |

## LIST OF SYMBOLS (Concluded)

$\sigma_{ij}$         Stress Components in the $x_1$-$x_2$ Coordinate System

$\sigma_x, \sigma_y, \sigma_{xy}$ Stress Components in the x-y Coordinate System

# SECTION I

## INTRODUCTION

Among the major advantages of laminated composite
structures over conventional metal structures are their
comparatively high strength to weight and stiffness to
weight ratios. As a result, fiber reinforced composite
materials have been gaining wide application in aircraft and
spacecraft construction. These applications require joining
composites either to composites or to metals. Most
commonly, joints are formed by using mechanical fasteners.
Therefore, suitable methods must be found to determine the
failure strengths and failure modes of mechanically-fastened
joints. A knowledge of the failure strength and failure
modes would help in selecting the appropriate size joint in
a given application.

Owing to the significance of the problem, several
investigators have developed analytical procedures for
calculating the strength of bolted joints in composite
materials. Among the recent studies are those of Waszczak
and Cruse (Reference 1), Oplinger and Gandhi (References 2 & 3), Agarwal
(Reference 4), Soni (Reference 5), Garbo and Ogonowski (Reference 6),
York, Wilson, and Pipes (References 7 & 8),and Collings (9). The
results of these investigations apply only to joints containing a
single hole, and, with the exception of Agarwal's method, none of the
previous methods can predict the mode of failure. Furthermore, as will be
discussed in Section VIII, the previous methods provide conservative
results and underestimate the failure strength, often by as much as 50
percent.

The first objective of the investigation was, therefore, to develop a method which a) can be used to estimate both the failure strength and the failure mode of pin-loaded holes in composites, b) applies to laminates containing either one pin-loaded hole or two pin-loaded holes in parallel, or two pin-loaded holes in series, c) provide results with better accuracy than the existing analytical methods and, d) can be used in the design of mechanically-fastened composite joints. The second objective was to develop a "user friendly" computer code which can be used to predict the failure strength and failure mode of loaded holes (joints) involving laminates with different ply orientations, different material properties, and different configurations-- including different hole sizes, hole positions, and joint thicknesses. The third objective was to generate data which can be used to assess the accuracies of analytical methods.

The analytical model and the corresponding numerical method of solution are presented in Sections III-VI. The experimental apparatus and procedures are given in Section VII. The data, and comparisons between the analytical and experimental results are presented in Section VIII. The use of the model in the design of joints is described in Section IX.

# SECTION II

## PROBLEM STATEMENT

Consider a plate (length L, width W, thickness H) made of N fiber reinforced unidirectional plies. The ply orientation is arbitrary, but must be symmetric with respect to the $x_3=0$ plane (symmetric laminate). Perfect bonding between each ply is assumed.

Three types of problems are being analyzed (Figure 1): a) A single hole of diameter D is located along the centerline of the plate; b) Two holes of diameter D are located at equal distances from the centerline of the plate (two holes in parallel); c) Two holes of diameter D are located along the centerline of the plate (two holes in series). A rigid pin, supported outside of the plate, is inserted into each hole.

A uniform tensile load P is applied to the lower edge of the plate and a uniform tensile load $P_2$ (referred to as the "by-pass" load) is applied to the upper edge. These loads are parallel to the plate (in-plane loading) and are symmetric with respect to the centerline. Hence, the loads cannot create bending moments about either the $x_1$, $x_2$, or $x_3$ axes. Moreover, for symmetric laminates, in-plane loading and bending effects are uncoupled. Transverse forces, (i.e., forces in the $x_3$ direction) are not applied, and transverse displacement of the laminate is not taken into account. For example, a washer on each side of the

4
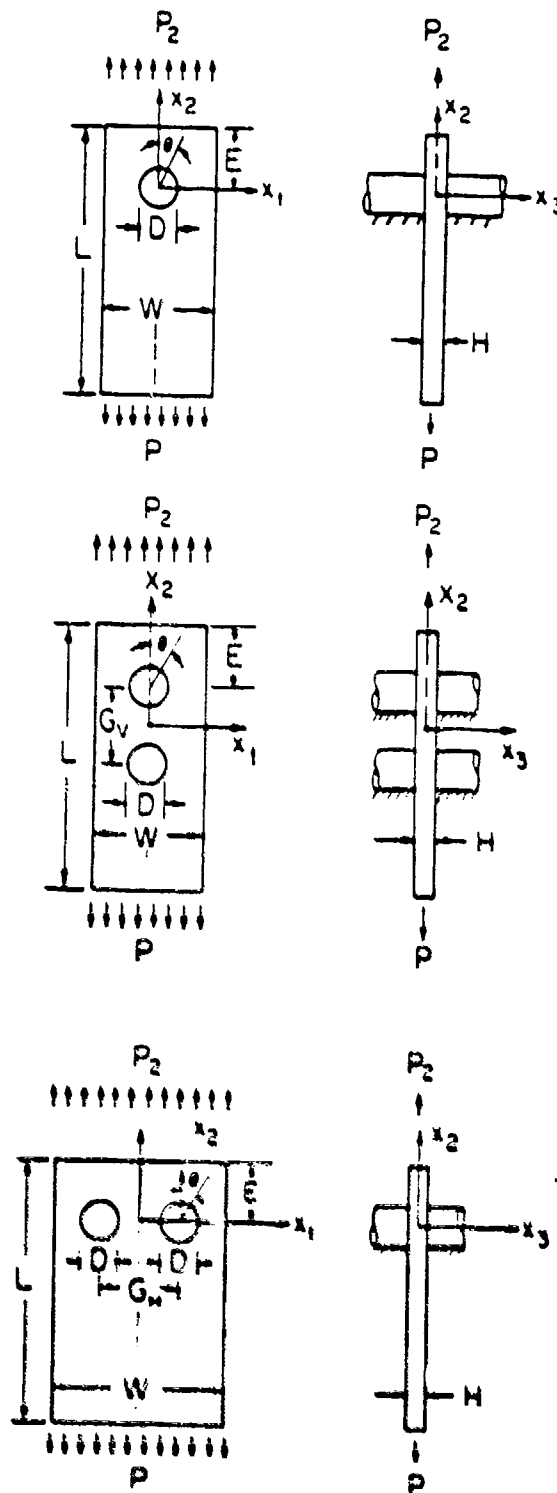


Figure 1. Descriptions of the Problem. Top: Single Hole Model; Middle: Two Holes in Series; Bottom: Two Holes in Parallel.

laminate, supported by a lightly-tightened ("finger-tight") bolt in the hole, would ensure that there is no transverse displacement, and that the condition of two dimensionality is satisfied [10].

It is desired to find :

1) the maximum (failure) load ($P_M$) that can be applied before the joint fails, and

2) the mode of failure.

Point 2 refers to the fact that, according to experimental evidence, mechanically-fastened joints under tensile loads generally fail in three basic modes, referred to as tension mode, shear-out mode, and bearing mode. The type of damage resulting from each of these modes is illustrated in Figure 2. The objective, listed in point 2 above, is to determine which of these modes will most be responsible for the failure.

The calculation proceeds in three steps. For a given geometry and load :

1) the stress and strain distributions around the hole are calculated,

2) the maximum (failure) load is predicted,

3) the mode of failure is determined.

The details of these steps are presented in Sections III and IV.

TENSION       SHEAROUT       BEARING
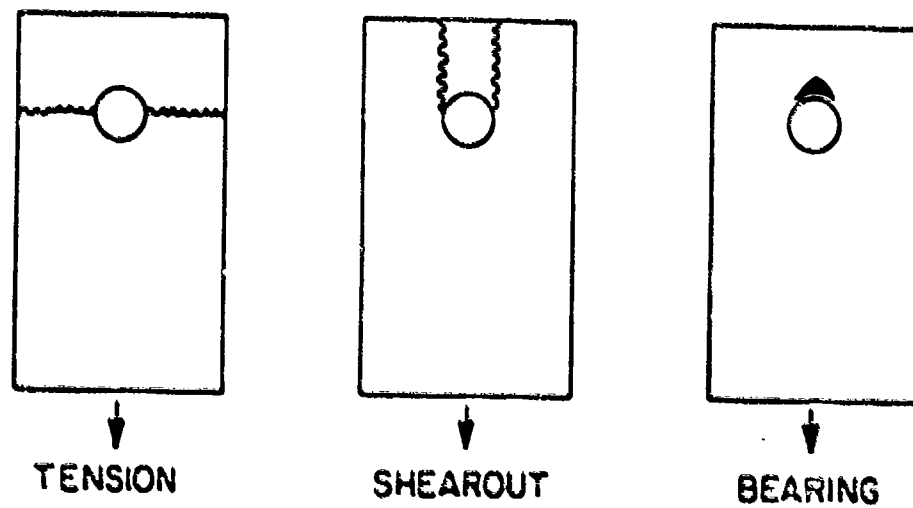
Figure 2.     Illustration of the Three Basic Failure Modes

# SECTION III

## STRESS ANALYSIS

The calculation of stresses raises the issue of whether a two or three dimensional stress analysis is required. If tests were to show that the stacking sequence did not affect the failure strength and the failure mode, then a two dimensional stress analysis would suffice. Existing experimental evidence indicates that the stacking sequence is important only when a) the laminate is narrow (and edge effects are not negligible [11]), or b) the laminate is unrestrained laterally [12]. However, even when the stacking sequence affects the results, it seems to affect the failure strength by only 10 percent to 20 percent [11-15]. Furthermore, the failure strength and the failure mode seem unaffected by the stacking sequence when there is a slight lateral constraint on the laminate, such as provided by lightly tightened (finger-tight) bolts [10,16,17].

For these reasons, a two dimensional stress analysis was chosen for the present work. As will be demonstrated in Section VIII, this analysis provides a useful estimate of the failure strength and the failure mode of loaded holes. In addition to being reasonably accurate, the two dimensional analysis adopted here also provides a simple and inexpensive means for calculating failure strengths and failure modes, making it an attractive design aid.

## 3.1) Governing Equations

The stresses in the laminate are calculated on the bases of theory of anisotropic elasticity and classical-lamination plate theory. Accordingly, in the analysis, planes are taken to remain planes, the strain across the thickness is taken to be constant $[\varepsilon_{ij}=f(x_1,x_2)]$, and only plane stresses are considered $(\sigma_{13}=\sigma_{23}=\sigma_{33}=0)$. Under these conditions, in the absence of body forces, the condition of force equilibrium can be expressed as [18]

$$\partial\sigma_{11}/\partial x_1 + \partial\sigma_{12}/\partial x_2 = 0$$

$$\partial\sigma_{21}/\partial x_1 + \partial\sigma_{22}/\partial x_2 = 0 \tag{1}$$

In index notation eq. (1) becomes

$$\sigma_{ij,j} = 0 \tag{2}$$

$\sigma_{ij}$ is the stress component in the plane normal to the $x_i$ axis and is in the $x_j$ direction. The subscripts i and j may have the values of 1 or 2. Now consider an elastic laminate of volume $V_0$ containing a single pin-loaded hole or two pin-loaded holes, as shown in Figure 3. Loads are applied over the surface area $\lambda_t$. The displacements along the surface area $\lambda_R$ are restricted in a manner described subsequently. The surface area $\lambda_F$ is free of applied stress.

TOTAL SURFACE: A

LOADED SURFACE: $A_L = A_{L_1} + A_{L_2}$

RESTRICTED SURFACE: $A_R$
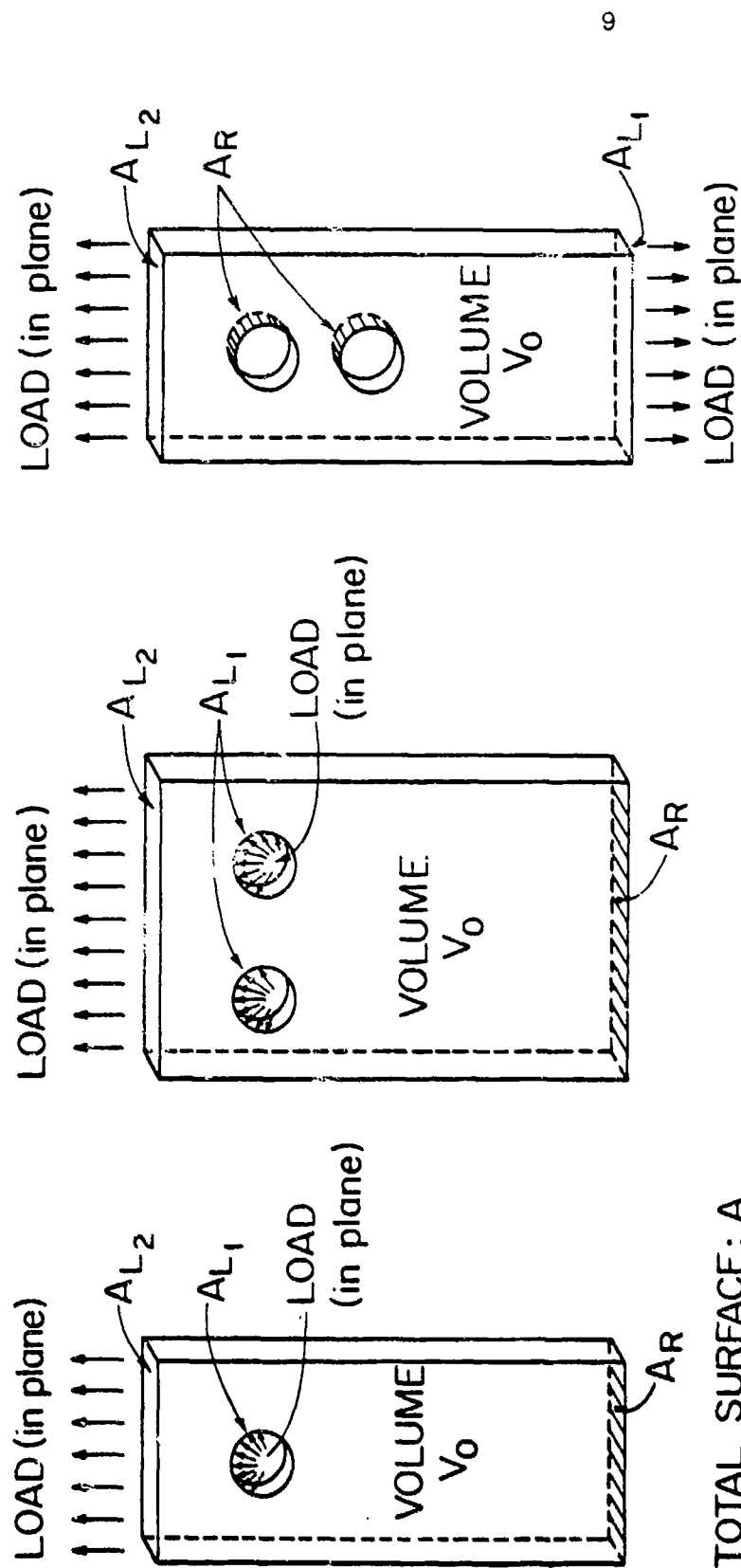
Figure 3. Elastic Laminates with One Hole (Left), Two Holes in Parallel (Middle), and Two Holes in Series (Right).

The total surface area is

$$A = A_L + A_R + A_F \tag{3}$$

Let us denote by $\bar{u}_i$ any arbitrary displacement inside the body. $\bar{u}_i$ is a test function. The only requirement is that $\bar{u}_i$ be continuous and differentiable. In addition, along the $A_R$ surface, the components of $\bar{u}_i$ normal to the surface must be zero. By multiplying eq.(2) by $\bar{u}_i$ and by taking the volume integral of the resulting expression, we obtain

$$\iiint_{V_o} \sigma_{ij,j} \, \bar{u}_i \, dV = 0 \tag{4}$$

By employing the identity

$$\sigma_{ij,j}\bar{u}_i = (\sigma_{ij}\bar{u}_i)_{,j} - \sigma_{ij}\bar{u}_{i,j} \tag{5}$$

and by utilizing Gauss' theorem, eq. (4) may be written as

$$\iint_A \sigma_{ij} \, n_j \, \bar{u}_i \, dA - \iiint_{V_0} \sigma_{ij} \, \bar{u}_{i,j} \, dV = 0 \tag{6}$$

where $n_j$ is the unit vector normal to the surface. By utilizing eq.(3), eq.(6) can be expressed as

$$\iint_{A_L} \sigma_{ij} n_j \bar{u}_i dA + \iint_{A_R} \sigma_{ij} n_j \bar{u}_i \, dA + \iint_{A_F} \sigma_{ij} \, n_j \, \bar{u}_i \, dA$$

$$= \iiint_{V_o} \sigma_{ij} \, \bar{u}_{i,j} \tag{7}$$

On the free surface $A_F$ the stresses are zero. This condition gives

$$\iint_{A_F} \sigma_{ij} \, n_j \, \bar{u}_i \, dA = 0 \tag{8}$$

The forces per unit area (called surface traction) at each point of the surface area $A_L$ are [18]

$$T_i = \sigma_{ij} \, n_j \tag{9}$$

Equations (7)-(9) yield

$$\iint_{A_L} T_i \bar{u}_i \, dA + \iint_{A_R} \sigma_{ij} n_j \bar{u}_i \, dA = \iiint_{V_0} \sigma_{ij} \bar{u}_{i,j} \, dV \tag{10}$$

The stress is related to the displacement through the stress -strain relationship, which for an elastic body is [18]

$$\sigma_{ij} = E_{ijkl} \, \varepsilon_{kl} \tag{11}$$

The subscripts $k$ and $l$ may take on the values of 1 or 2. In order to reduce the analysis from three dimensions to two dimensions, the reduced modulus $E_{mn}$ is introduced

$$E_{ijkl} = E_{mn} = \sum_{p=1}^{N} (h^p/H) \, \bar{Q}^p_{mn} \tag{12}$$

where $h^p$ is the thickness of the p-th ply, and $[\bar{Q}]^p$ is the transformed reduced stiffness matrix for the P-th ply [19]

(Appendix A). The subscripts $i,j,k,$ and $l$ are related to $m$ and $n$ as follows

$$i=j=1 \rightarrow m=1 \qquad k=l=1 \rightarrow n=1$$
$$i=j=2 \rightarrow m=2 \qquad k=l=2 \rightarrow n=2$$
$$i \neq j \rightarrow m=3 \qquad k \neq l \rightarrow n=3 \qquad (13)$$

Note that this reduced modulus is a constant and is independent of the thickness of the laminate. The strains are related to the displacements $u_j$ by the expression

$$\varepsilon_{kl} = (1/2)( \partial u_k/\partial x_l + \partial u_l/\partial x_k ) \qquad (14)$$

By combining eqs (10)-(14) we obtain

$$\iiint_{V_0} E_{ijkl} \bar{u}_{i,j} u_{k,l} \, dV = \iint_{A_L} T_i \bar{u}_i \, dA + \iint_{A_R} \sigma_{ij} n_j \bar{u}_i \, dA \qquad (15)$$

Since the problem is treated as two dimensional, the displacements and, consequently the strains are constant across the laminate. Hence the stresses, as defined by eq.(11), are also constant across the laminate. However, the on axis stresses in each ply vary from ply-to-ply, and are given by

$$\left\{ \begin{array}{c} \sigma^p_x \\ \sigma^p_y \\ \sigma^p_{xy} \end{array} \right\} = [T][\bar{Q}]^p \left\{ \begin{array}{c} \varepsilon_1 \\ \varepsilon_2 \\ \gamma_{12} \end{array} \right\} \qquad (16)$$

where the subscripts x and y represent the directions parallel and normal to the fibers, respectively. The matrix [T] is the coordinate transformation matrix given in Appendix B.

### 3.2) Boundary Conditions; Single Hole and Two Holes in Parallel

For problems involving a single hole and two holes in parallel, it is assumed that a portion of the surface of each hole is subjected to a surface traction $T_i^*$ (Figure 4). The parameter $T_i^*$ is related to the applied load. The spatial distribution of $T_i^*$ depends on the magnitude of the applied load, on the material properties, and on the geometry in a complex manner. It is extremely difficult to determine the exact distribution of $T_i^*$ inside the hole [20-22]. To overcome this difficulty, a cosine normal load distribution was assumed. With this approximation, a force balance in the $x_2$ direction gives

$$P = P_2 + H \int_{-\pi/2}^{\pi/2} (D/2) T_{x_2} \cos^2\theta \, d\theta \qquad (17)$$

where $T_{x_2}$ is the normal stress at the hole surface at $\theta=0$. At any arbitrary angle $\theta$ $(-\pi/2 \leq \theta \leq \pi/2)$, the stress normal to the surface is

$$T_i^* = T_{x_2} n_i \cos\theta \qquad (18)$$
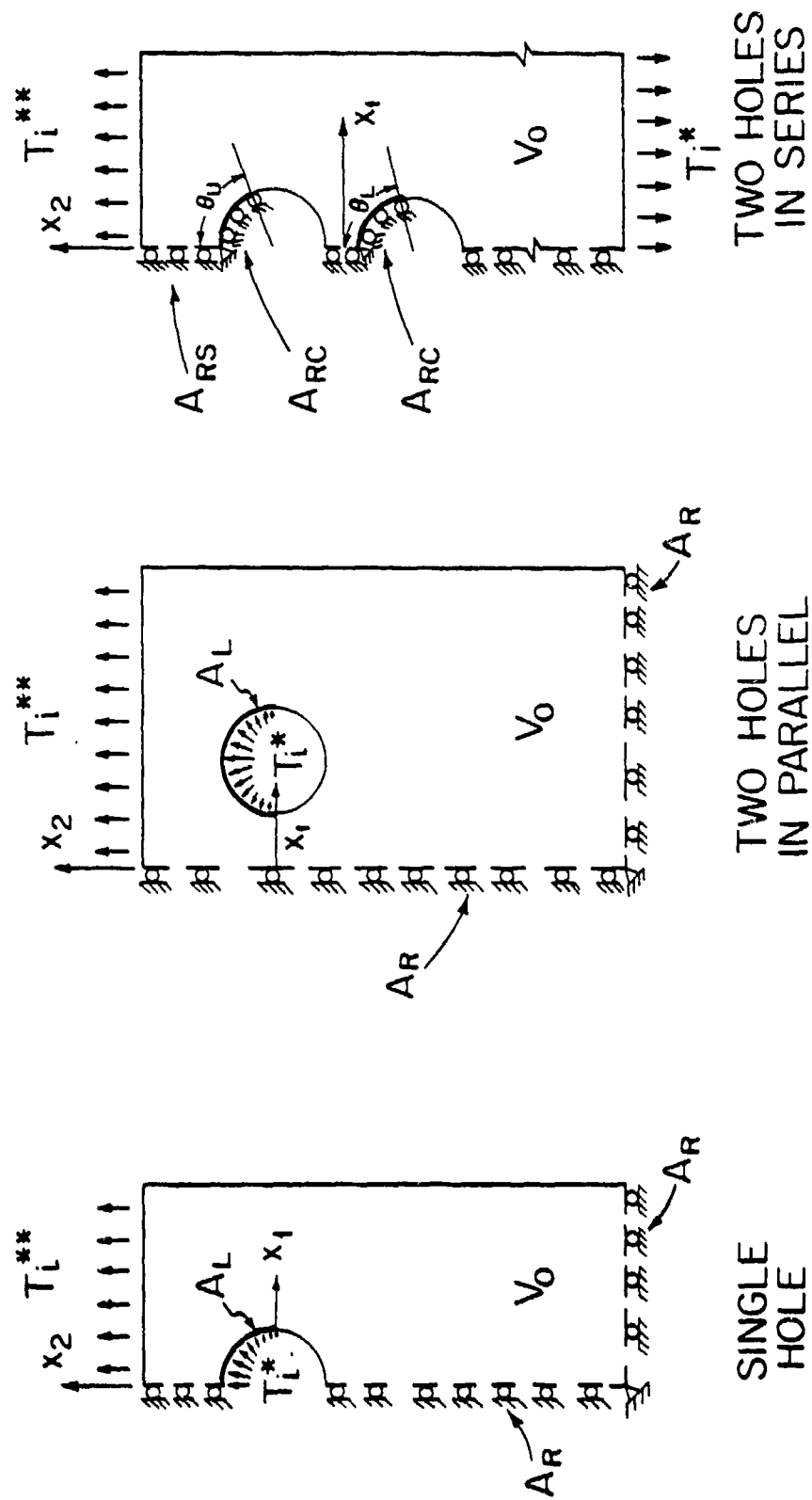
Figure 4. Configurations Used in the Finite Element Calculations.

Eq(17) and (18) give

$$T_i^* = -4 \ C((P-P_2)/\pi DH) \ n_i \ \cos\theta \qquad (19)$$

where $P_2$ is the by-pass load which is a fraction f of the total load P

$$P_2 = fP \qquad (20)$$

The values of either P and $P_2$ or P and f must be specified. Thus, the surface traction on $A_{L1}$ can be written as

$$T_i^* = -C \ (P(1-f)/\pi DH)n_i \ \cos\theta \qquad (21)$$

The surface traction on $A_{L2}$ is

$$T_i^{**} = (P_2/HW) \ n_i = (fP/HW) \ n_i \qquad (22)$$

For a single hole C is equal to 1 and, for two holes in parallel it is equal to 1/2. The angle $\theta$ varies from $-\pi/2$ to $\pi/2$ in each hole. The angle $\theta$ is in the $x_1$-$x_2$ plane, and is measured clockwise from the $x_2$ axis (Figure1). For isotropic materials, the cosine normal load distribution (eq.21) was found to represent closely the actual load distribution [23]. Calculations performed by previous investigators also showed that, for composite materials, the stress distribution inside the body is insensitive to the

assumed load distribution [1, 6, 24]. Therefore, eq. (21)
should suffice for the purpose of the present analysis,
which is to determine the overall strength of the joint.

Equations(10),(20),(21) and (22) give

$$\iiint_{V_0} E_{ijkl}\bar{u}_{i,j}u_{k,l} \ dV = \iint_{A_{L1}} -C(4p(1-f)/\pi DH)n_i\bar{u}_i\cos\theta \ dA +$$

$$\iint_{A_{L2}} (fp/HW) \ n_i \ \bar{u}_i \ dA + \iint_{A_R}\sigma_{ij} \ n_j \ \bar{u}_i \ dA \qquad (23)$$

We recall that $\bar{u}_i$ are functions that can be selected
arbitrarily. The unknowns in eq.(23) are the displacements
$u_k$. Once $u_k$ are known, the stresses at every point can be
calculated from eqs (14) and (16).

Solutions to eq.(23) must be obtained subject to the
following constraints: a) Along the symmetry axis and along
the lower edge, displacements are allowed only in the
direction tangential to the surface. These tangential
displacements may occur freely without any restraints. b)
The intersection of the symmetry axis and the lower edge
must not move (i.e., the intersection is rigidly fixed).

The integral (eq. 23) over the $A_R$ surface now applies to
the surfaces along the symmetry axis and along the lower
edge (Figure 4). On these surfaces, the normal component of
the displacement and the tangential component of the surface
traction are zero. Accordingly, we have

$$\iint_{A_R} \sigma_{ij}n_j\bar{u}_i \ dA = 0 \qquad (24)$$

Equation (23) can now be simplified, and becomes

$$\iiint_{V_o} E_{ijkl}\bar{u}_{i,j}u_{k,l} \ dV = \iint_{A_{L1}} - C(4P(1-f)/\pi DH)n_i\bar{u}_i\cos\theta \ dA$$

$$+ \iint_{A_{L2}}(fP/HW)n_i\bar{u}_i \ dA \tag{25}$$

The method of solution of eq.(25) is described in Section 3.4.

### 3.3) Boundary Condition; Two Holes in Series

For the problems of two holes in series, the fractions of the load carried by each pin are unknown. To analyze the the problem, it is assumed that a uniform load distribution is applied along the lower edge of the plate, and it is further assumed that a rigid pin is inside each hole. The assumption of the rigid pins implies that the normal displacements are zero along the contact surface (Figure 4). The extent of the contact surfaces are as yet unknown and need to be determined.

The uniform load distribution on the $A_{L1}$ surface is

$$T_i^\circ = -(P/HW) \ n_i \tag{26}$$

where H and W are the thickness and the width of the plate, respectively (Figure 1).

Equations (15), (22), (26) give

$$\iint E_{ijkl}\bar{u}_{i,j}u_{k,1}dV = \iint_{A_{L1}} -(P/HW)n_i\bar{u}_i dA + \iint_{A_{L2}}(fP/HW)n_i\bar{u}_i dA$$

$$+ \iint_{A_R} c_{ij} r_{ij} \bar{u}_i dA \qquad (27)$$

As before, $\bar{u}_i$ can be selected arbitrarily, but must satisfy the displacement boundary conditions. Hence, the unknowns in eq.(27) are the displacements $u_k$. The solution to eq.(27) must be obtained with the displacement $u_k$ subject to the following constraints:

a) Along the symmetry axis, displacements are allowed only in the direction tangential to the surface (i.e., in the $x_2$ direction). This tangential displacement may occur freely.

b) The contacts between the rigid pins and the surfaces of the holes are assumed to be frictionless and are assumed to take place through arcs bounded by the angles $\theta_U$ and $\theta_L$ (Figure 4). Along the arcs the surface displacements can take place only in the direction tangential to the surface. Because of the assumption of frictionless contact, this displacement may occur freely.

c) The radial displacements at the intersections of the symmetry axis and the upper edge of each hole are zero (i.e., these intersections are rigidly fixed ). This corresponds to the rigid supporting pins being fixed in space.

The integral over the $A_R$ area now applies to the symmetry axis and to contact surfaces. We express $A_R$ as the sum of two surfaces

$$A_R = A_{RS} + A_{RC} \tag{28}$$

$A_{RS}$ is the surface area along the symmetry axis and $A_{RC}$ is the total contact surface inside the upper and lower holes. Along the symmetry axis, the normal component of the displacement and the tangential component of surface traction are zero. Accordingly, we have

$$\iint_{A_{RS}} \sigma_{ij} n_j \bar{u}_i \, dA = 0 \tag{29}$$

Equation (27) gives

$$\iiint_{V_o} E_{ijkl} \bar{u}_{i,j} u_{k,l} \, dv = \iint_{A_{L1}} -(P/HW) n_i \bar{u}_i \, dA +$$
$$\iint_{A_{L2}} (fp/HW) n_i \bar{u}_i \, dA + \iint_{A_{RC}} \sigma_{ij} n_j \bar{u}_i \, dA \tag{30}$$

Solution to eq.(30) require that the contact area $A_{RC}$ (i.e., the contact angles $\theta_U$ and $\theta_L$ , Figure 4) be known. However, the contact angles $\theta_U$ and $\theta_L$ are as yet unknown; therefore, these angles must be determined before solutions for $u_k$ can be obtained. Procedures for calculating $\theta_U$ and $\theta_L$ are described in Section 3.4. Note that the procedure was also performed for a single hole. Little difference was found between the predicted failure load and the one predicted using the stress boundary condition.

## 3.4) Finite Element Analysis

Solutions to eq.(25) and (30) were obtained by a finite element method. As a first step in the solution procedure, the volume $V_o$ is subdivided into M subdomains of volume $v_g$

$$V_o = \sum_{g=1}^{M} v_g \tag{31}$$

Eqs.(25) and (30) may now be written as

$$\sum_{g=1}^{M} \iiint_{V_g} E_{ijkl} \bar{u}_{i,j} u_{k,1} \, dV = \sum_{g=1}^{M} \iint_{A_{Lg_1}} T_i^* \bar{u}_i \, dA +$$

$$\sum_{g=1}^{M} \iint_{A_{Lg_2}} T_i^{**} \bar{u}_i \, dA + \sum_{g=1}^{M} \iint_{A_{cg}} \sigma_{ij} n_j \bar{u}_i \, dA \tag{32}$$

$T_i^*$ and $T_i^{**}$ are the surface tractions given by eqs.(21) and (22) for a single hole and two holes in parallel, and by eqs. (22) and (26) for two holes in series. $A_{Lg}$ is the surface of an element where the surface traction is applied. At any surface where load is not applied, $A_{Lg}$ is zero. $A_{cg}$ is the surface of an element along the contact surfaces. For problems involving a single hole and two holes in parallel the summation over $A_{Lg}$ is zero.

Advantage is now taken of the assumption that the strains ($\epsilon_{11}, \epsilon_{22}$, and $\epsilon_{12}$), the reduced modulus $E_{mn}$, and the stress (eq. 11) are independent of the thickness. Thus, the three dimensional grid, consisting of M volume elements, may be
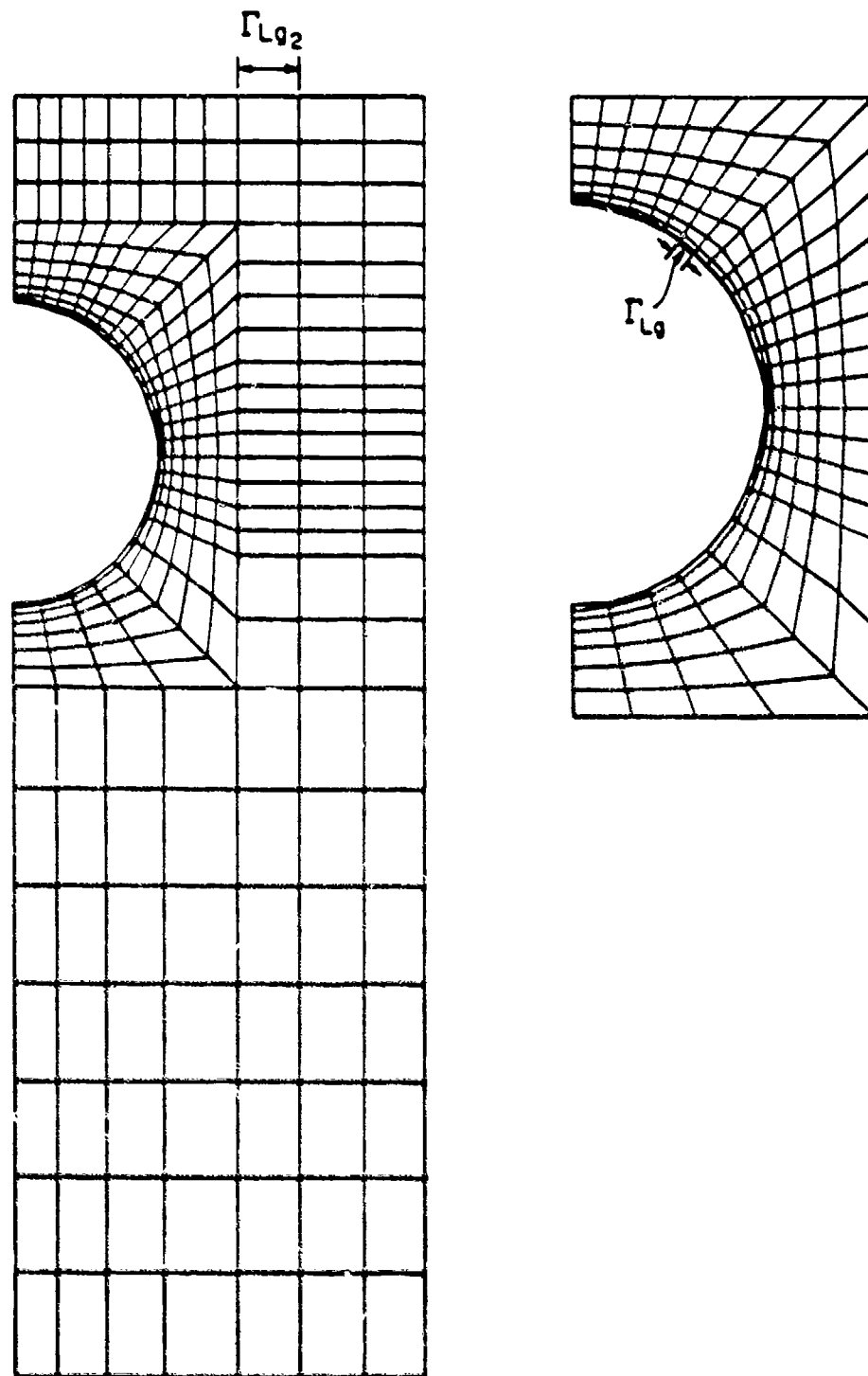
Figure 5. Grid Used in the Finite Element Analysis for a Single Hole. Right Hand Figure is an Enlarged View of the Grid Around the Hole.
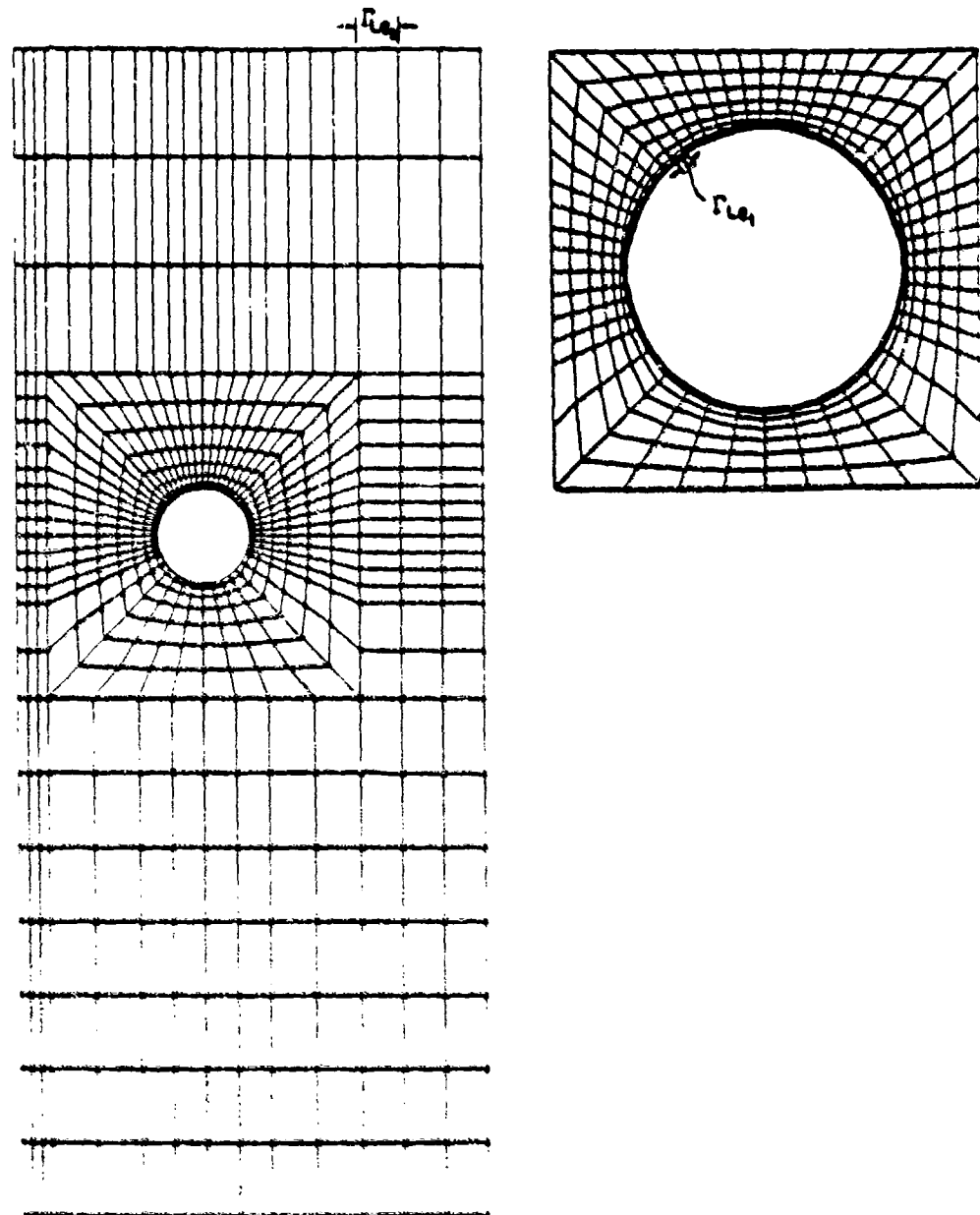
Figure 6.  Grid Used in the Finite Element Analysis for
Two Holes in Parallel.  Right Hand Figure is an
Enlarged View of the Grid Around One of
the Holes.
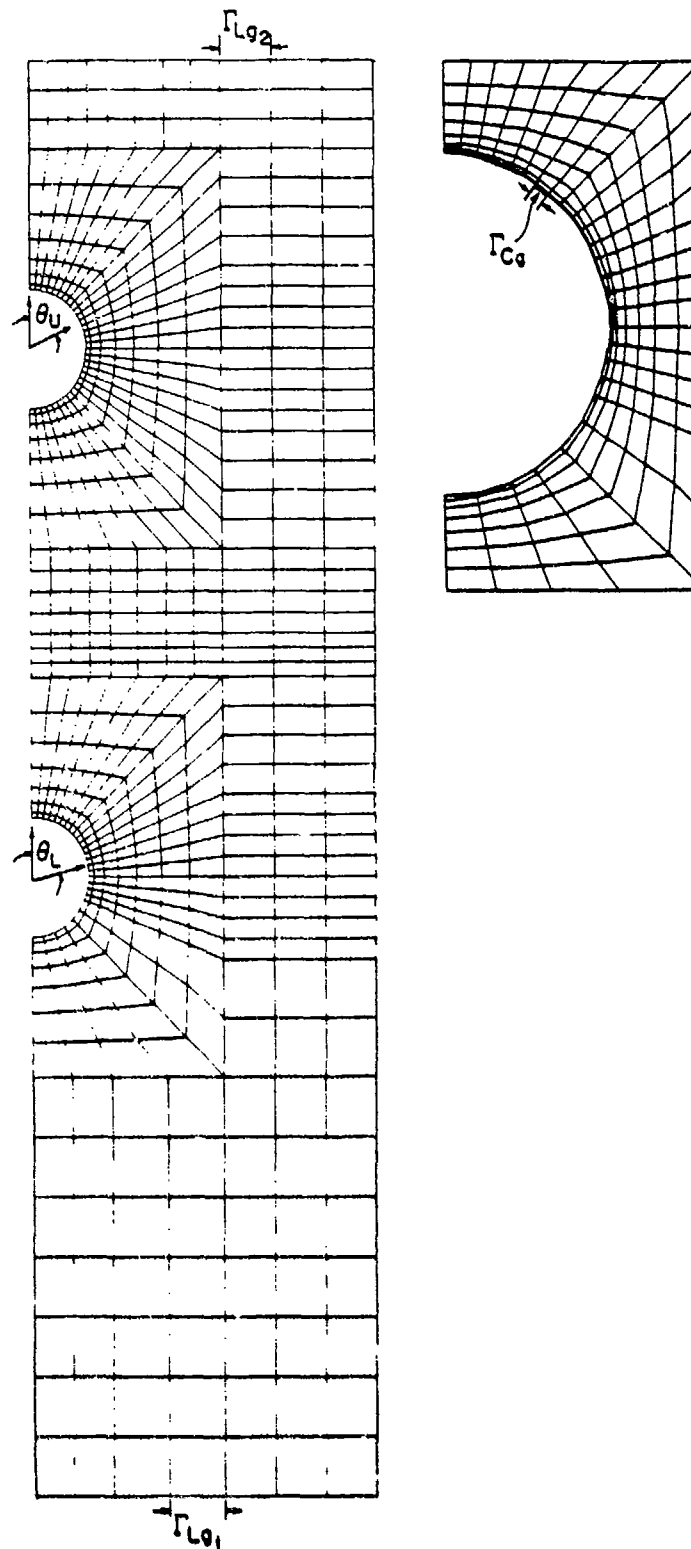
**Figure 7.** Grid Used in the Finite Element Analysis for Two Holes in Series. Right Hand Figure is an Enlarged View of the Grid Around Hole.

replaced by a two dimensional grid consisting of M surface elements of area s (Figures 5-7)

$$s = \int_{g=1}^{M} s_g \tag{33}$$

Equation (32) thus becomes

$$\sum_{g=1}^{M} \iint_{s_g} E_{ijkl} \bar{u}_{i,j} u_{k,l} \; ds = \sum_{g=1}^{M} \iint_{\Gamma_{Lg1}} T_i^{*} \bar{u}_i \; dP +$$

$$\sum_{g=1}^{M} \iint_{\Gamma_{Lg2}} T_i^{**} \bar{u}_i dA + \sum_{g=1}^{M} \iint_{\Gamma_{cg}} \sigma_{ij} n_j u_i \; d\Gamma \tag{34}$$

where $\Gamma_{Lg_1}$ and $\Gamma_{Lg_2}$ are segments of a line which coincide with the boundary of an element g where the load is applied (Figure 5-7). $\Gamma_{cg}$ denotes the boundary of an element along the contact regions bounded by $\theta_U$ and $\theta_L$ (Figure 7).

Isoparametric 4-node elements were used in the investigation. The mesh was generated using a mesh generator. This mesh generator was designed to automatically generate grid sizes around the hole (or holes) in a manner which ensures accurate resolution of the stresses in the vicinity of the holes (Appendix C). Smaller grids were used around the holes to obtain a better resolution of the stresses. Utilizing the symmetry about the $x_2$ axis, grids were placed on one half of the laminate, as illustrated in Figures 5-7. Grids consisting of 306, 612 and 655 elements were used for problems involving a single hole, two holes in parallel, and two holes in series, respectively.

### 3.4.1 Method of Solution; Single Hole and Two Holes in
Parallel

For problems involving a single hole and two holes in parallel, the displacements in each element can be expressed in terms of the displacements of the four nodal points [25, 26]

$$u_i = N_\alpha \, q_{i\alpha}$$
$$\bar{u}_i = N_\alpha \, \bar{q}_{i\alpha} \tag{35}$$

The subscript $\alpha$ designates the nodal points ($\alpha = 1,2,3,$ or 4). $N_\alpha$ is the shape function described in detail in Appendix D. $q_{i\alpha}$ is the displacement at the nodal point $\alpha$ in the i direction.

We define a stiffness matrix for the q-th element as

$$K^g_{i\beta k\alpha} = \iint_{s_g} E_{ijkl} N_{\alpha,l} N_{\beta,j} \, ds \tag{36}$$

$K^g_{i\beta k\alpha}$ is an eight by eight matrix. The subscript $\beta$ may take on the values 1, 2, 3, and 4. The nodal displacements $q_{k\alpha}$ and $\bar{q}_{i\beta}$ are independent of the surface and line integrations.

Accordingly, eqs(34), (35), and (36) yield

$$\sum_{g=1}^{M} K^q_{i\beta k\alpha} \, q_{k\alpha} \, \bar{q}_{i\beta} = \sum_{g=1}^{M} \bar{q}_{i\beta} (\int_{\Gamma_{Lg1}} -C(4P/\pi DH) n_i \, N_\beta \cos\theta \, d\Gamma$$
$$+ \int_{\Gamma_{Lg2}} (fP/HW) \, n_i \, N_\beta d\Gamma) \tag{37}$$

The nodal displacements $\bar{q}_{i\beta}$ are arbitrary functions and hence eq. (37) can be written

$$\bar{K}_{i\beta k\alpha}\, q_{k\alpha} = \bar{F}_{i\beta} \tag{38}$$

where the global stiffness matrix $\bar{K}_{i\beta k\alpha}$ and the load vector $\bar{F}_{i\beta}$ are given by

$$\bar{K}_{i\beta k\alpha} = \sum_{g=1}^{M} K^{g}_{i\beta k\alpha} \tag{39}$$

$$\bar{F}_{i\beta} = \sum_{g=1}^{M} \left( \int_{\Gamma_{Lg_1}} -(4P/\pi DH) n_i\, N_\beta \cos\theta\; d\Gamma \right.$$

$$+ \int_{\Gamma_{Lg_2}} (fP/HW) n_i N_\alpha\; d\Gamma \tag{40}$$

The elements of $\bar{K}_{i\beta k\alpha}$ and the components of the vector $\bar{F}_{i\beta}$ are known; hence, $q_{k\alpha}$ can be obtained from eq. (38), using the Gaussian elimination method [27]. Once $q_{k\alpha}$ are known, the displacements $u_i$ are calculated from eq. (35).

### 3.4.2 Method of Solution; Two Holes in Series

For problems involving two holes in series, a local coordinate system is employed along the contact surfaces. The coordinates of this system ($x'_1$ and $x'_2$) are everywhere normal and tangential to the contact surfaces as illustrated in Figure 8.
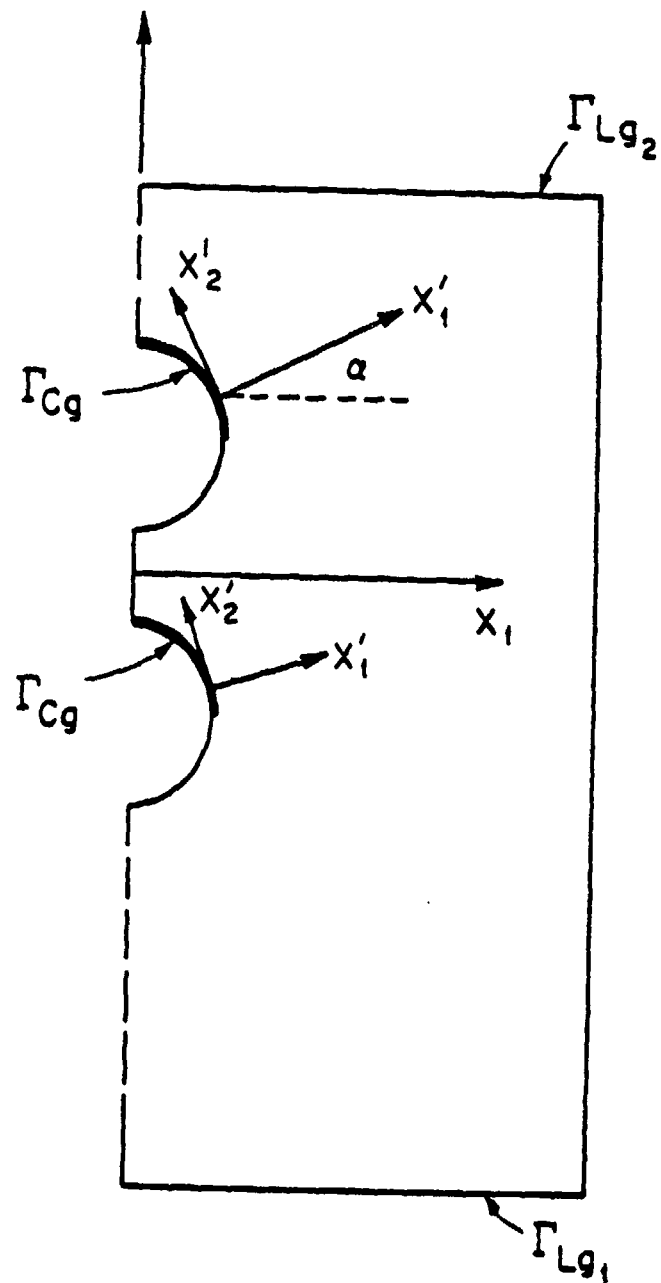
Figure 8. Illustration of the Local Coordinate System $x'_1$ and $x'_2$ along the Contact Surfaces

In this coordinate system the component of $u_i$, $\bar{u}_i$ and $\sigma_{ij}$ are denoted by the symbols, $u'_1$, $\bar{u}'_i$, and $\sigma'_{ij}$, respectively. These parameters in the local coordinate system are related to the parameters in the fixed $x_1$, $x_2$ coordinate system by the expressions

$$u_i = A_{im} u'_m$$
$$\bar{u}_i = A_{im} \bar{u}'_m$$
$$\sigma_{ij}n_j = A_{im}\sigma'_{mk}n'_k \tag{41}$$

The above transformations (eq.40) are only used for the elements adjacent to the contact surfaces. For all other elements these transformations are not employed, and we have

$$u_i = u'_i$$
$$\bar{u}_i = \bar{u}'_i$$
$$\sigma_j n_j = \sigma'_{ij}n'_j \tag{42}$$

Therefore, for elements adjacent to the contact surface, the matrix [A] is :

$$[A] = \begin{bmatrix} \cos\alpha & \sin\alpha \\ -\sin\alpha & \cos\alpha \end{bmatrix} \tag{43}$$

$\alpha$ is the angle measured clockwise from the $x'_1$ axis to the $x_1$ axis [26] (Figure 8). For any other elements which are not

adjacent to the contact surfaces, the matrix [A] is

$$[A] = \begin{bmatrix} 1 & 0 \\ 0 & 1 \end{bmatrix} \tag{44}$$

Substitution of eqs(41) and (42) into eq.(34) gives

$$\sum_{g=1}^{M} \iint_{s_g} A_{im}E_{ijkl}A_{kn}\bar{u}'_{m,j}u'_{n,l}ds = \sum_{g=1}^{M} \int_{\Gamma_{Lg1}} (-P/HW)A_{im}A_{in}n'_m\bar{u}'_n \, d\Gamma$$
$$+ \sum_{g=1}^{M} \int_{\Gamma_{Lg2}} (fP/Hw)A_{im}A_{in}n'_m\bar{u}'_n d\Gamma + \sum_{g=1}^{M} \int_{\Gamma_{cg}} A_{im}A_{in}\sigma_{mr}n'_r\bar{u}'_n dA \tag{45}$$

On the contact surfaces, the normal component of the displacements and the tangential component of the stress are zero (in the new coordinate system $x'_1$ and $x'_2$). Accordingly, the line integral along the contact surfaces is zero. With this simplicification, eq.(45) becomes

$$\sum_{g=1}^{M} \iint_{s_g} A_{im}A_{kn}E_{ijkl}\bar{u}'_{m,j}u'_{n,l} \, ds =$$
$$\sum_{g=1}^{M} \int_{\Gamma_{Lg1}} -(P/HW)A_{im}A_{in}n'_m\bar{u}'_n d\Gamma + \sum_{g=1}^{M} \int_{\Gamma_{Lg2}} (fP/HW)A_{im}A_{in}n'_m\bar{u}'_n \, d\Gamma \tag{46}$$

The displacements at the nodal point $\alpha$ are now designated by the symbol $q'_{i\alpha}$. With this notation, the displacements in each element become

$$u'_i = N_i \, q'_{i\alpha}$$

$$\bar{u}'_i = N_\alpha \, \bar{q}'_{i\alpha} \tag{47}$$

$N_\alpha$ is the shape function given in Appendix D. The calculation now proceeds along the line developed previously for problems involving either a single hole or two holes in parallel (Section 3.4.1). The stiffness matrix of the g-th element is defined as

$$K^g_{m\beta n\alpha} = \iint_{S_g} A_{im} A_{kn} E_{ijkl} N_{\alpha,l} N_{\beta,j} \, ds \tag{48}$$

As before, the nodal displacements $q'_{i\alpha}$ are independent of the surface and line integrations. Thus eqs(48)-(49) yield

$$\sum_{g=1}^{M} K^g_{m\beta n\alpha} \, q'_{n\alpha} \, \bar{q}'_{m\beta} = \sum_{g=1}^{M} \bar{q}'_{m\beta} ( \int_{\Gamma_{Lg1}} -(P/HW) A_{im} A_{in} n'_n N_\beta \, d\Gamma$$

$$+ \int_{\Gamma_{Lg2}} (P_2/HW) A_{im} A_{in} n'_n N_\beta d\Gamma \tag{49}$$

The nodal displacements $\bar{q}'_{m\beta}$ are arbitrary functions. Thus eq.(49) can be written as

$$\bar{K}_{m\beta n\alpha} \, q'_{n\alpha} = \bar{F}_{m\beta} \tag{50}$$

Where $\bar{K}_{m\beta n\alpha}$ and $\bar{F}_{m\beta}$ are given by

$$\bar{K}_{m\beta n\alpha} = \sum_{g=1}^{M} K^g_{m\beta n\alpha} \tag{51}$$

$$\bar{F}_{m\beta} = \sum_{g=1}^{M} (\int_{\Gamma_{Lg1}} - (P/HW)A_{im}A_{in}n_n N_\beta d\Gamma$$

$$+ \int_{\Gamma_{Lg2}} (fP/HW) A_{im} A_{in} n_n N_\beta d\Gamma) \tag{52}$$

The elements of $\bar{K}_{m\beta n\alpha}$ and the components of the vector $\bar{F}_{m\beta}$ are known, provided that the components of the matrix [A] in eq.(50), are known. Hence, eq(50) can be solved, once the contact angles have been determined. This can be accomplished as follows.

Values of $\theta_U$ and $\theta_L$, $\theta^a_U$ and $\theta^a_L$, are assumed such that $\theta^a_U$ and $\theta^a_L$ are greater than $\pi/2$. The displacements $u_i$ are then calculated from eqs (41), (42) and (47). Using eqs(11), (14), (41) and (42), the normal stresses along the contact surfaces bounded by the arcs $\theta^a_U$ and $\theta^a_L$ are then calculated. For contact angles greater than the actual contact angles compressive stresses become tensile (stress reserval), as illustrated in Figure 9. The angles $\theta^a_U$ and $\theta^a_L$ are then decreased slightly (by one grid length, say), and the stresses are calculated again. This procedure is repeated until no reversal in sign of the normal stresses occurs along the arcs, 0 to $\theta_U$ and 0 to $\theta_L$ (i.e., both contact surfaces are in compression) . These values, $\theta_U$ and $\theta_L$, are taken to be the contact angles. As an illustration, values of the contact angles were calculated for Fiberite T300/1034-C composites with different width ratios. The variation in the contact angles with the width ratios are given in Figure 10.
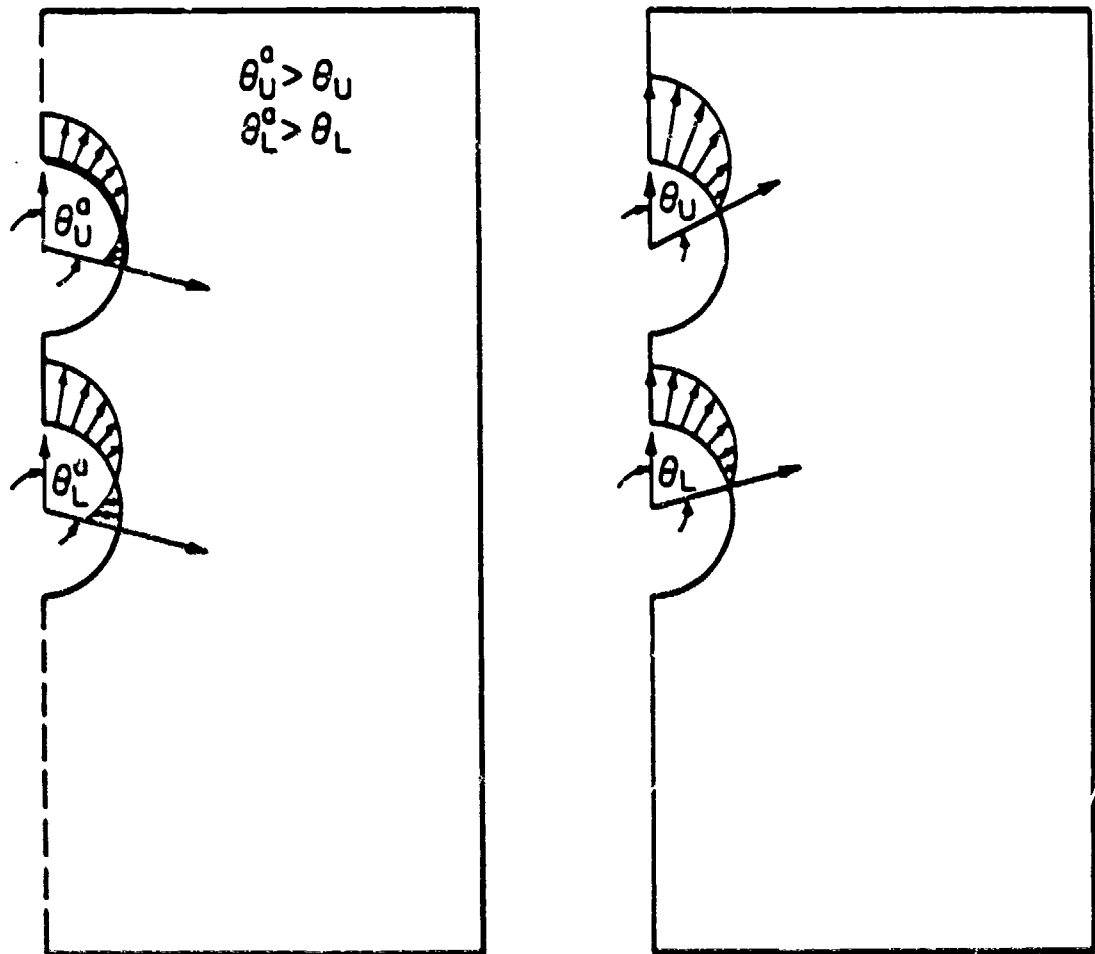
Figure 9. Illustration of the Reversal of the Normal Stresses When the Assumed Contact Angles $\theta^a_U$ and $\theta^a_L$ are Greater than the Actual Contact Angles (Left). No Stress Reversal Occurs for the Actual Contact Angles $\theta_U$ and $\theta_L$ (Right).
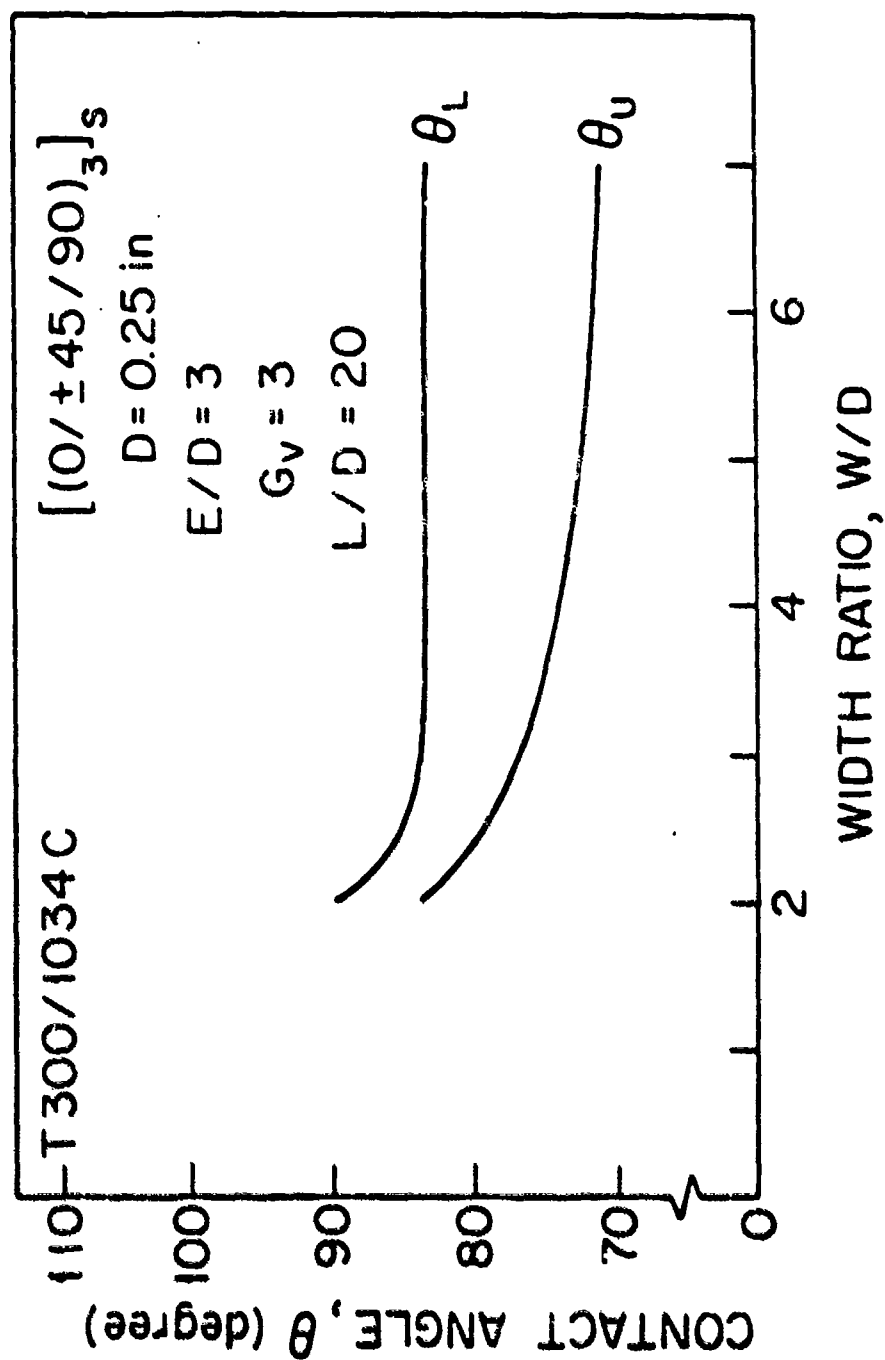
Figure 10. Variation of the Contact Angle With the Width Ratio for a Laminate Containing Two Holes in Series.

# SECTION IV

## PREDICTION OF FAILURE

In order to determine the load at which a joint fails (failure load) and the mode of failure, the conditions for failure must be established. In this investigation, the joint is taken to have failed when certain combined stresses have exceeded a prescribed limit in any of the plies along a chosen curve(denoted as the characteristic curve). The combined stress limit is evaluated using the failure criterion proposed by Yamada-Sun [28].

### 4.1) Failure Criterion

Numerous criteria for failure have been proposed in the past [29, 30-33]. Although the concepts underlying the different failure criteria may be different, the results of the various criteria are generally quite similar. In this investigation, the Yamada-Sun failure criterion was adopted [28]. This criterion is based on the assumption that just prior to failure of the laminate ,every ply has failed due to cracks along the fibers. This criterion states that failure occurs when the following condition is met in any one of the plies

$$(\sigma_x/X)^2 + (\sigma_{xy}/S)^2 = e^2 \quad \begin{cases} e < 1 & \text{no failure} \\ e \geq 1 & \text{failure} \end{cases} \quad (53)$$

34

As indicated in eq. (53) failure occurs when e is equal to or greater than unity. In the above equation, $\sigma_x$ and $\sigma_{xy}$ are the longitudinal and shear stresses in a ply, respectively (x and y being the coordinates parallel and normal to the fibers in the ply). S is the rail shear strength of a symmetric, cross ply laminate $[0/90]_s$. X is either the longitudinal tensile strength or the longitudinal compressive strength of a single ply. The tensile strength ($X=X_t$) is used when the stress $\sigma_x$ is in tension ($\sigma_x>0$). The compressive strength ($X=X_c$) is used when $\sigma_x$ is compressive ($\sigma_x<0$).

## 4.2) Failure Hypothesis-Characteristic Curve

The hypothesis is proposed here that failure occurs when, in any one of the plies, the combined stresses satisfy an appropriately-chosen failure criterion at any point on a characteristic curve. The characteristic curve (Figure 11) is specified by the expression

$$r_c(\theta) = D/2 + R_t + (R_c - R_t) \cos\theta \tag{54}$$

The angle $\theta$, measured clockwise from the $x_1-x_2$ axis, may range in value from $-\pi/2$ to $\pi/2$. $R_t$ and $R_c$ are referred to as the characteristic lengths for tension and compression.
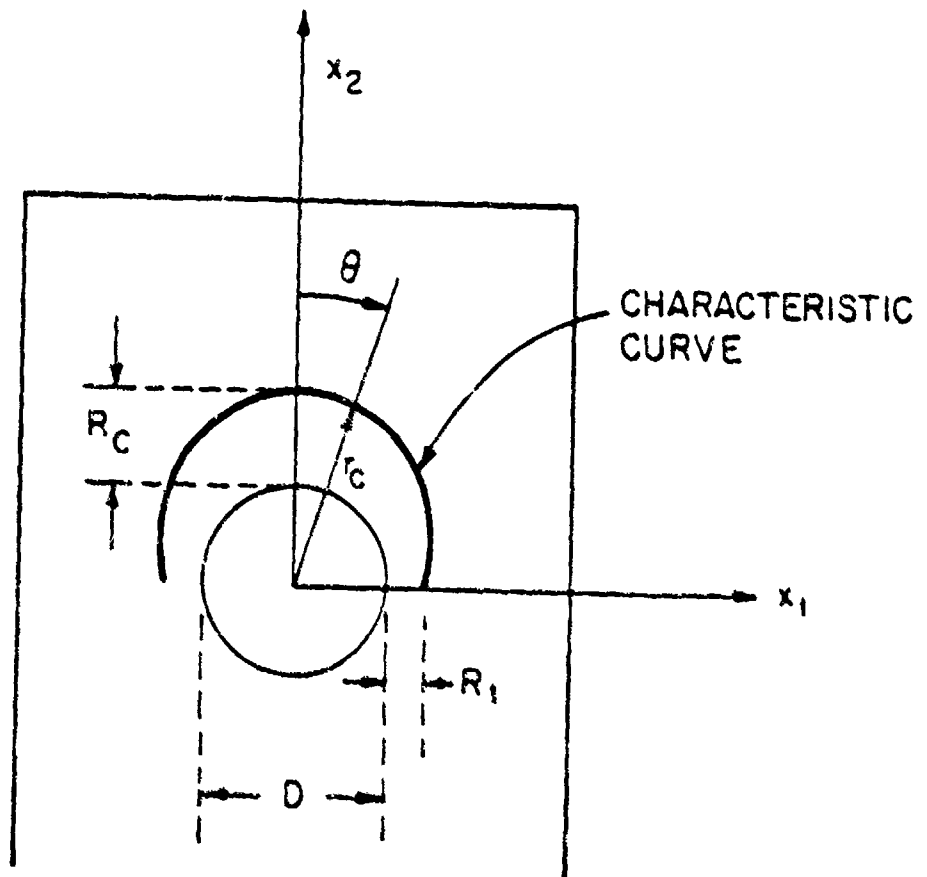
Figure 11. Description of the Characteristic Curve.

These parameters must be determined experimentally.

The concept of the characteristic length in tension $R_t$ was introduced by Whitney and Nuismer [34-37]. In recent years, several investigators utilized this concept in analyzing the strength of loaded holes. However, different investigators used different definitions of $R_t$, and employed different procedures for determining the value of $R_t$. As will be discussed in Sections VI and VII, the method proposed here for determining $R_t$ differs from that proposed by previous investigators [7, 34, 35]. It is also noted that the characteristic length in compression $R_c$ has not yet been employed in the strength analysis of loaded holes.

In this investigation, the characteristic curve is used together with the Yamada-Sun failure criterion. Accordingly (see eq. 53), failure occurs when the parameter e is equal to, or is greater than unity at any point on the characteristic curve

$$\left. \begin{array}{ll} \text{No failure} & e < 1 \\ \text{Failure} & e \geq 1 \end{array} \right\} \text{at } r = r_c \qquad (55)$$

It is emphasized that the above failure hypothesis is used here in conjunction with the Yamada-Sun failure criterion (eq. 53). However, the hypothesis is general and is not restricted to the Yamada-Sun criterion. The characteristic curve proposed here may be used with any other failure criterion.

4.3) <u>Solution Procedure</u>

Whether or not a joint fails under a given condition is determined as follows. For a given load

a) The components of strains of $\varepsilon_{11}$, $\varepsilon_{22}$ and $\varepsilon_{12}$ are calculated, using the method of solution described in Section III.

b) The longitudinal and shear stresses in each ply are calculated using eq.(16').

c) The parameter e is calculated (eq.53) along the characteristic curve.

d) If e equals or exceeds the value of unity (e≥1) in any ply along the characteristic curve, the joint is taken to have failed.

The procedure outlined above is used to predict whether or not failure occurs under a given load. Due to the assumption of a linear stress-strain relationship, the calculated stresses are linearly proportional to the applied load P. This fact, together with Yamada-Sun failure criterion (eq.53) gives

$$p \sim e \qquad (56)$$

This relationship is utilized to determine the maximum load ($P_{max}$) which can be imposed on the joint. For a given

load P, values of e are calculated on the characteristic curve, as discussed above (points a-d). Note that there are two characteristic curves when there are two holes. The highest value of e ($e_o$) is then determined, and the maximum load is calculated by the expression

$$P_{max} = P/e_o \tag{57}$$

The calculation procedure described in the foregoing also provides the location (angle $\theta_f$) at which e first reaches the value of unity (e=1) on the characteristic curve (Figure 12). A knowledge of $\theta_f$ provides an estimate of the mode of failure. When $\theta_f$ is small ($\theta_f=0°$), failure occurs by the bearing mode. When $\theta_f=45°$, failure is due to shearout; when $\theta_f=90°$, failure is caused by tension. In summary

$$
\begin{array}{lll}
-15° \le \theta_f \le 15° & \text{bearing mode} & \\
30° \le \theta_f \le 60° & \text{shearout mode} & (58) \\
75° \le \theta_f \le 90° & \text{tension mode} &
\end{array}
$$

At intermediate values of $\theta_f$, failure may be caused by a combination of these modes.
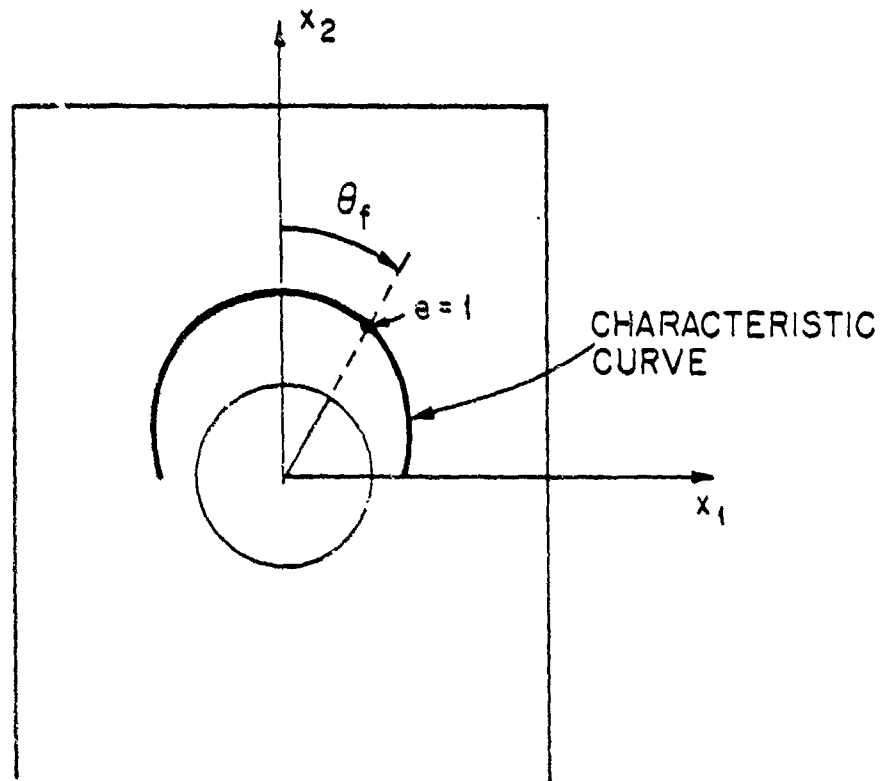
Figure 12.    Location of Failure (e=1) Along the
Characteristic Curve.

# SECTION V

## NUMERICAL SOLUTION

A "user friendly" computer code (designated as BOLT) was developed which is suitable for generating solutions to the problem formulated in Sections III-IV. The required input parameters and the output provided by the code are summarized in Table 1. The input-output is illustrated by the sample calculations included in Appendix E.

In order to assess the accuracy of the numerical method, solutions were generated to problems for which analytical solutions were available. Specifically, stress distributions were calculated in isotropic plates containing both unloaded (open) and loaded holes, and in orthotropic plates containing unloaded holes.

An analytical solution for the stress distribution in an infinite ($W \to \infty$) isotropic plate containing an unloaded hole was given by Timoshenko [38]. The stress distribution in such a plate was also calculated by the present method. The parameters used in the numerical calculations are given in Figure 13. A large width ($W/D=14$) was used in the calculation to approximate an infinite plate. The results of the present method and the analytical solution of Timoshenko are compared in Figure 13. There is excellent agreement between the stresses calculated by the two methods.

41

Table 1.  Input parameters required by the computer code and
          the output provided by the code.

INPUT PARAMETERS

1) Material Properties

    a) Longitudinal and transverse Young's moduli; $E_1$ and $E_2$

    b) Shear modulus, $G_{12}$

    c) Poisson's ratio, $\mu_{12}$

    d) Longitudinal tensile and compressive ply strength,
       $X_t$ and $X_c$.

    e) Rail shear strength of a cross ply laminate

       $[0/90]_s$, $S_{50}$

    f) Characteristic lengths, $R_t$ and $R_c$

2) Geometry

    a) hole diameter, D

    b) thickness, H

    c) width, W

    d) length, L

    e) edge distance, E

    f) distance between two holes, G (for two holes only)

3) Ply orientations

OUTPUT PARAMETERS

1) Failure load

2) failure mode
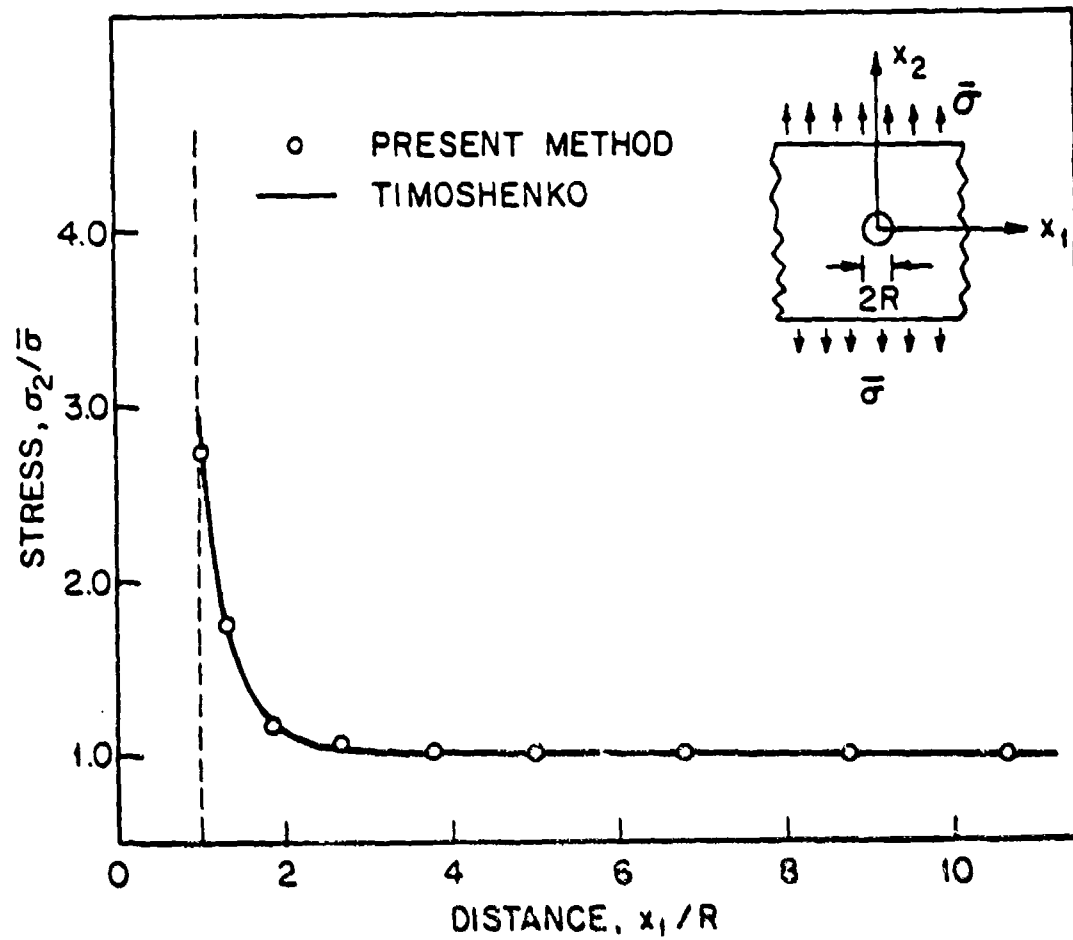
Figure 13. Stress $\sigma_2$ Along $x_1$-axis in an Isotropic Infinite Plate Containing a Circular Hole. Comparison of Present Results with Theoretical Results Given by Timoshenko [38]. Parameters Used in Numerical Calculations: $\bar{\sigma}$=2.37 ksi, D=2R=0.3 in, W/D=14. E/D=8, L/D=28.

The stresses in isotropic plates containing loaded holes were also calculated. Plates of infinite and finite width were considered. Calculations were performed for the parameters given in Figure 14.

As shown in Figure 14, the stresses calculated by the present method are in excellent agreement with De Jong's approximate solution [24].

The stress distribution in an orthotropic plate of finite width containing an open (unloaded) hole was also calculated. The calculations were performed for a plate with the symmetric laminate lay up of $[0/90]_s$. An analytical solution for this problem was provided previously by Nuismer and Whitney [35], who modified Lekhnitskii's earlier solution [39] for an infinite plate. The results given in Figure 15 show excellent agreement between the stresses calculated by the present method and by the analytical solution.

The aforementioned comparisons indicate that the present method predicts the stress distribution around loaded and unloaded holes with high accuracy.
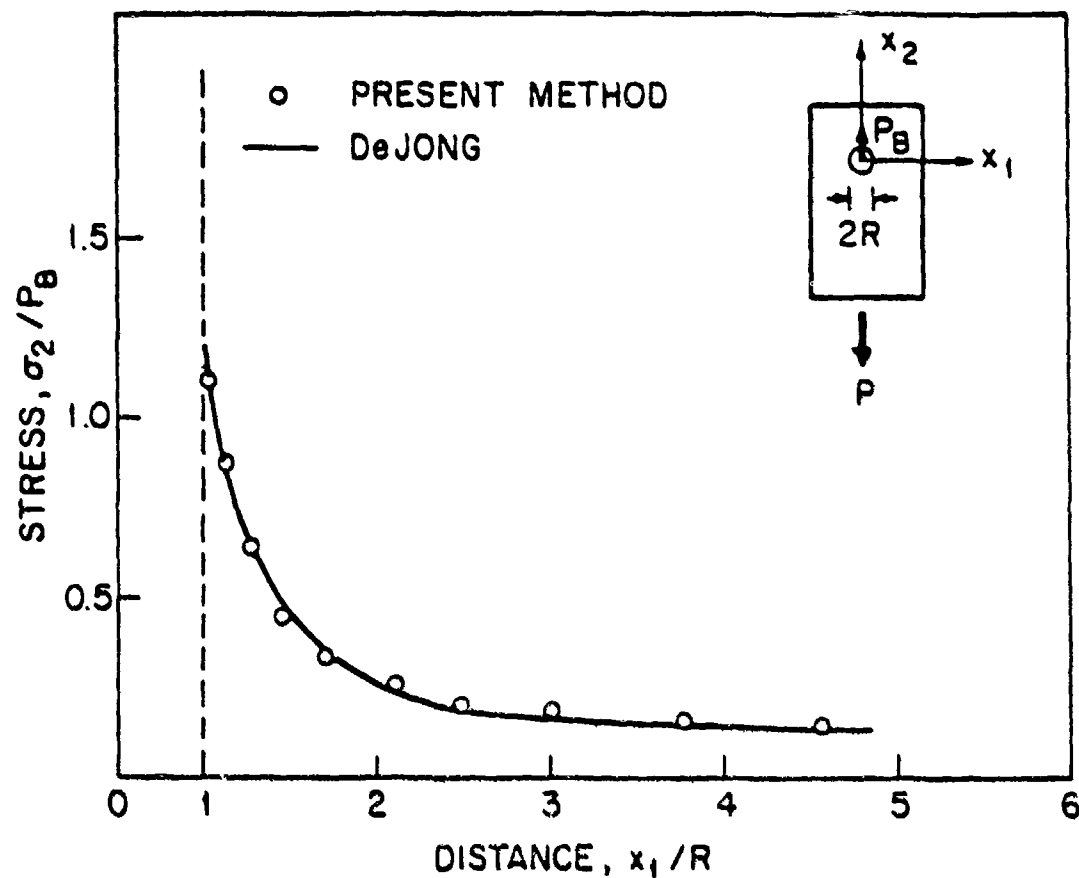
Figure 14. Stress $\sigma_2$ Along the $x_1$-axis in an Isotropic Plate of Finite Width Containing a Loaded Hole. Comparison of the Present Results With the Theoretical Results Given by De Jong [24]. Parameters Used in the Numerical Calculations: D=0.3 in, W/D=5, E/D=4, L/D=14.
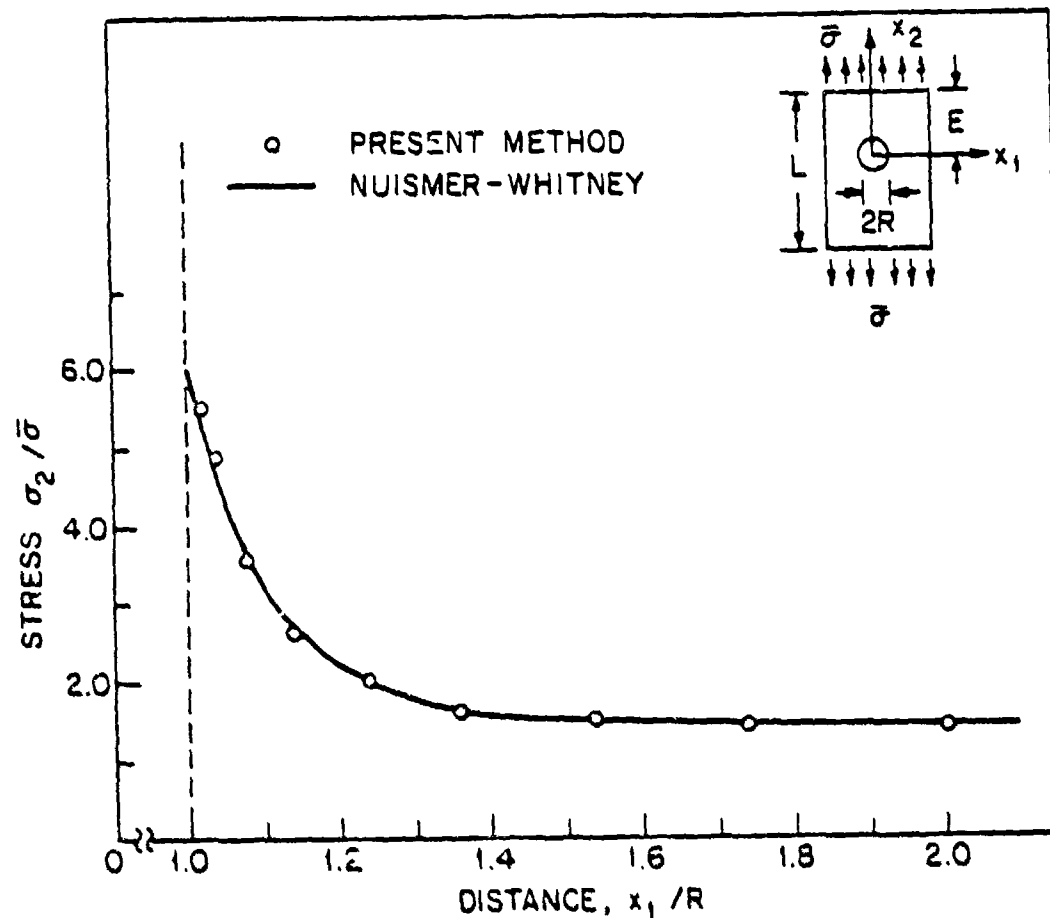
Figure 15. Stress $\sigma_2$ Along the $x_1$-axis in an Orthotropic Finite Plate $[0/90]_s$ Containing a Circular Hole. Comparison of the Present Results With the Theoreticla Results Obtained by Nuismer and Whitney [34]. Parameters Used in the Numerical Calculations: Material: Graphite/Epoxy T300/5208, $E_1$=21.4x10$^3$ ksi, $E_2$=1.6x10$^3$ ksi, $G_{12}$=0.77x10$^3$ ksi, $\mu_{12}$=0.29, $\bar{\sigma}$=2.3 ksi, D=1 in, W/D=3, E/D=4, L/D=14

# SECTION VI

## EXPERIMENT

An experiment was performed to measure the mechanical
properties of composite laminates (with and without holes),
and the failure strengths and failure modes of mechanically-
fastened composite joints.

The apparatus and procedures used in the tests are
described in this section. A brief description of the
procedure used to fabricate the test specimens is also
given.

### 6.1) Measurement Procedure for the Laminate Shear Strength S

Rail shear tests were performed to measure the laminate
shear strength. Cross ply $[0/90]_s$ laminates made of either
20 or 24 plies were used in the tests. Laminates with
different volume fractions $v_o$ of 0 plies were tested. $v_o$ is
the number of zero degree plies divided by the total number
of plies.

The specimens ranged from 8 in to 7.75 in in length and
2 in to 1.5 in in width. These specimen dimensions were
selected because it was demonstrated by previous
investigators that for such specimens, edge effects are
negligible [40,41]. The configurations of the rail-shear
specimens are shown in Appendix E.
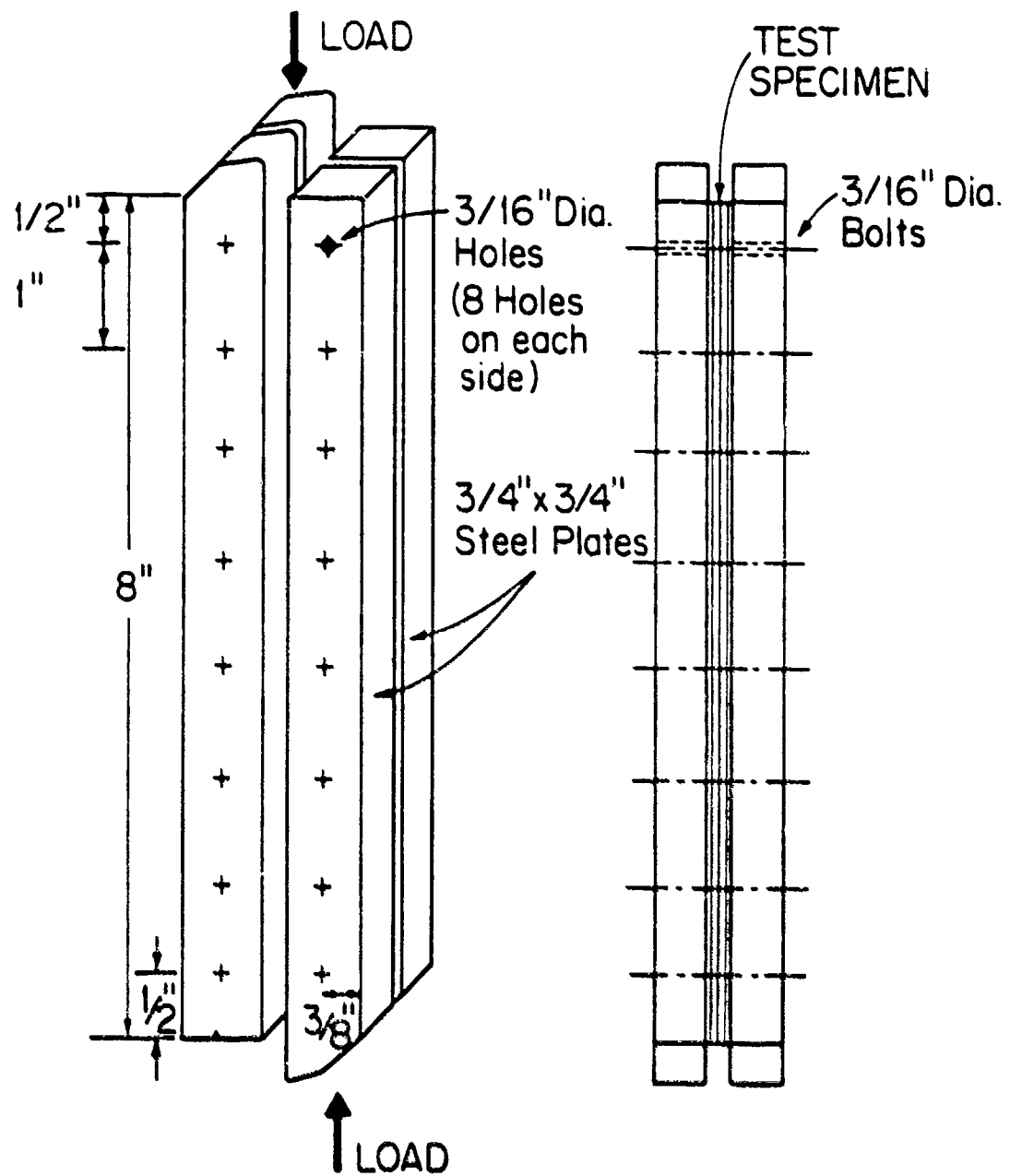
Figure 16. Schematic of Rail Shear Test Fixture.

Eight 3/16 in diameter holes were drilled along two sides of the specimens, as illustrated in Figure 16. The specimens were placed between a rail-shear fixture. The geometry and dimension of this fixture are given in Figure 16. The specimen was fastened to the rail-shear fixture by 16 bolts. The bolts were tightened to at least 80 ft-lbf torque.

The shear tests were performed by placing the rail-shear fixture into a mechanical testing machine and by applying a compressive load. The ultimate failure load of the laminate was recorded.

## 6.2) Measurement Procedure for the Characteristic Length $R_t$

The characteristic length $R_t$ was measured using rectangular specimens with an open hole in the center of the specimen. Tests were performed with specimens having different ply orientations, different hole sizes, and different dimensions (Appendix F). During each test, the specimen was subjected to a tensile load and the ultimate load was recorded. In addition, (after failure) the specimens were inspected visually to establish the mode of failure.

From the measured tensile strength the value of $R_t$ was determined as follows :

At the failure load, the stresses in the laminate were

calc·lated, using the model described in Section III for a
laminate containing and open hole.  The stresses calculated
in each ply along the $\theta=90$  line were substituted into the
Yamada-Sun failure criterion (eq. 53).  The point
along this line was found at which the value e became unity.
The distance between this point and the edge of the hole was
taken to be $R_t$.  The values of $R_t$ thus measured are
presented in Section VII.

## 6.3) Measurement Procedure for the Characteristic
###    Length $R_C$

The characteristic length $R_C$ was determined by the
following method.  A single hole was drilled into the
specimen.  The position and the diameter of the hole, the
specimen geometry, and the laminate configurations used in
the tests are given in Appendix F.  The specimen was
inserted into a fixture shown in Figure 17.  The top part of
the fixture consisted of two 3 in wide and 5 in long steel
plates ("main plates").  A 1.25 in diameter and 3.5 in long
rod was inserted between these plates. The rod was fastened
to the main plates by bolts.  A 0.5 in diameter hole was
drilled along the center line of each main plate, 1.5 in
from the bottom edge.  A 0.5 in dowel pin was inserted into
this hole.

The bottom part of the fixture consisted of two 3 in
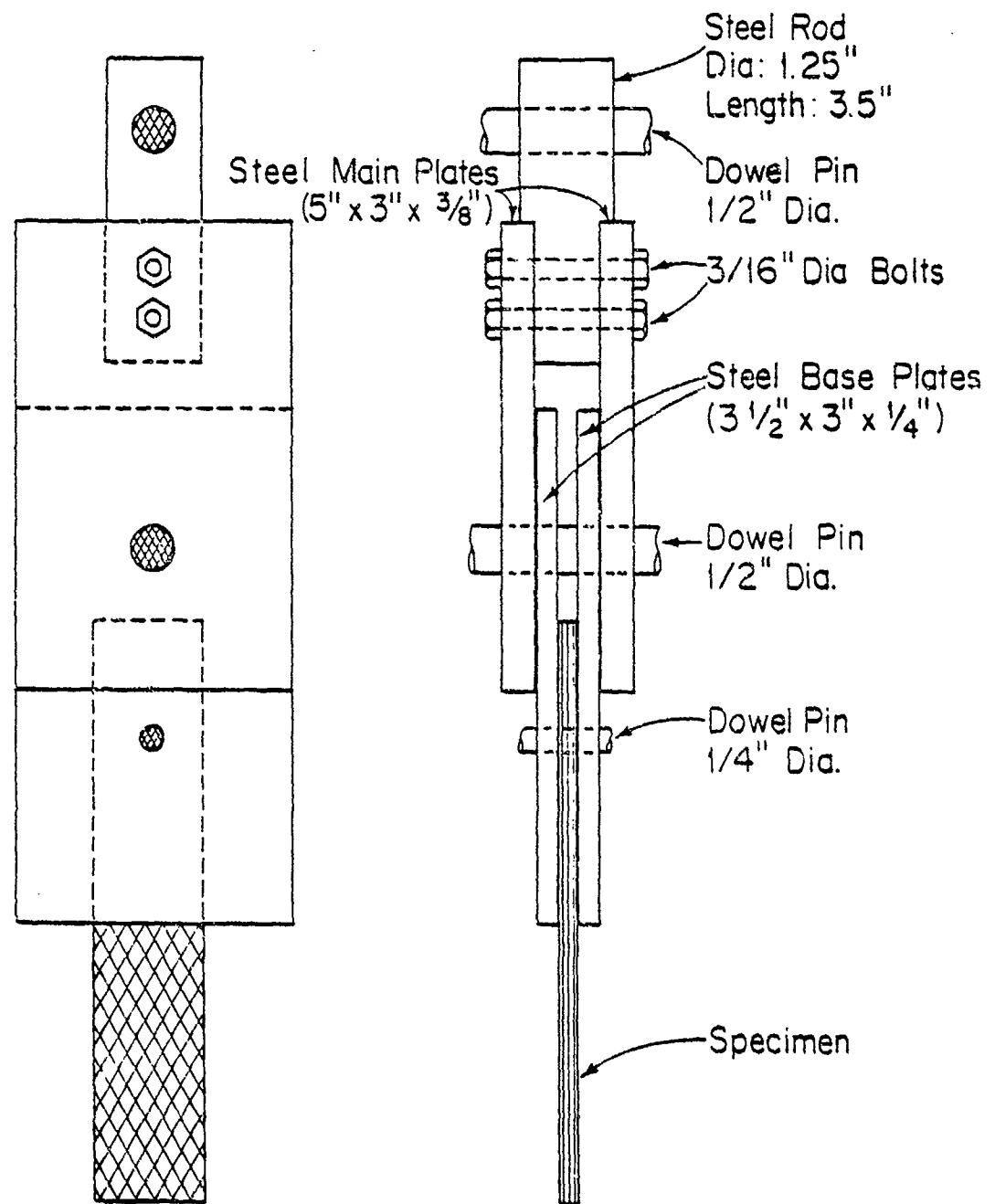
Figure 17.    Fixture Used in Testing Loaded Holes (Base Plate
Geometry Given in Figure 18 and Table 2).

wide and 5 in long "base plates." These plates were
supported by the dowel pin. The material to be tested was
placed between the two base plates. A second 0.5 in
diameter dowel pin was passed through the base plates and
the laminate.

A C clamp was placed around the base plates near the
lower dowel pin and tightened by hand. The purpose of this
clamp was to simulate the lateral force which would be
provided by "finger-tight" bolts in the hole.

During the tests the rod protruding from the main plates
was inserted into the upper grips, and the laminate was
inserted into the lower grips of a mechanical testing
machine. A tensile load was applied by the machine and the
ultimate tensile strength was recorded.

From the measured tensile strength, the characteristic
length $R_c$ was determined . The stresses were calculated
using the model described in Section III for a loaded hole.
A value of $R_c$ was assumed and the characteristic curve was
constructed in the manner given in Section IV. The value e
in the Yamada-Sun failure criterion (eq.53) was determined
in each ply along a segment of the characteristic curve,
ranging from $\theta = 15$ to $\theta = -15$. The procedure was repeated for
different assumed values of $R_c$ until (in any ply) the value
e=1 was reached along the characteristic curve segment
($-15 \leq \theta \leq +15$). This value was then taken to be $R_c$. The
measured values of $R_c$ are presented subsequently (Section
7.3).

## 6.4) Strength of Mechanically Fastened Composite Joints

The strengths of mechanically fastened joints (loaded holes) were determined using rectangular specimens. Either a single hole or two holes in parallel or in series were drilled in each specimen. The geometries of the specimens and the laminate configurations used in the tests are described in Appendix G.

The test was performed by placing the laminate into the fixture described previously and illustrated in Figure 17. In each test the same main plate and the dowel pin were uesd. The dimensions of the base plates were different, depending upon the specimen configurations. The dimension of the base plates are given in Figure 18 and Table 2. During the test, a lateral force was applied with one C clamp to simulate the lateral force that would be provided by "finger-tight" bolts placed in the hole. The fixture was inserted into a mechanical testing machine. A tensile load was applied and the ultimate tensile strength as recorded. After the test, each specimen was inspected and the mode of failure was determined.

## 6.5) Specimen Preparation

The laminates were constructed from Fiberite T300/1034-C prepreg tape. The panels were cured in an autoclave [43]. The test specimens were cut by a diamond saw. The holes were drilled with solid carbide drills for hole diameters less than one half inch and by carbide tip drills for 1/2 in diameter holes. The nominal sizes of holes were 0.125 in, 0.1875 in, 0.25 in, and 0.5 in. The nominal size dowel pins were the same. To provide a close fit, each dowel pin was dressed down by about 0.001 in. The properties of Fiberite T300/1034-C are listed in Table 3.

55
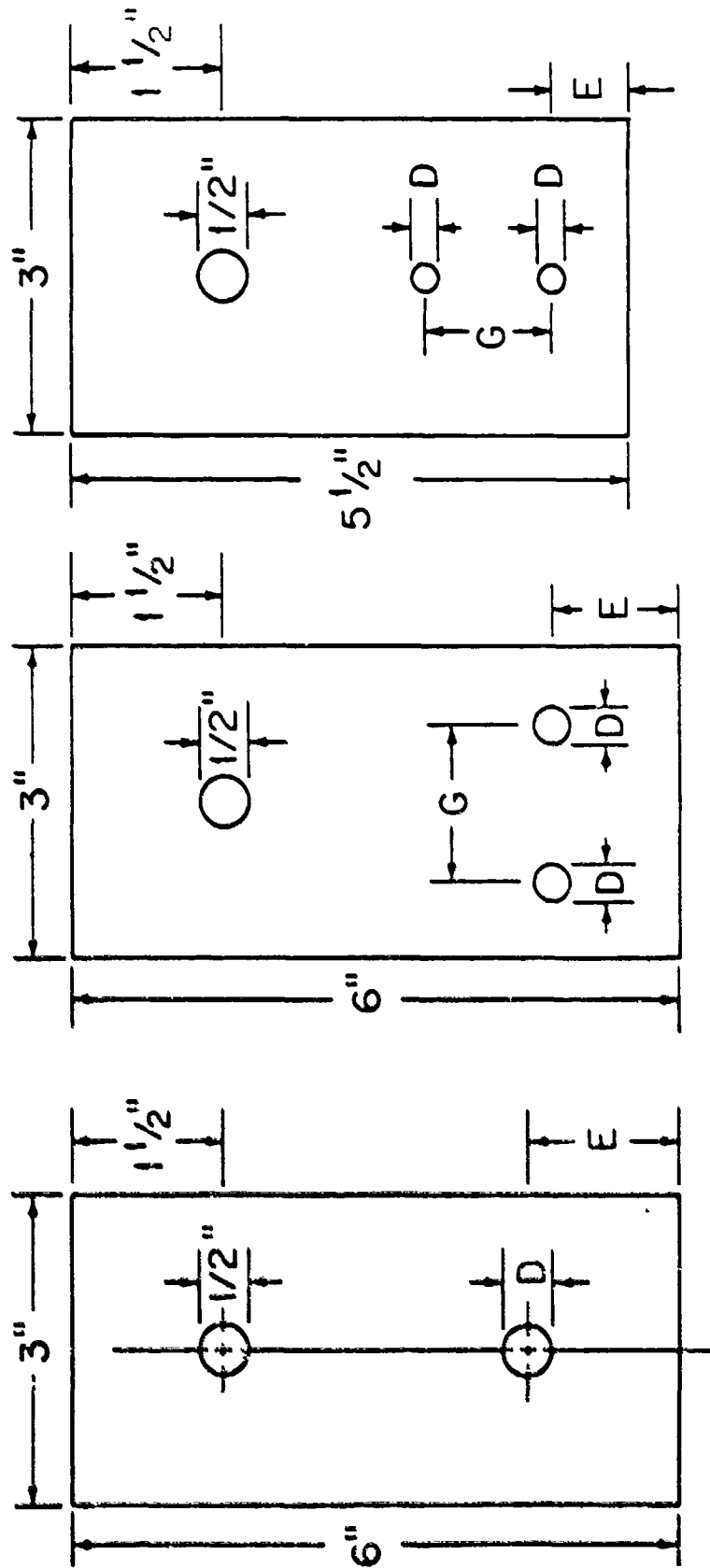


Figure 18. Base Plates Configurations (See Figure 17). Plate Thickness 1/4 in. The Dimensions G, D, and E are Given in Table 2.

Table 2    Dimensions of the base plates shown in Figures 17
           and 18. All units in inches.

| Single Hole | D | G | E |
|---|---|---|---|
| plate 1 | 0.5 | | 1.5 |
| plate 2 | 0.25 | | 1.0 |
| plate 3 | 0.1875 | | 0.75 |
| plate 4 | 0.125 | | 0.5 |
| | | | |
| Two Holes in Parallel | | | |
| plate 1 | 0.5 | 2.5 | 1.5 |
| plate 2 | 0.5 | 1.5 | 1.5 |
| plate 3 | 0.25 | 1.25 | 1.0 |
| plate 4 | 0.25 | 0.75 | 1.0 |
| | | | |
| Two Holes in Series | | | |
| plate 1 | 0.25 | 1.25 | 0.75 |
| plate 2 | 0.25 | 0.75 | 0.75 |
| plate 3 | 0.1875 | 0.625 | 0.5 |
| plate 4 | 0.1875 | 0.375 | 0.5 |

Table 3    Properties of Fiberite T300/1034-C graphite/epoxy
           composite


Longitudinal Young's modulus, $E_1$          $=$ 21300000 psi

Transverse Young's modulus, $E_2$            $=$  1700000 psi

Shear Modulus, $G_{12}$                       $=$   897000 psi

Poisson's Ratio $\mu_{12}$                    $=$      0.3

Longitudinal tensile strength, $X_t$         $=$   251000 psi

Longitudinal compressive strength, $X_c$     $=$   200000 psi

Rail shear strength, $S=S_{50}$              $=$    19400 psi

Characteristic length in tension, $R_t$      $=$    0.018 in

Characteristic length in compression, $R_c$  $=$     0.07 in

## MEASUREMENTS OF S, $R_t$, AND $R_c$

Tests were performed to determine the rail-shear
strength S and the characteristic lengths $R_t$ and $R_c$ of
Fiberite T300/1034-C composites. These data were generated
because they are required in the numerical calculation of
the failure strength and the failure mode of loaded holes.
The data obtained also indicate the sensitivities of S, $R_t$,
and $R_c$ to such parameters as specimen geometry and laminate
configuration.

The material properties used in deducing S, $R_t$, and $R_c$
from the measured data are listed in Table 3. In these
tables the values of S, $R_t$, and $R_c$ obtained in this
investigation are also included.

### 7.1) Rail Shear Strength S

Rail shear tests were performed with symmetric cross-ply
laminates $[0/90]_s$ having different volume fractions of zero
degree plies and different geometries. The test conditions
and the test results are summarized in Appendix F. During
some of the tests, cracks were observed near the top and
bottom holes of the rail-shear fixture. These cracks
resulted in a reduction of shear strength. Specimens with
such cracks were not used in calculating the rail-shear
strengths. Accordingly, the rail-shear strength of cross-

ply $[0/90]_s$ specimens having 50 percent zero-degree plies by volume was found to be $S_{50} = 19.4$ ksi.

The rail-shear strength depends on the volume fraction of the zero degree plies in the laminates. At volume fractions above 50 percent the rail shear strength decreases (Figure 19). At volume fractions above 60 percent the rail shear strength remains nearly constant. Therefore, when the volume fraction of zero-degree plies is higher than 50 percent, the rail-shear strength corresponding to the appropriate volume fraction should be used in calculating the failure strength and the failure mode.

It was observed that the shear stress to shear strain relationship was nonlinear. However, in the present model, this nonlinearity was not taken into account. The assumption of linear stress-strain relation may result in some error in the calculated values of the failure strength (Section VIII), especially for joints consisting predominantly of $[0/90]_s$ and $[\pm45]_s$ laminates.

## 7.2) Characteristic length $R_t$

The characteristic length $R_t$ was determined using laminates with different geometries and different ply orientations. The detailed results of the measurements are given in Appendix F. The data are summarized in Figures 20 and 21. Each data point in these figures is the average of four measurements. Figure 20 shows the variations in $R_t$ with laminate lay up. In Figure 21, all but one set of data

are presented in a single plot. The data for $[(\pm 45)]_s$ laminates were excluded from Figure 21, because with these laminates failure occurred not by tension, but by tear-out along the 45 dwgree fibers.

The results in Figure 20 show that the value of $R_t$ depends on the hole diameter, the width ratio (W/D), and the ply orientation. The value of $R_t$ increases with increasing hole diameter (Figures 20 and 21). As was discussed previously (Section 4.2), different investigators use different definitions of the characteristic length. It is still noteworthy that an increase in characteristic length with hole diameter was also observed by Whitney and Nuismer [34, 35] and by Pipes et al. [7] in their tests with T300/5208 and AS-3501-6 graphite/epoxy laminates. It is difficult to discern definite trends in $R_t$ with width ratio and ply orientation. In calculating the strength of loaded hole, the $R_t$ value appropriate to the laminate and hole configurations should be used. When this value is unavailable, an approximate value of $R_t$ must be used. Fortunately, it was found that strength prediction is not too sensitive to the value of $R_t$. For example, the failure strengths of loaded holes in T300/1034-C laminates were calculated with the values of $R_t$ =0.007, 0.018, and 0.04 in. The use of the lower and higher $R_t$ values yielded failure strengths which were about 10 percent to 20 percent different from the one obtained by the average $R_t$ value ($R_t$=0.018 in ).
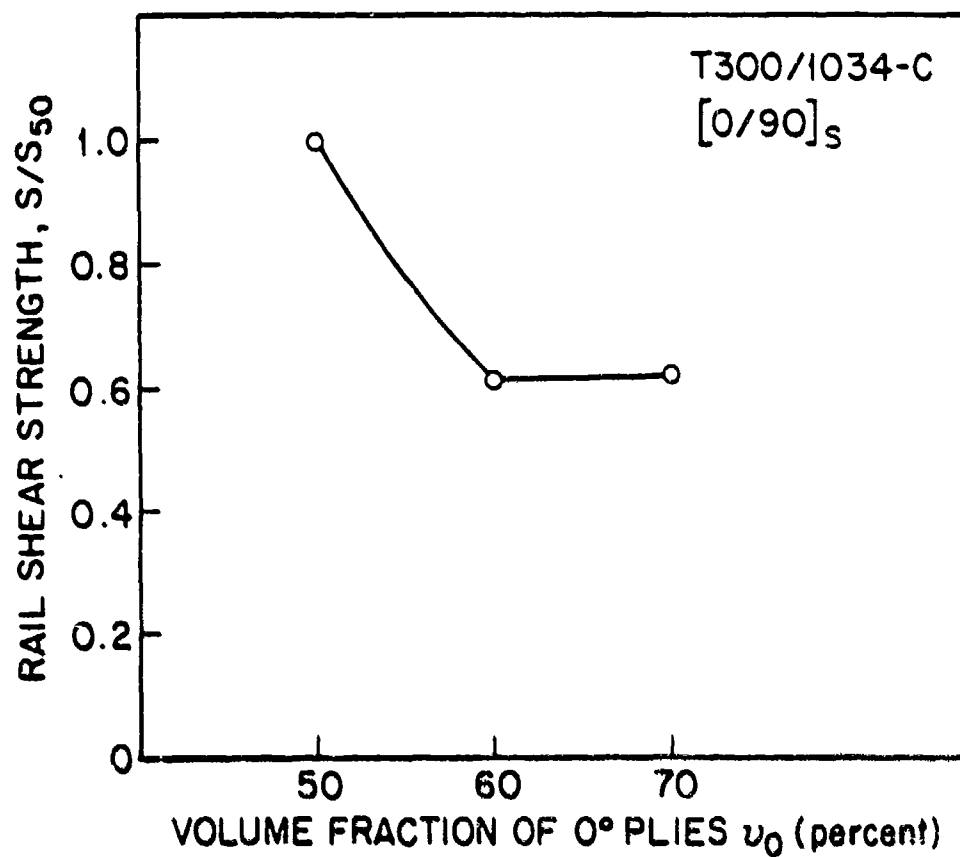
Figure 19. Variation in Rail Shear Strength with the Volume Fraction of 0 Degree Plies of Cross Ply Laminates. o Data. ——— Fit to Data. $S_{50}$ =50% Volume Fraction of 0 Degree Plies = 19400 psi
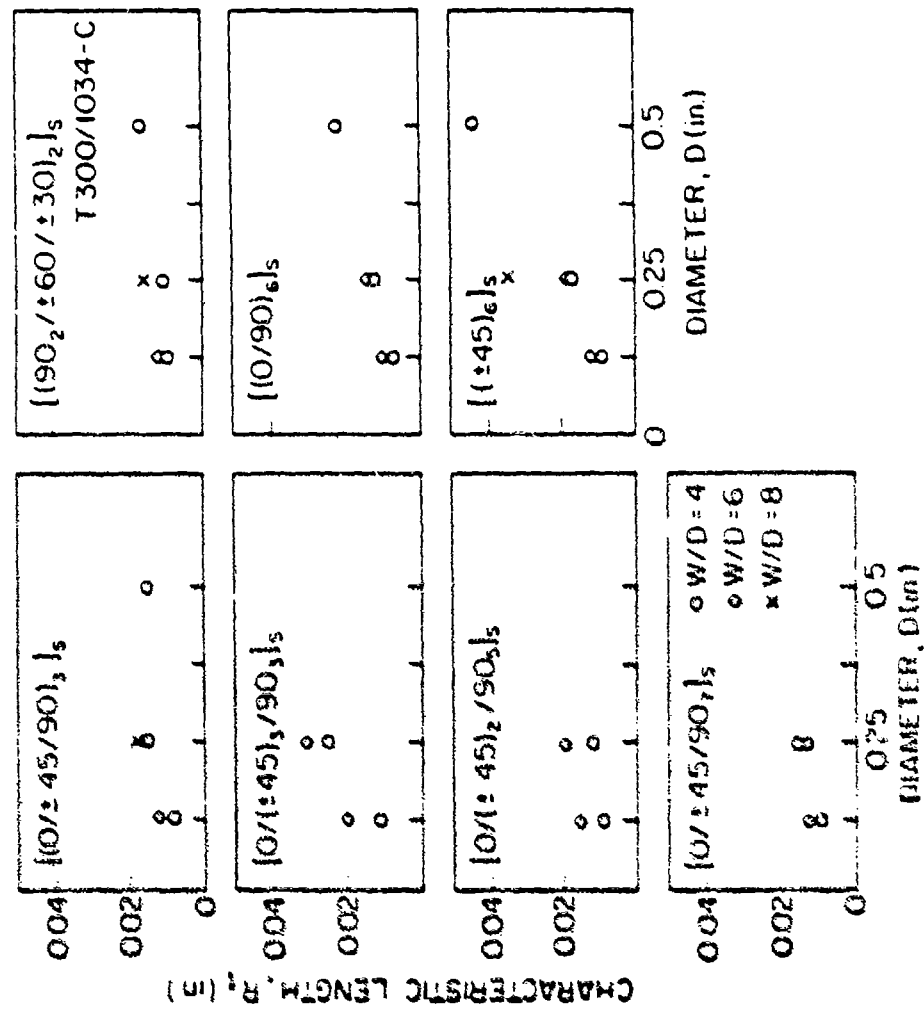
Figure 20. Characteristic Length in Tension $R_t$ as Function of Hole Diameter, Width Ratio, and Ply Orientation.
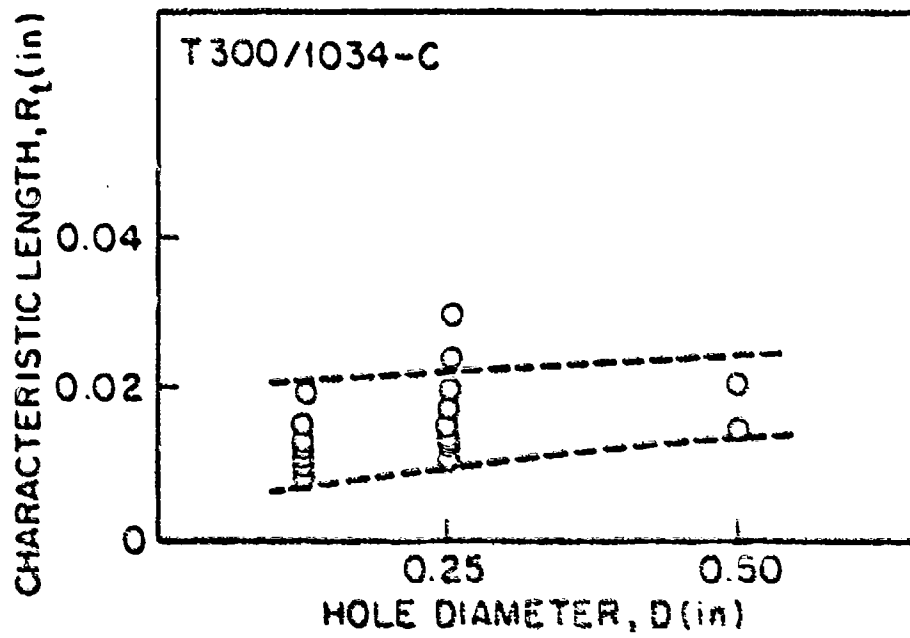
Figure 21. Variation of Characteristic Length With Hole Diameter. Data are for Laminate Configurations Given in Figure 20.

7.3) <u>The Characteristic Length</u> $R_c$

The value of $R_c$ was determined for four different ply orientations, as indicated in Appendix F. The data are summarized in Table 4. Each $R_c$ value in this table is the average of four measurements.

As was discussed in Section 6.3, the values of $R_c$ were obtained from data generated using loaded holes and from the Yamada-Sun failure criterion (eq.53). Both the longitudinal and shear stresses play a role in this criterion. Thus, both of these stresses may affect the value of $R_c$. The shear stress has a significant effect in those laminates in which the shear stress to shear strength ratio $(\sigma_{xy}/S)$ is comparable to the longitudinal stress to longitudinal compressive strength ratio $(\sigma_x/X_c)$. This situation arises, for example, in $[0/90]_s$ and $[\pm 45]_s$ laminates.

In calculating $R_c$, the stresses were assumed to vary linearly with strains. As was noted previously (Section 6.1), for shear stresses this assumption may be invalid, since the value $R_c$ may depend on the shear stress. This assumption may have affected the values of $R_c$, especially for the two cross-ply laminates in Table 4. The effects introduced in $R_c$ by the assumption of linear stress-strain relationship is unknown; therefore, the value of $R_c$ $(=0.07$ in.) obtained for quasi-isotropic laminates was adopted in this investigation.

Table 4    The Characteristic Length in Compression $R_c$
           for Fiberite T300/1034-C.  Data obtained for
           D=0.25 in, W=2.0 in, L=7.0 in , E=1.25 in

| Ply Orientation | Characteristic Length $R_c$ (in) |
|---|---|
| $[(0/\pm45/90)_3]_s$ | 0.07 |
| $[(90_2/\pm60/\pm30)_2]_s$ | 0.08 |
| $[(0/90)_6]_s$ | 0.09 |
| $[\pm45)_6]_s$ | 0.13 |

# SECTION VIII

## EXPERIMENTAL VALIDATION OF THE MODEL

In this section, comparisons between data and the results of the model are presented. The data used in the comparisons were generated during the course of this investigation with Fiberite T300/1034-C graphite/epoxy composite having different geometries and different ply orientations. The failure strength and the failure modes were measured with composites containing either one pin-loaded hole or two pin-loaded holes in parallel, or two pin-loaded holes in series. The experimental results are presented in Figures 22 through 29.

To facilitate comparisons between the data and the results of the model, the ordinates in these figures represent the bearing strength $P_B$. For laminates with a single hole or with two holes in series, the bearing strength is expressed as $P_B = P/DH$. For laminates containing two holes in parallel, the bearing strength is taken as $P_B = P/2DH$. P is the failure load and DH represents the cross sectional area of the hole. In Figures 22-29 the measured bearing strengths and failure modes are represented by different symbols.

The bearing strengths and failure modes were also calculated by the model. The numerical calculations were performed using the material properties listed in Table 3. The numerical results are included in these figures. The

66

calculated bearing strengths are given by solid lines. The calculated failure modes were not identified separately as long as they were the same as those given by the data. In those cases where the calculated failure model differs from the data, the calculated failure mode is identified by the letters T, B, or S, next to the corresponding data point. These letters represent failure in tension, bearing, and shearout modes.

As indicated in Figures 22-29, for $[(0/\pm45/90)_3]_s$ and $[(90_2/\pm60/\pm30)_2]$ laminates the calculated failure strengths agree with the data within 10 percent to 30 percent. The specimen geometry (hole diameter, edge distance, and width) has little effect on the accuracy of the model.

For cross-ply laminates($[0/90]_s$ and $[\pm45]_s$) the difference between the calculated bearing strengths and the data ranges from about 10 to 40 percent. The accuracy is better for smaller holes (10 percent for D= 1/8 in) and decreases as the hole size increases. The differences between the calculated and measured bearing strengths become about 40 percent for 1/2 in diameter holes. In all cases, the calculated values are conservative and underestimate the actual bearing strengths. The reason for the lower accuracy of the model for cross ply laminates is most likely due to the assumption that the shear stress is linearly proportional to the shear strain. Since shear stresses are important in determining the failure strengths of cross ply laminates (Section VII), the use of nonlinear shear stress-

strain relationships should improve the accuracy of the model for such laminates.

The results in Figures 22-29 show that the model predicts the failure mode with good accuracy. Of the 83 specimen configurations tested, the model failed to predict accurately the failure mode only in 9 cases - - these cases being indicated by the letters, T, B, or S, in Figures 22-29. In 3 of those cases where the model gave different failure modes than the data, the data were ambiguous. Failure, in fact, may have occurred by the combination of two different modes.

The results discussed in the foregoing, and represented in Figures 22-29, show that the model provides the failure strengths and failure modes of loaded holes with reasonable accuracy. The accuracy of the present model could be improved further if, instead of the average values of S, $R_t$ and $R_c$, the values corresponding to the specific geometry and laminate configuration were used in the calculations.

It is worthwhile to compare the accuracy of the present model with the accuracy of the models developed by previous investigators. A summary of the accuracies of the various models is presented in Table 5.

The accuracy may depend on the geometry, ply orientation, and material properties. Therefore, the accuracies in Table 5 must be viewed with caution. Nevertheless, the numbers in this provide an estimate of the magnitudes of error of the different models. The present

model appears to be more accurate than any of the other models.

Two points are worth noting: First, the models developed previously apply only to laminates containing a single hole. None of the models except the present one applies to laminates containing two holes. Second, of the existing models, only the present one and the one by Garbo and Ogonowski [6] have been supplemented with "user friendly" computer codes. Therefore, presently, only these two models can be used readily. Furthermore, the Garbo and Ogonowski model yields the failure strength, but does not provide the mode of failure.
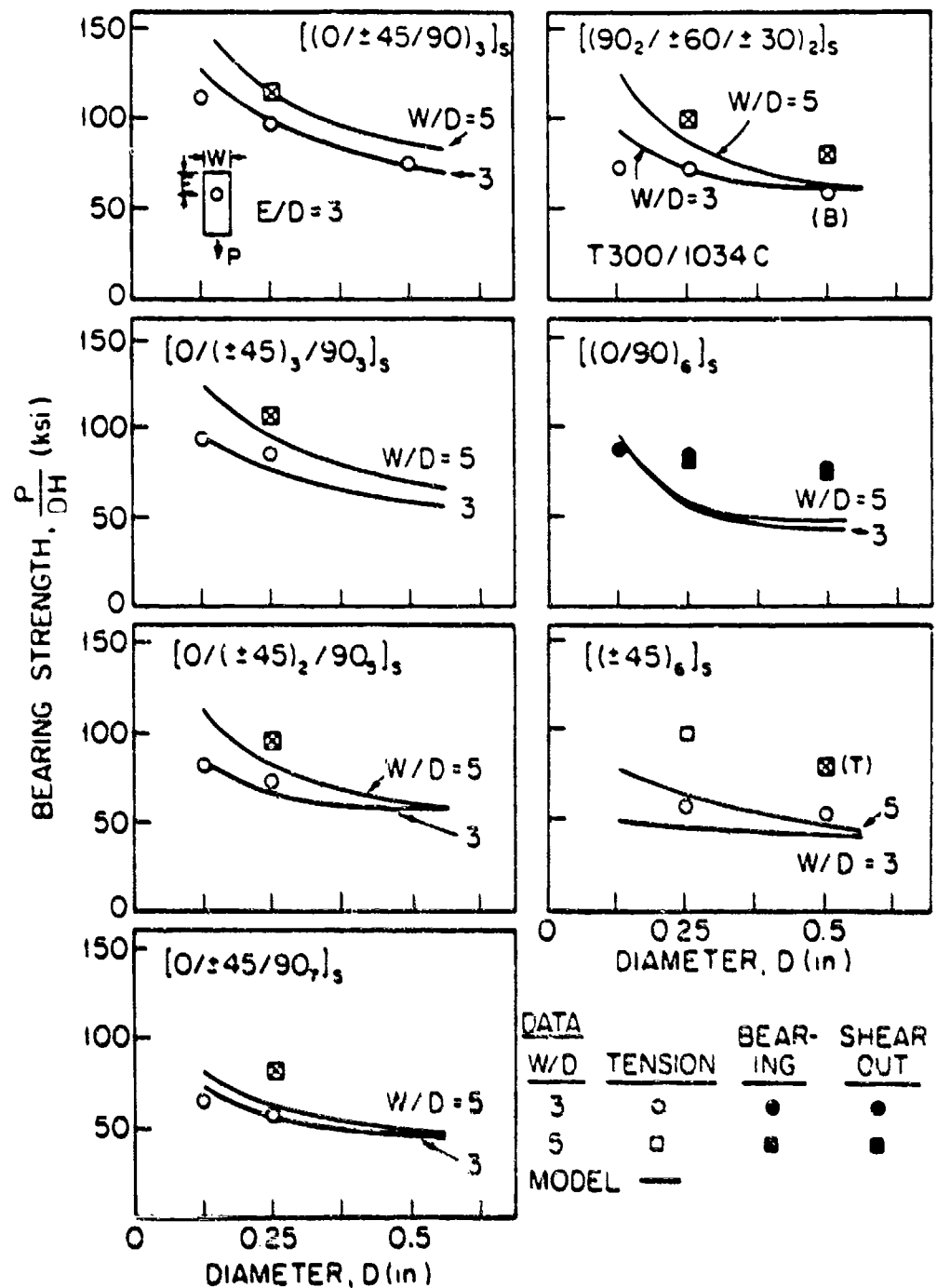
Figure 22. Bearing Strengths of Fiberite T300/1034-C Laminates Containing a Single Loaded Hole. Comparisons Between the Data and the Results of the Model. The Failure Modes Calculated by the Model are the Same as Those of the Data Unless Indicated by a Letter in Parentheses next to the Data Point.
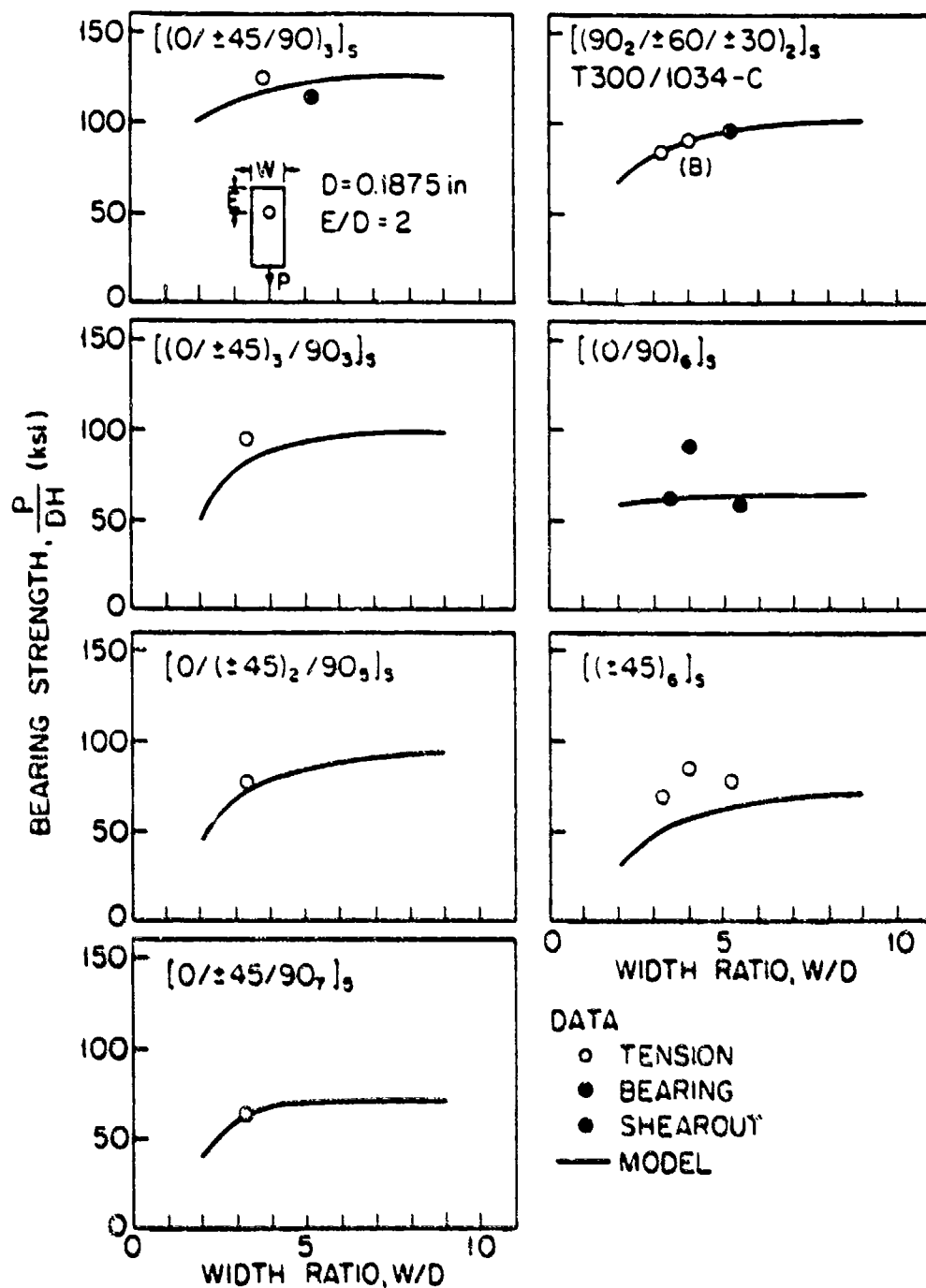
Figure 23. Bearing Strengths of Fiberite T300/1034-C Laminates Containing a Single Loaded Hole. Comparisons Between the Data and the Results of the Modle. The Failure Modes Calculated by the Modle are the Same as Those of the Data Unless Indicated by a Letter in Parentheses next to the Data Point.
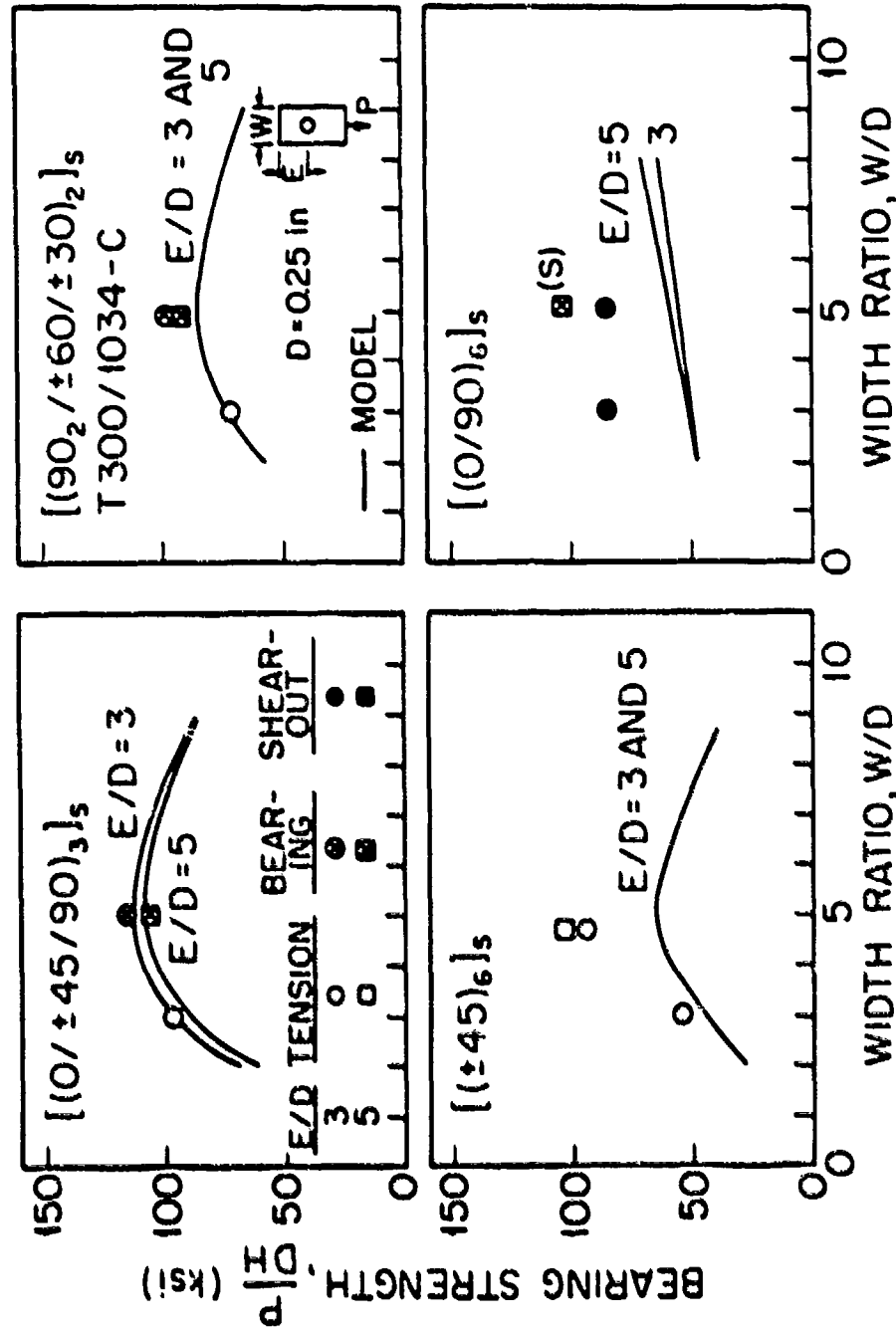
Figure 24. Bearing Strengths of Fiberite T300/1034-C Laminates Containing a Single Loaded Hole. Comparisons Between the Data and the Results of the Model. The Failure Modes Calculated by the Model are the Same as Those of the Data Unless Indicated by a Letter in Parentheses next to the Data Point.
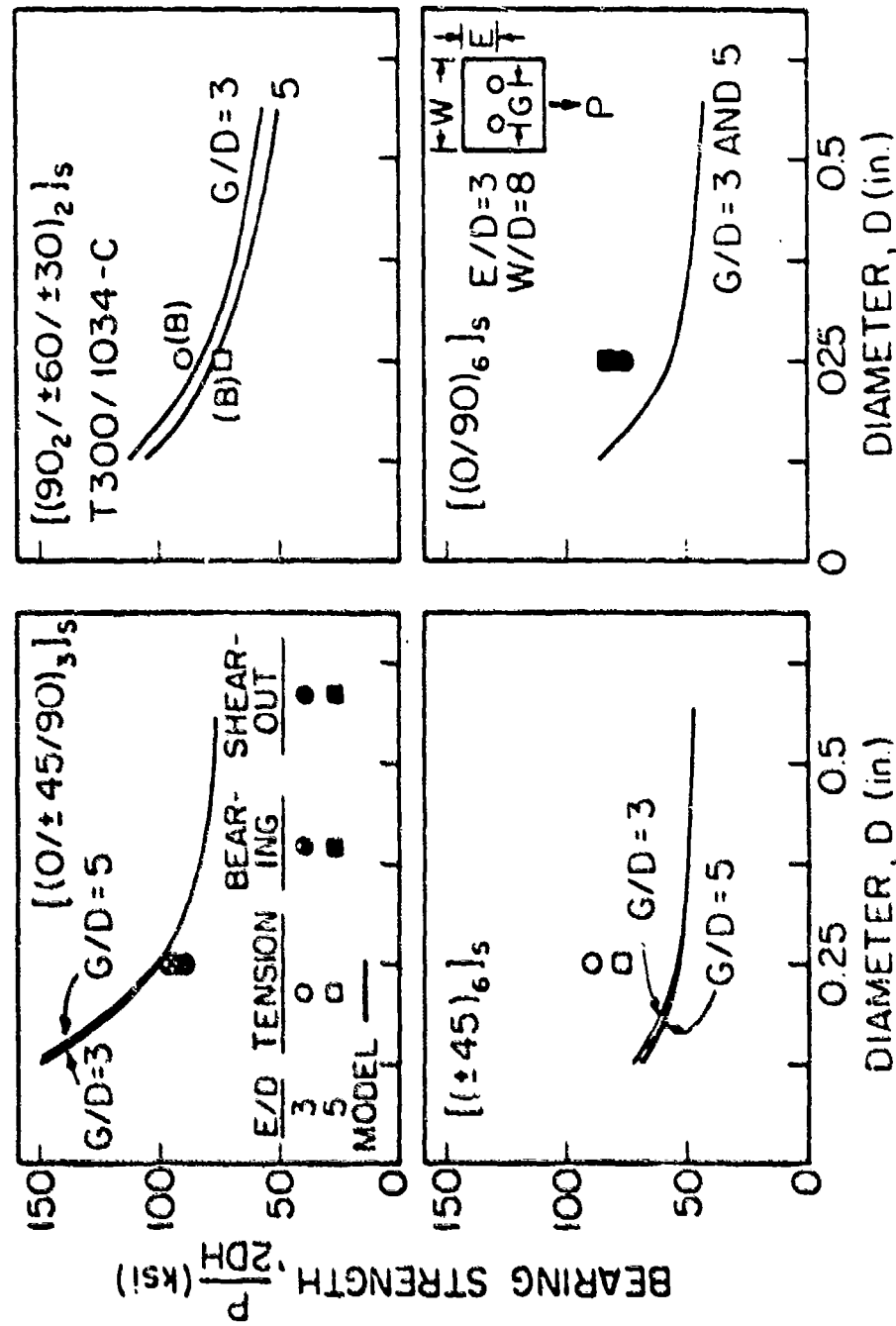
Figure 25. Bearing Strengths of Fiberite T300/1034-C Laminates Containing Two Loaded Holes in Parallel. Comparisons Between the Data and the Results of the Model. The Failure Modes Calculated by the Model are the Same as Those of the Data Unless Indicated by a letter in Parentheses next to the Data Point.
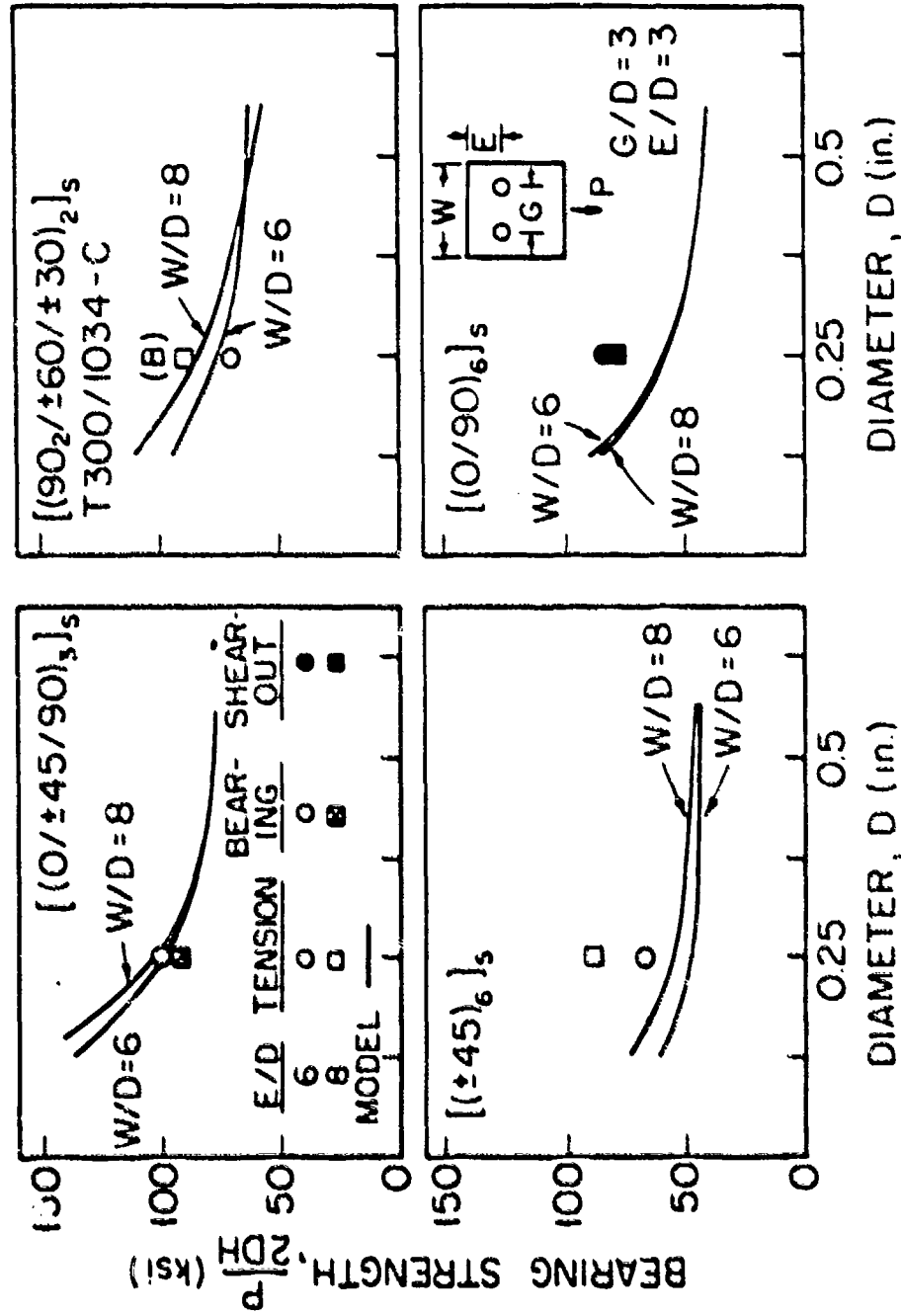
Figure 26. Bearing Strengths of Fiberite T300/1034-C Laminates Containing Two Loaded Holes in Parallel. Comparisons Between the Data and the Results of the Model. The Failure Modes Calculated by the Model are the Same as Those of the Data Unless Indicated by a Letter in Parentheses next to the Data Point.
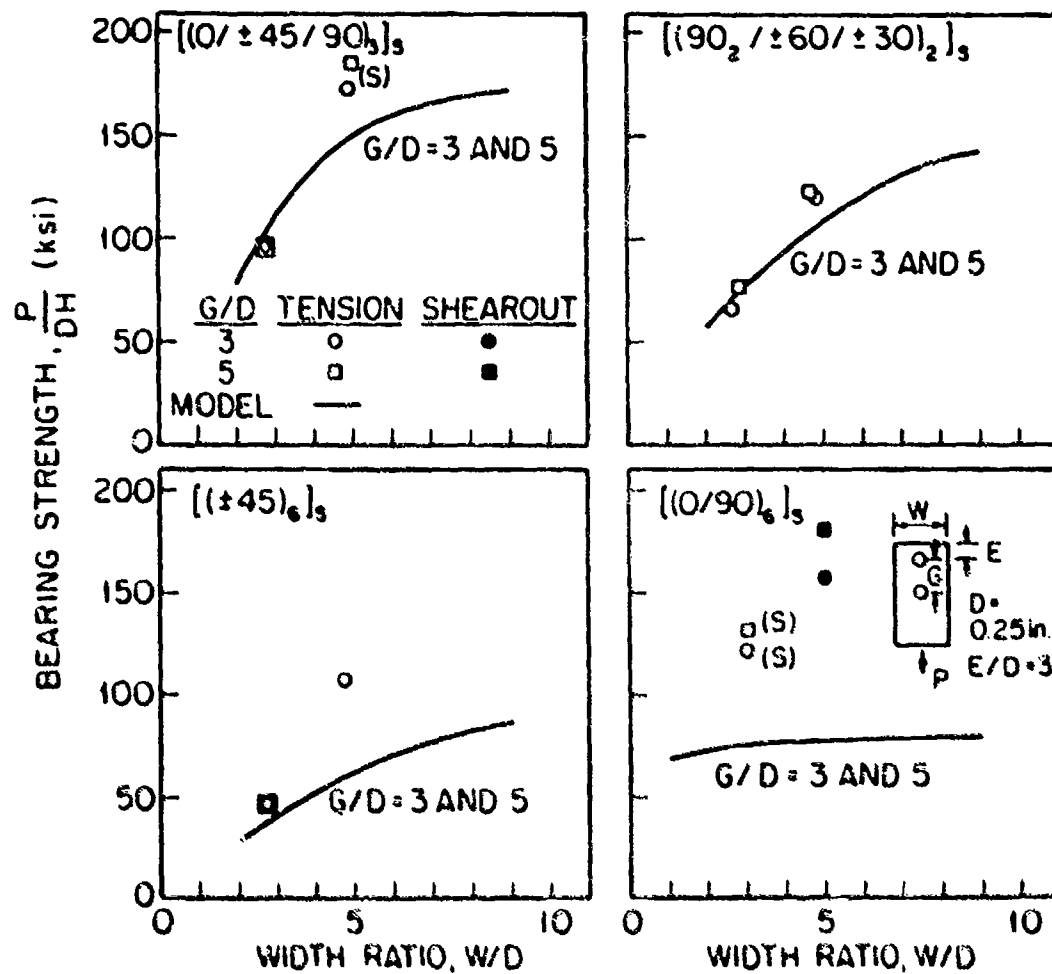
Figure 27. Bearing Strengths of Fiberite T300/1034-C Laminates Containing Two Loaded Holes in Series. Comparisons Between the data and the Results of the Model. The Failure Modes Calculated by the Model are the Same as Those of the Data Unless Indicated by a Letter in Parentheses next to the Data Point.
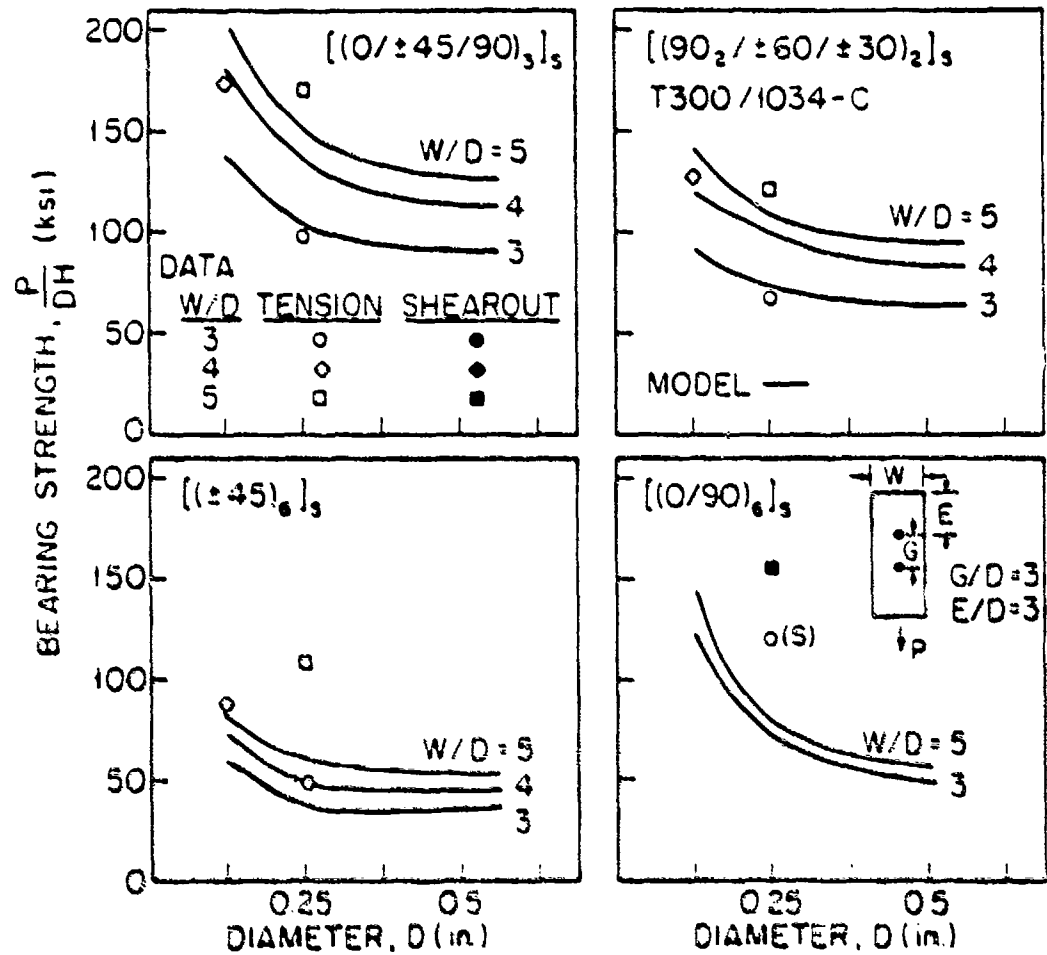
Figure 28. Bearing Strengths of Fiberite T300/1034-C Laminates Containing Two Loaded Holes in Series. Comparisons Between the Data and the Results of the Model. The Failure Modes Calculated by the Model are the Same as Those of the Data Unless Indicated by a Letter in Parentheses next to the Data Point.
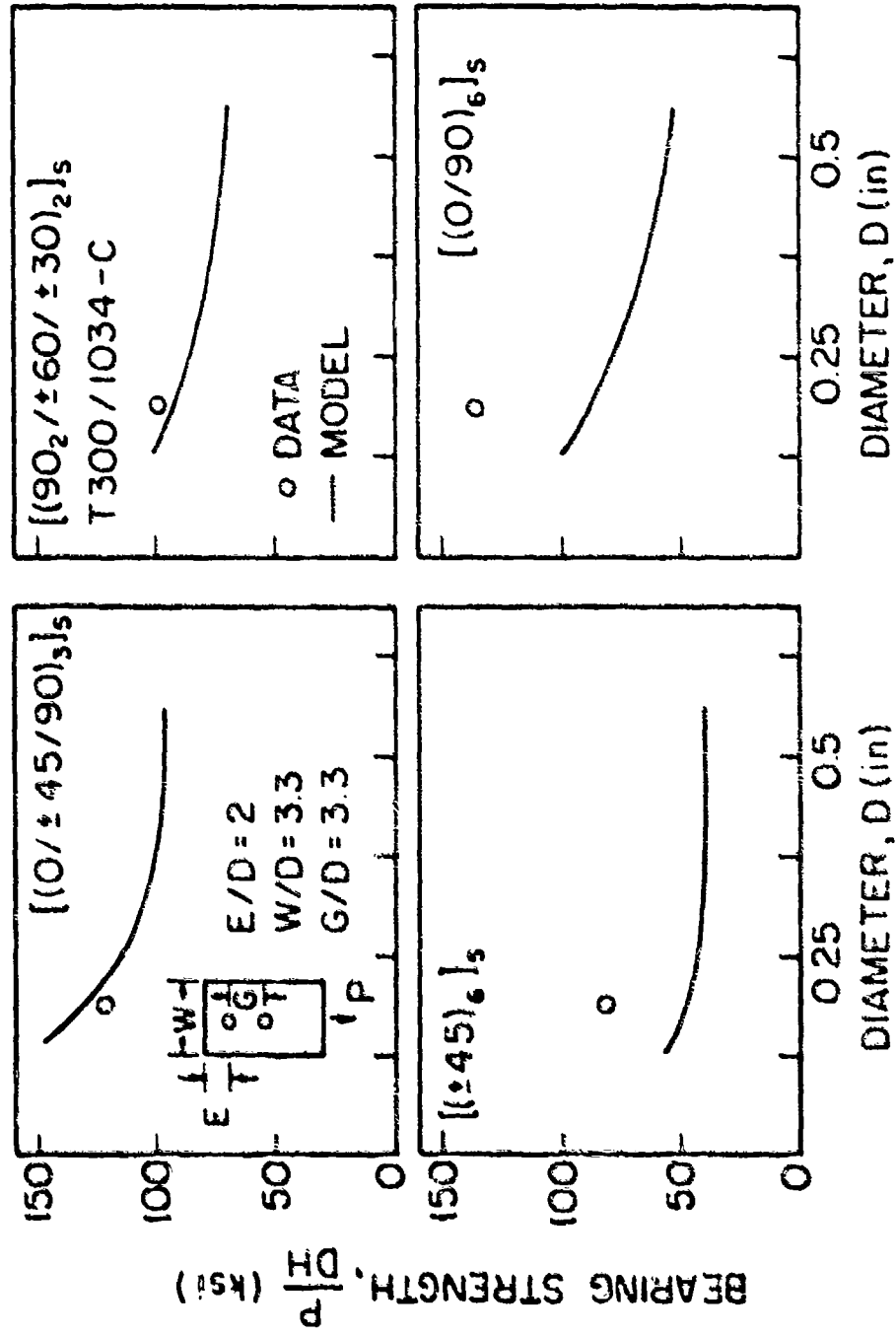
Figure 79. Bearing Strengths of Fiberite T300/1034-C Laminates Containing Two Loaded Holes in Serie. Comparisons Between the Data and the Results of the Model The Failure Modes Calculated by the Model are the Same as Those of the Data.

Table 5 Approximate Differences Between Experimental (P) and Calculated (P_c) Failure Loads of Laminate Containing a Single Loaded Hole. The Numbers Indicate the Maximum Differences (in Percent) for the Indicated Hole Diameters and Ply Orientation.

| Investigator | Diameter | $[0/\pm45/90]_s$ 10-20 | $[\pm30/\pm60/90]_s$ 10-30 | $[\pm45/90]_s$ | $[0/\pm45]_s$ | $[0/90]_s$ 10-40 | $[\pm45]_s$ 10-40 |
|---|---|---|---|---|---|---|---|
| Present T300/1034-C | 1/8-1/2 | 10-20 | 10-30 | | | 10-40 | 10-40 |
| Agarwal[4] SP286 | 1/16 | 10 | | | 20 | 50 | 50 |
| Collings[5] HTS/914,XAS/914 HTS/MC3501 | 1/4 | 20 | | 20 | | 20 | |
| Garbo[6] AS/3501-6 | 1/4 | 40 | | | | | |
| Hart-Smith[42] T300/5208 | 1/4 | 10 | | | | | |
| Pipes[7,8] AS/3501-6 | 1/8,1/4,3/8 | 20 | | | | | |
| Soni[5] AS/3501-6, T300/5208 | | 10 | | 50 | | | |
| Waszczak[1] GR/EP,B/EP | | 50 | | 50 | | 50 | 50 |

# SECTION IX

## DESIGN CONSIDERATIONS

As illustrated by the sample computer input-output in Appendix E, the model, together with the computer code, can readily be used to calculate the failure strengths and failure modes of laminates containing a single pin-loaded hole, two pin-loaded holes in parallel, or two pin-loaded holes in series. The model can also be used to design joints containing many pin loaded holes. In joint design, it is desired to determine the number of holes, the hole diameter, and the hole positions which result in the maximum failure load $P_M$ and the maximum failure load per unit weight $P^*_M$. The failure load per unit weight is defined as

$$P^* = P/w \tag{59}$$

where P is the failure load, and w is the combined weight of the composite $w_c$ and the pin $w_s$

$$w = w_c + w_s \tag{60}$$

In this section, procedures suitable for calculating $P_M$ and $P^*_M$ are illustrated via two sample problems. In these problems, the failure load of 24-ply (thickness H=0.125 in) $[(0/\pm45/90)_3]_s$ Fiberite T300/1034-C graphite-epoxy composites are determined. The material properties used in

the calculations are listed in Table 1. The density of the composite is $\rho_c = 0.00194$ lbm/in$^3$. The pin or pins are assumed to be 3/4 in long and to be made of steel (density $\rho_s = 0.0093$ lbm/in$^3$).

The calculation procedures are presented in Section 9.3 for joints containing one or two holes, and in Section 9.4 for joints containing three or more holes. First, however, interferences between two adjacent holes, between the edge and an adjacent hole, and between the side and an adjacent hole are discussed.

## 9.1) Interaction Coefficients

It is desired to know under what conditions, if any, the proximity of two holes, or the proximity of a hole to the edge or to the side of the laminate, affects the failure load. The interaction between two holes, between a hole and the edge, and between a hole and the side, can best be evaluated by the use of interaction coefficients.

Two Holes in Parallel     The parallel hole interaction coefficient $g_H$ is defined as

$$g_H = P_S/(P_H/2) \tag{61}$$

Where $P_S$ is the failure load of a $G_H$ wide laminate containing a single hole, and $P_H$ is the failure load of a $2G_H$ wide laminate containing two loaded holes separated by a

distance $G_H$ (Figure 30). When $G_H$ becomes large, the
interaction between two holes becomes small $(P_H/2 \rightarrow P_S)$ and
the interaction coefficient approaches unity $(g_H \rightarrow 1)$.

<u>Two Holes in Series</u>    The series hole interaction
coefficient $g_V$ is defined as

$$g_V = P_V/P_T \qquad (62)$$

where $P_V$ is the failure load of a laminate (width W)
containing two loaded holes separated by a distance $G_V$. $P_T$
is the failure load of a laminate with the same width
containing two holes; one located at a distance E from the
edge, and the other located at the center of the laminate
(Figure 31). When the hole distance increases, the
influence of one hole on the other becomes small; the
failure load $P_V$ approaches $P_T (P_V \rightarrow P_T)$ and $g_V$ approaches
unity $(g_V \rightarrow 1)$.

<u>Edge Interaction</u>    The edge interaction coefficient $g_E$ is
defined as

$$g_E = P_S/P_C \qquad (63)$$

where $P_S$ is the failure load of laminates (width W) with a
single loaded hole at distance E from the edge. $P_C$ is the
failure load of a laminate of width W with a hole in the
center (Figure 32). The influence of the edge on the

failure load becomes smaller as the edge distance increases. When the hole is moved to the center ($E=L/2$), $P_S$ becomes $P_C$ and the interaction coefficient becomes unity ($g_E \rightarrow 1$).

Side Interaction Coefficient    The side interaction coefficient $g_S$ is defined as

$$g_S = P_H/P_G \tag{64}$$

where $P_H$ is the failure load of a laminate (width W) containing two loaded holes separated by a distance $W/2$. $P_G$ is the failure load of a laminate with the same width containing two loaded holes separated by a distance $G_H$ ($G_H \geq W/2$, Figure 33). As the distance Q between the side and the hole increases $P_G \rightarrow P_H$ and the interaction coefficient $g_S$ approaches unity.

9.2) Numerical values of the Interaction Coefficients

In order to illustrate the trend in the interaction coefficients these coefficients were calculated for Fiberite T300/1034-C graphite-epoxy composite laminates with ply orientations of $[(0/\pm45/90)_3)]_s$ and $[(0_2/\pm45)_3]_s$. The results, obtained using the computer code, are presented in Figures 30-33. The most significant feature of these results is that the failure load is not affected significantly

a) by the proximity of two holes in parallel when the distance between two holes is larger than 3D

b) by the proximity of two holes in series when the distance between two holes is larger than 2D

c) by the edge when the distance between the edge and the hole is greater than 3D.

d) by the proximity of side when the distance between the hole and the side is larger than 2D

Mathematically, these conditions can be expressed as

$$\left.\begin{array}{llll} g_H \rightarrow 1 & P_H \rightarrow 2P_S & \text{as } G_H/D \geq 3 \\ g_V \rightarrow 1 & P_V \rightarrow P_T & \text{as } G_V/D \geq 2 \\ g_E \rightarrow 1 & P_S \rightarrow P_C & \text{as } E/D \geq 3 \\ g_S \rightarrow 1 & P_G \rightarrow P_H & \text{as } Q/D \geq 2 \end{array}\right\} \begin{array}{l} \text{for } [(0/\pm 45/90)]_s \\ \\ [(0_2/\pm 45)_3]_s \end{array} \qquad (65)$$

It is emphasized that the conditions expressed by the above equations (eq. 65) may not apply for every ply orientation. The conditions at which the different coefficients become unity must be evaluated separately for each laminate lay up.

84
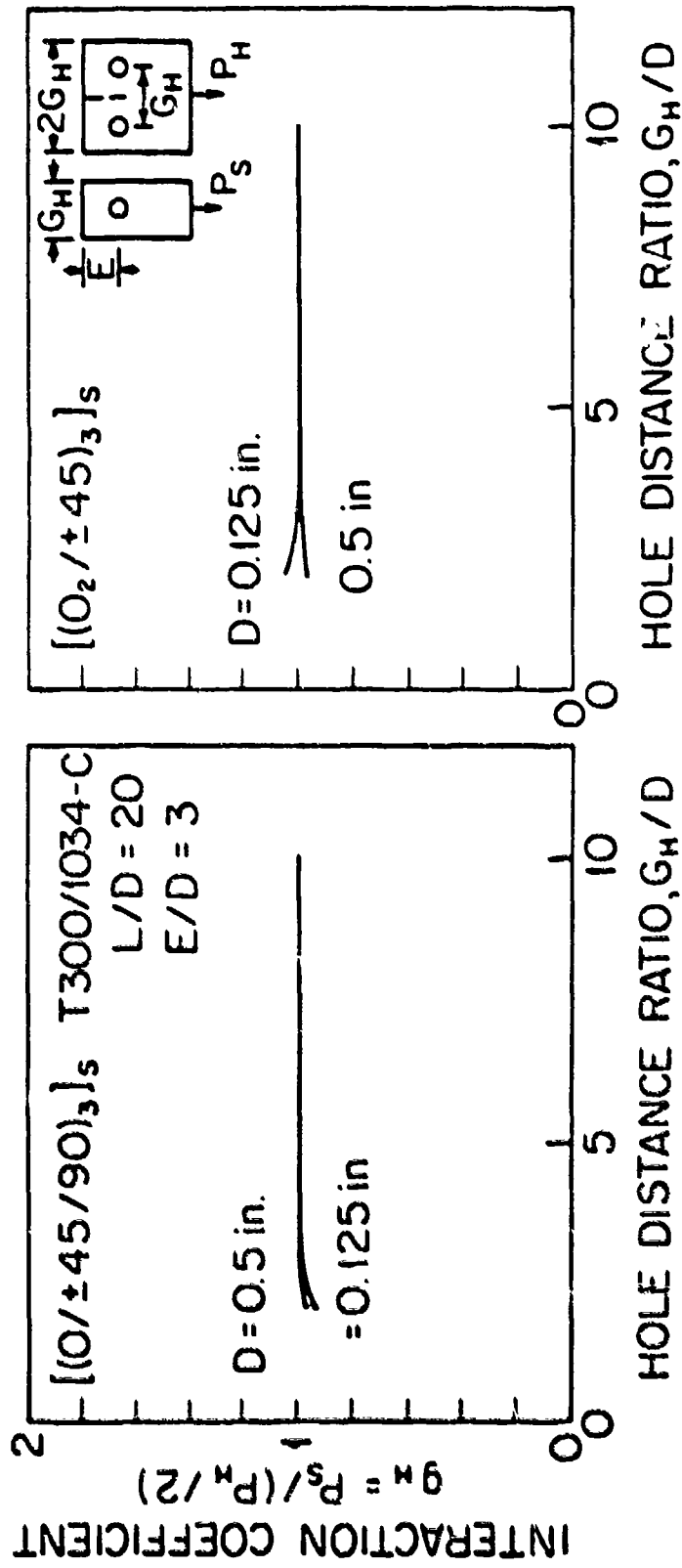


Figure 30. Interaction Coefficient for Two Holes in Parallel. Results of the Model.
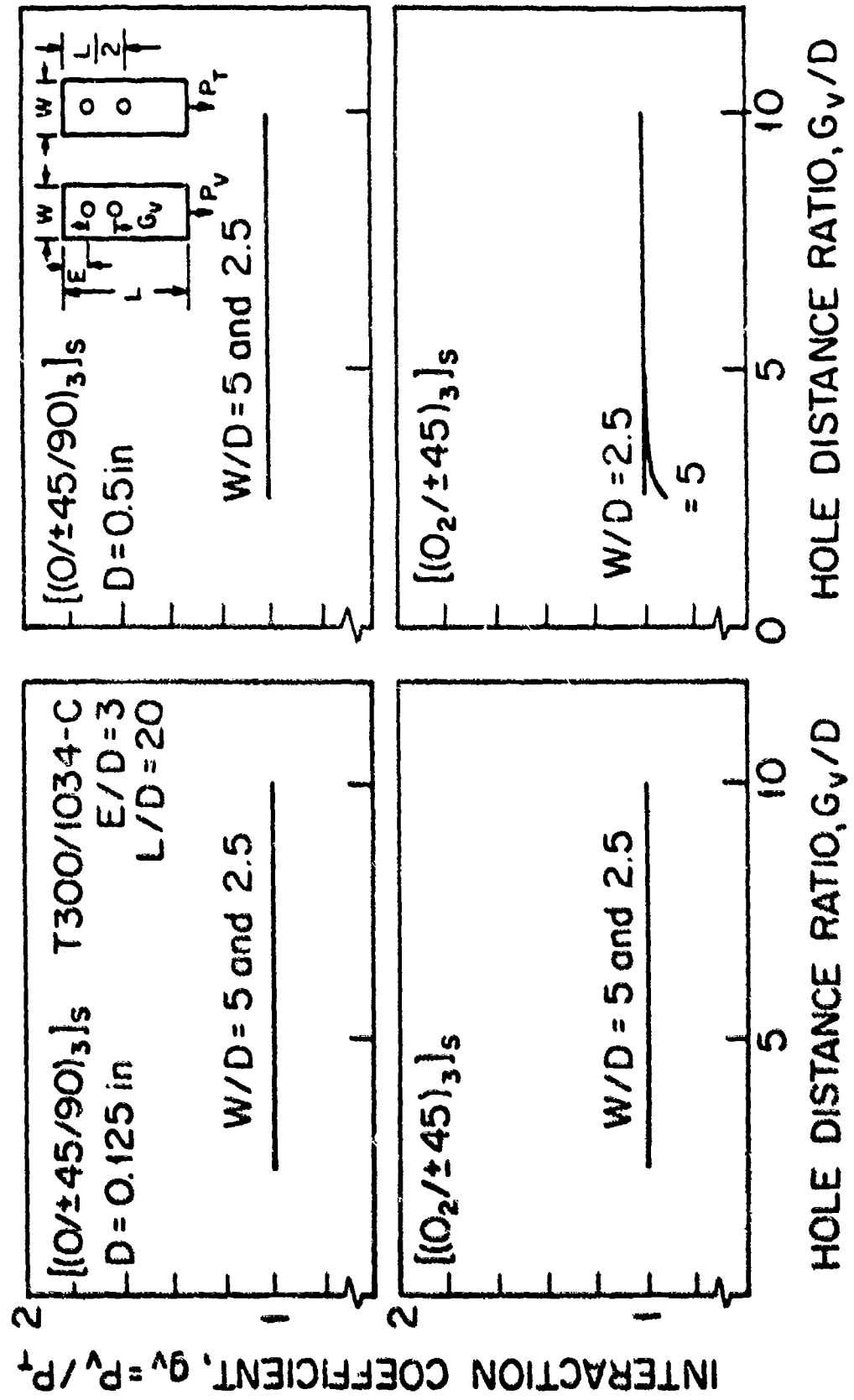
Figure 31.   Interaction Coefficient for Two Holes in Series.   Results of the Model.
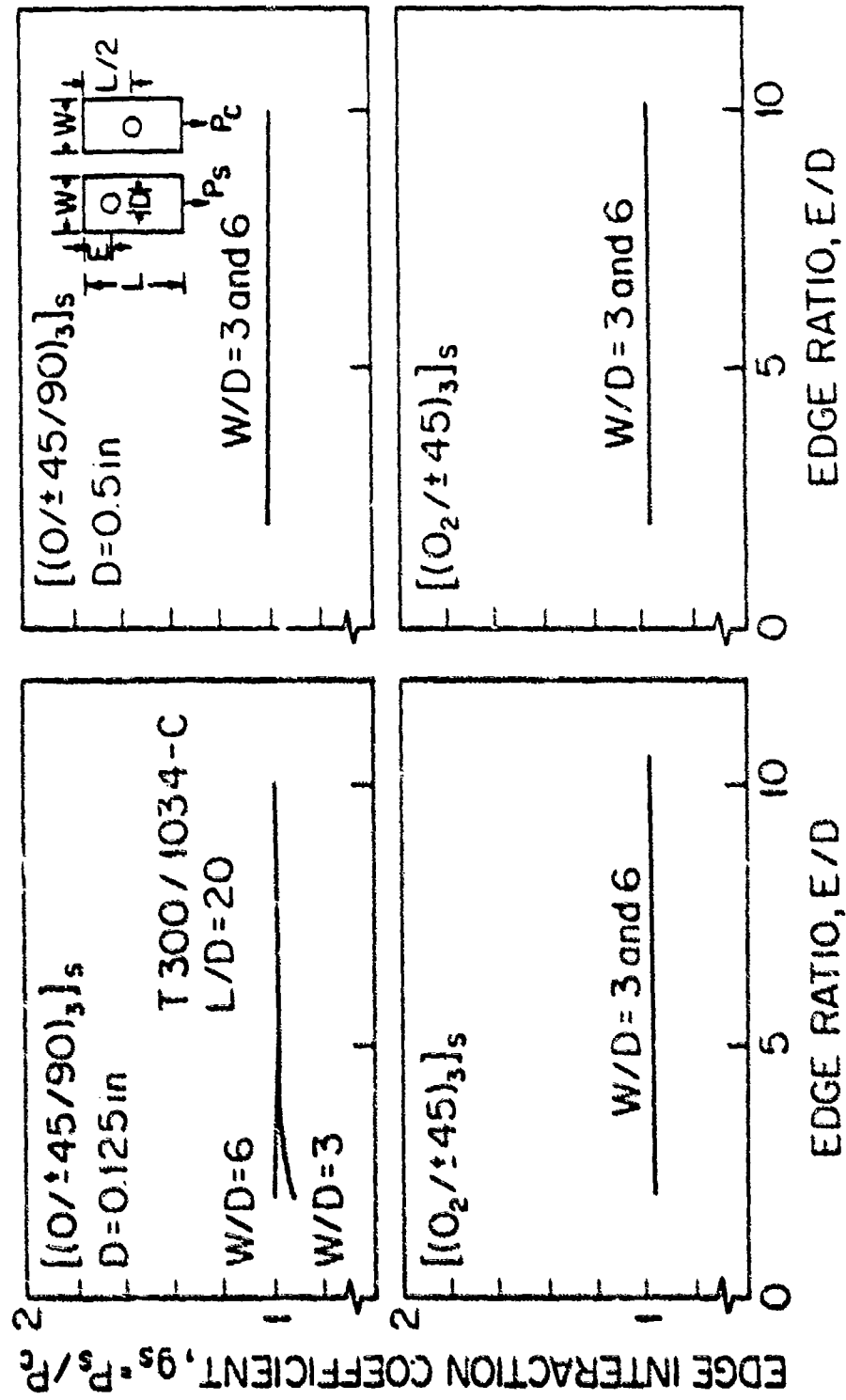
Figure 12.    Edge Interaction Coefficient. Results of the Model.
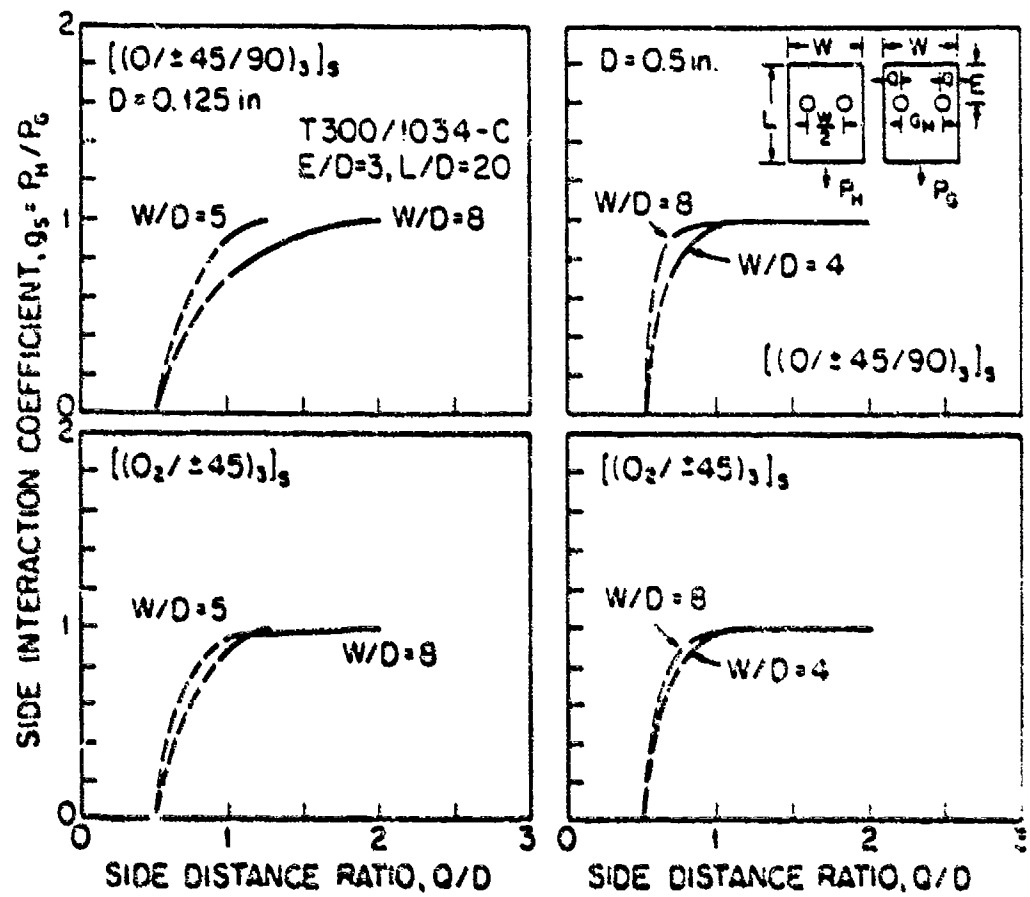
Figure 33.    Side Interaction Coefficient. Results of the Model.

### 9.3) <u>Laminates with One or Two Holes</u>

In this subsection, a procedure is described which can be used to size a laminate containing either one or two pin-loaded holes.

We consider a laminate of known width (W=1 in), length (L=8 in) and thickness (H= 0.125 in ). The laminate may contain either one pin-loaded hole or two pin-loaded holes in parallel or in series, as illustrated in Figure 34.

It is desired to find the number of holes ( one or two holes), the hole diameter D, the edge distance E, and the distance between two holes G, which result in the maximum failure load $P_M$ and in the maximum failure load per unit weight $P^*_M$.

The calculation proceeds along the following major steps:

a) Using the computer code, the failure loads of
   a laminate containing a single-loaded hole are
   calculated for different hole diameters D and
   for different edge distance ratios E/D.
   The failure load is plotted versus the edge ratio
   E/D (Figure 35). The desired edge ratio
   (E/D) is selected.

Here, the edge ratio E/D=3 was selected because the failure load reaches a maximum at the edge ratio of about 3 and remains nearly constant at higher edge ratios. This
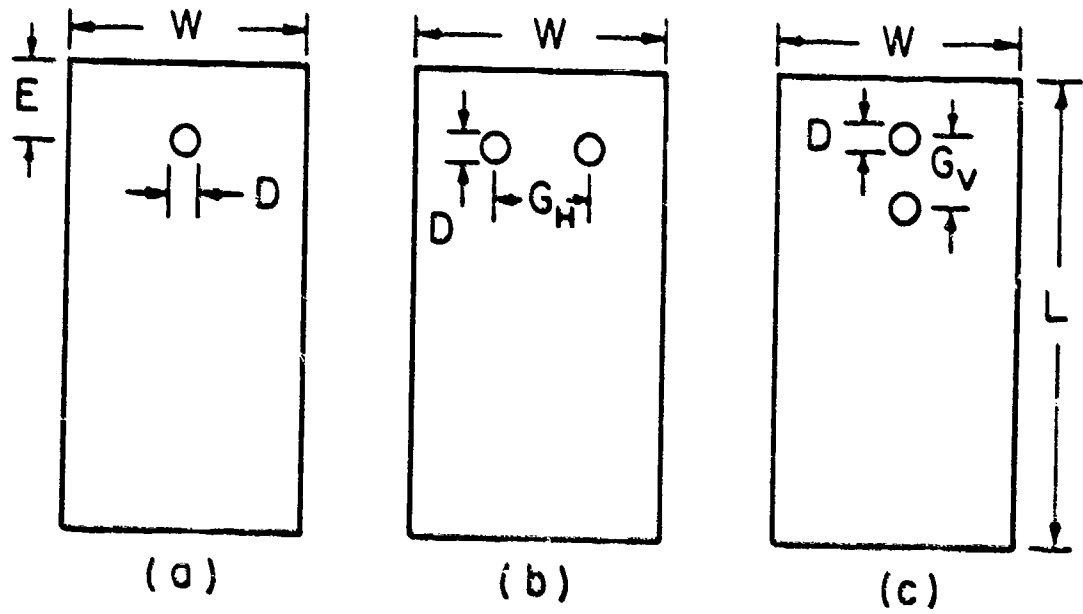
Figure 34. Description of Problem Used in Desiging Laminates
With a) Single Pin-Loaded Hole, b) Two Pin-
Loaded Holes in Parallel, c) Two Pin-Loaded
Holes in Series.
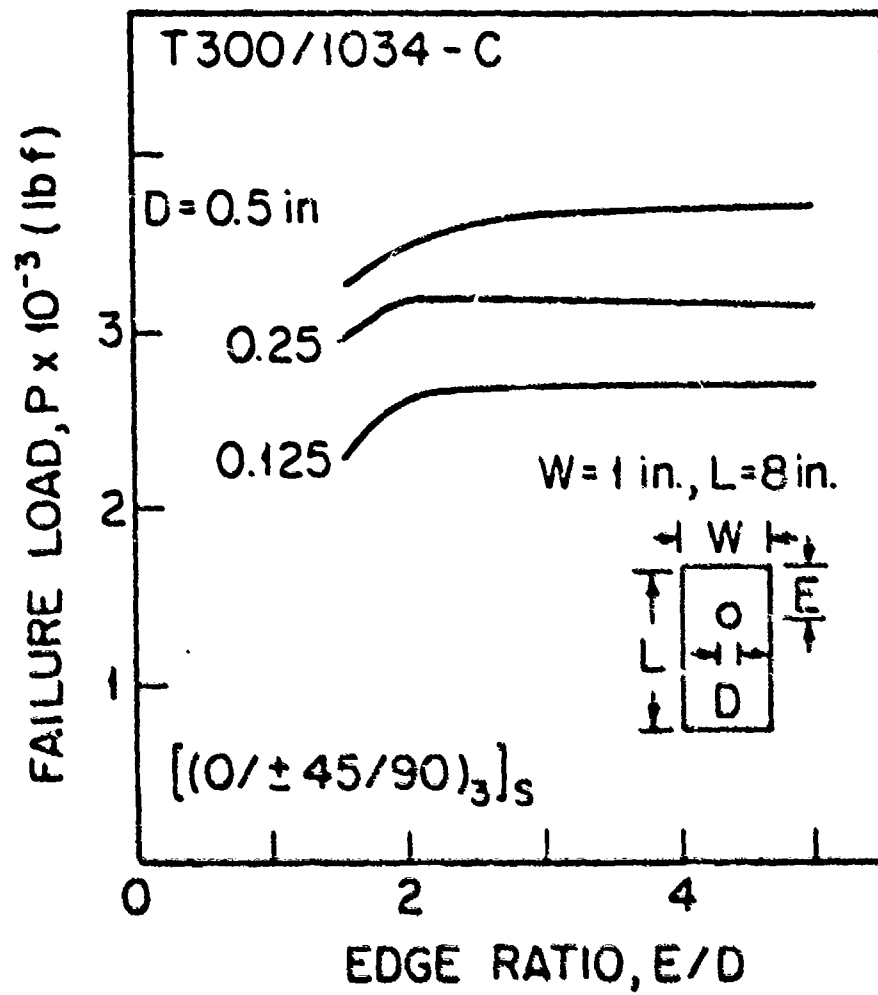
Figure 35.  Failure Load as a Function of Edge Ratio for
Laminates Containing a Single Pin-Loaded Holes.
Results of the Model.

value (E/D) will also be used for joints containing two
loaded holes in parallel and two holes in series. The
reasons for this choice of E/D are as follows:  1) For
parallel holes the interaction between two holes has almost
no effect on the failure load ($g_H \to 1$ and $P_H/2 \to P_S$,
Section 9.2 ). Hence, when $G_H/D>3$ (as is the case in the
present problem), two parallel holes can be treated as two
independent holes.  2) For two holes in series, the
interaction between the holes is unimportant, when $G_V/D>3$
($g_V \to 1$ and $P_V \to P_C$, Section 9.2). Two holes can be
considered as two independent holes sharing part of the
total load.  Hence the value of E/D=3 is a suitable choice
for the present problem when $G_V/D>3$.

b) Using the computer code, the failure loads are
   calculated for different hole diameters, and
   for different hole separations G for two holes in
   parallel and for two holes in series.  The failure
   loads are plotted as functions of the hole distance
   ratio G/D (Figure 36, top).  From these plots,
   the maximum failure load $P_M$ can be obtained.
For the problem under consideration, the maximum failure
load is 5000 lb.  This load is achieved by two 0.125in pins
in parallel separated by a distance $G_H=0.5$ in ($G_H/D = 4$).

c) From the known values of the failure load P,
   the failure load per unit weight $P^*$ is
   calculated using the expression

$$P^* = P/[\rho_c WHL + a\ (\pi D^2/4)(\rho_s L_s - \rho_c H)] \tag{66}$$

where $L_s$ is the length of the pin. The
parameter a=1 for a single hole, a=2 for
two holes.  The failure load per unit weight
is plotted as a function of G/D
(Figure 36, bottom).

For the present problem, the maximum failure load per unit
weight $P^*_M$ is 8000 lbf/lbf and occurs with two 0.125-in
diameter pins separated by a horizontal distance $G_H$ = 0.5 in
$(G_H/D = 4)$.

## 9.4) Laminates with Multiple Holes

This problem is concerned with laminates containing
several pin-loaded  holes spaced evenly, either in a single
row or in two parallel rows, as illustrated in Figure 37.

The number of holes in the laminate with a single row of
holes, or the number of columns in the laminates with two
rows of holes is

$$N_o = W/G_H \tag{67}$$

It is desired to determine the number of holes $N_o$, the
hole size D, the positions of the holes $G_H$ and $G_V$, and the
edge distance E, which result in the maximum failure load.
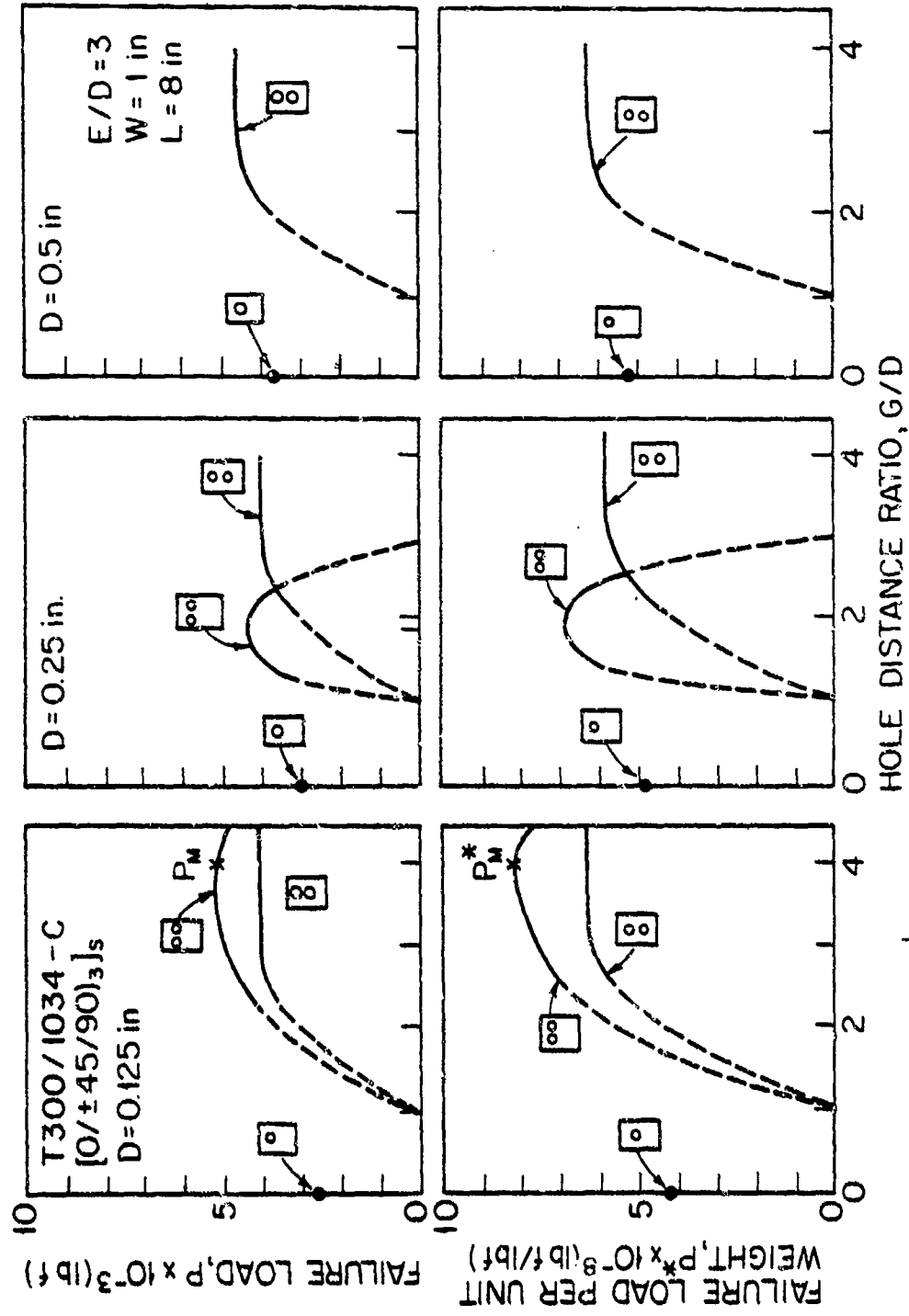
Figure 36. Failure Load (Top) and Failure Load Per Unit Weight (Bottom) of Laminates Containing a Single Pin-Loaded Hole, Two Pin-Loaded Holes in Parallel and Two Pin-Loaded Holes in Series. Results of the Model.
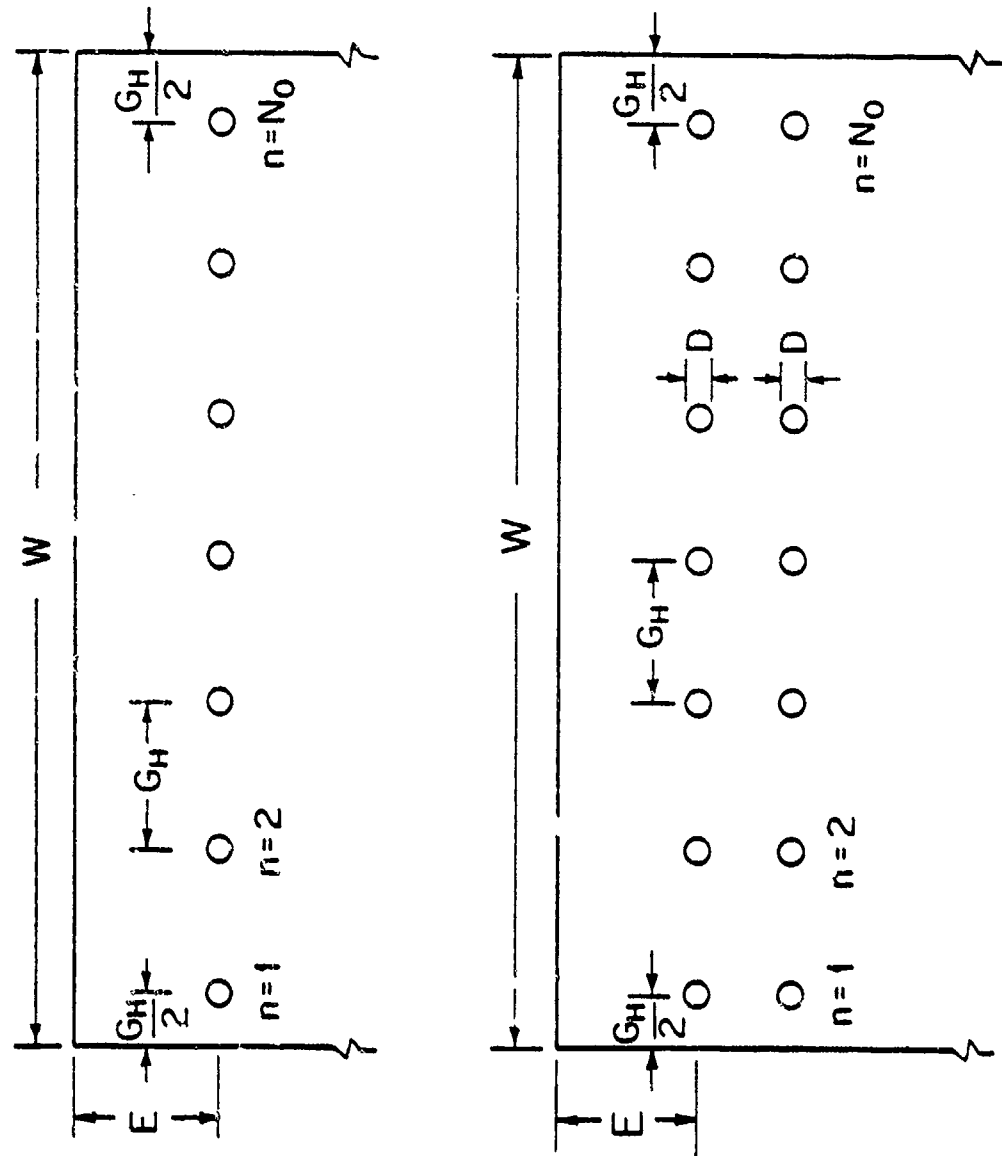
Figure 37. Geometry of Single Row of Holes (Top) and Two Rows of Holes (Bottom).

The model developed in this investigation can be applied only to laminates containing either a single pin-loaded hole, or two pin-loaded holes in parallel or in series. Therefore, the model can not be used directly to calculate the failure load of laminate containing several holes. The failure loads of such laminates can still be estimated with the use of the model by the procedure described below.

a) The interaction coefficients $g_E$ and $g_V$ are calculated and plotted in the manner described in Section 9.1.

b) The ratios $E/D$ and $G_V/D$ are selected, which correspond to the conditions $g_E \rightarrow 1$ and $g_V \rightarrow 1$. In this investigation, the values of both $E/D$ and $G_V/D$ were selected to be 3 because both $g_E$ and $g_V$ reach unity at this ratio. This $E/D$ ratio is used for a single row of holes. This is also a reasonable choice for two rows of holes, because the first row of holes acts independently of second rows of holes, to a very large degree.

c) Values are assumed for the number of holes and the hole diameter. The distance $G_H$ is calculated form

$$G_H = W/N_o \tag{68}$$

d) Using the computer code, the failure load is calculated
   for a $2G_H$ wide laminate containing two loaded holes in
   parallel $P_H$, and for a $G_H$ wide laminate containing two
   loaded holes in series $P_V$. The interaction parameter $g_H$
   is then calculated for the geometry under consideration,
   according to the method given in Section 9.2.

e) The failure load is approximated by the expression

$$P = P_{N_o-2} + 2\ P_{side} \tag{69}$$

where $P_{N_o-2}$ is the load carried by the second (n=2) through
the next to last $(n=N_o-1)$ pins, and $P_{side}$ is the load
carried by the first (n=1) and last $(n=N_o)$ pins. Thus, the
failure load of a laminate containing one or two rows of
holes is

$$P_{r1} = ((N_o-2)/2)g_H P_H + g_S P_H \qquad \text{(one row)} \tag{70}$$
$$P_{r2} = (N_o-2)g_H^2 P_V + 2g_H g_S P_V \qquad \text{(two rows)} \tag{71}$$

If $Q = G_H/2$ then $g_S$ is equal to unity. This is the case
in the present problem. Accordingly,

$$P_{r1} = ((N_o-2)/2)g_H P_H + P_H \tag{72}$$

$$P_{r2} = N_o-2)g_H^2 P_V + 2g_H P_V \tag{73}$$

f) The failure load per unit weight $P^*$ is calculated

$$P^*_{r1,r2} = P_{r1,r2}/[\rho_C WHL + aN_o(\pi D^2/4)(\rho_S L_S - \rho_C H)] \qquad (74)$$

where the subscripts r1 and r2 refer to one row or two rows of holes, respectively.

g) The calculations are repeated for different values of $N_o$ and D. The failure load $P_{r1,r2}$ and the failure load per unit weight $P^*_{r1,r2}$ are plotted as functions of $N_o$. From these figures, the maximum failure load $F_M$ and the maximum failure load per unit weight $P^*_M$ are determined.

In the present problem a 4 in wide and 10 in long composite laminate was considered. The ply orientation is $[(0/\pm 45/\pm 90)_3]_S$. The material properties are listed in Table 3. The procedures gave the maximum failure load $P_M$ = 23400 lbf when there are twelve 0.125 in diameter holes arranged in two rows of holes (Figure 38). The maximum failure load per unit weight ($P^*_M$ = 67000 lbf/lbf) is achieved with twelve 0.125 in diameter holes in a single row (Figure 38).

## 9.5) Failure Mode

The results generated by the computer code also show the modes of the failure. The changes in the modes of failure with the number of holes $N_o$ are illustrated in Figure 39. In the present sample problem, at the condition of the

maximum failure load ($N_O$=12) the failure mode is in tension. Failure in such mode often happens quite suddenly. In some situations it might be preferable to choose a design in which failure occurs by a less sudden failure mode. For example, failure would have occurred in bearing mode if, in the present problem, a hole diameter of 0.125 in were chosen, and the number of holes were taken to be $N_O$=6. However, this would have resulted in a 30 percent to 40 percent reduction in the failure load.
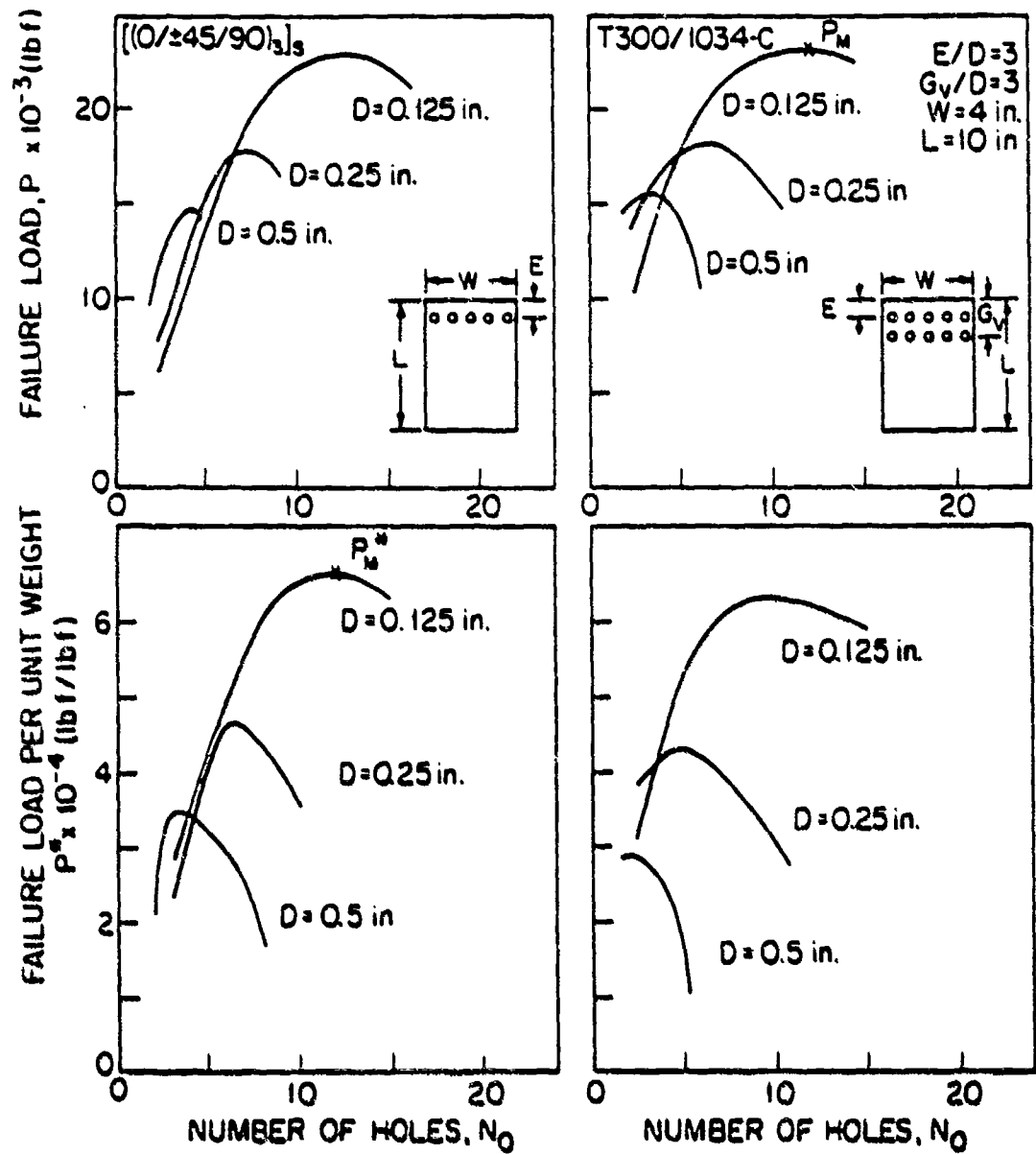
Figure 38.    Failure Load (Top) and Failure Load Per Unit
Weight (Bottom) of Laminates Containing One Row
(Left) and Two Rows (Right) of Pin-Loaded Holes.
Results of the Model.
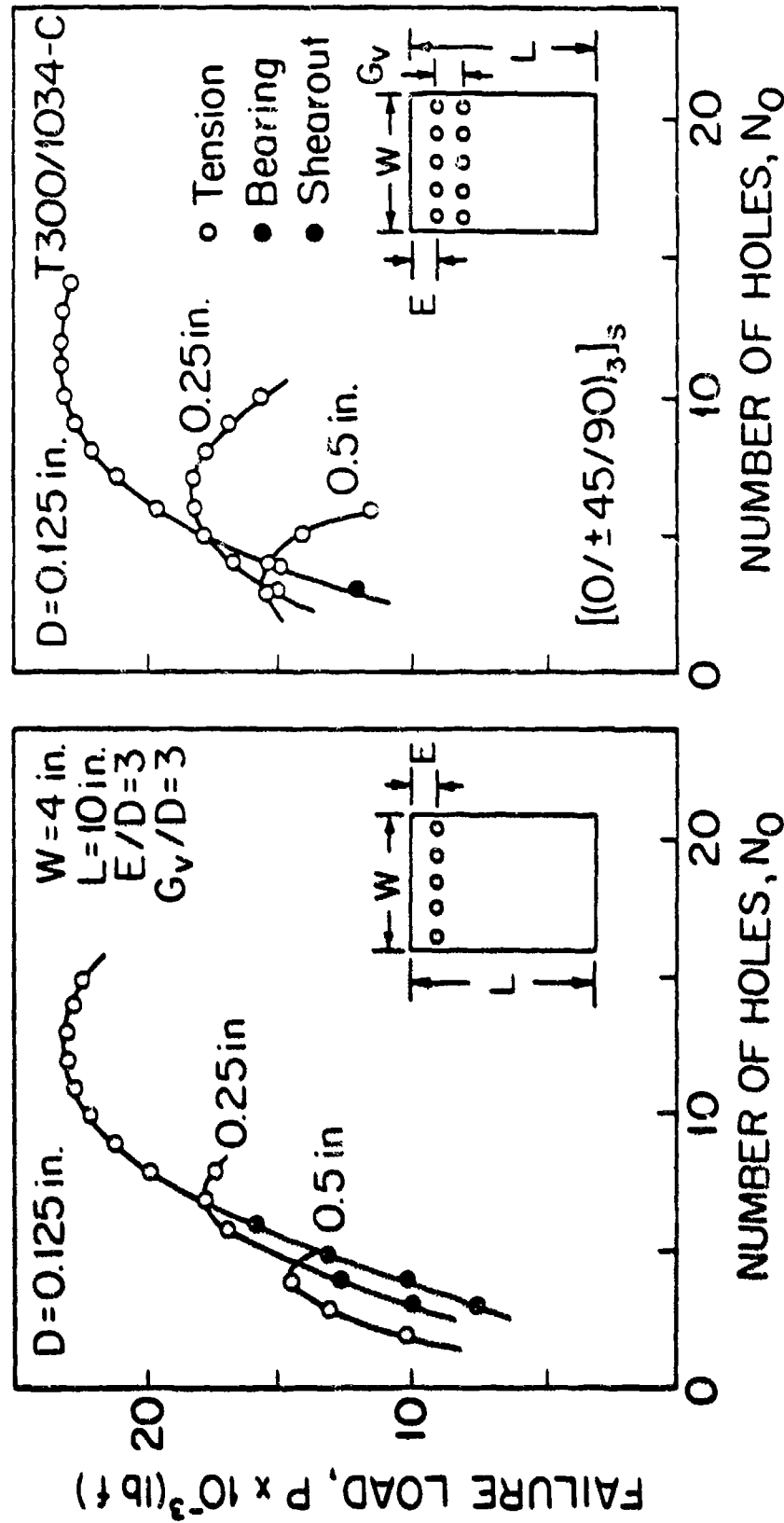
Figure 39. Failure Modes of Single Row (Left) and Two Rows (Right) of Pin-Loaded Holes. Results of the Model.

# SECTION X

## SUMMARY AND CONCLUSIONS

The following major tasks were completed during the course of this investigation:

a)  A model and a computer code were developed which can be used in the design of mechanically-fastened composite joints involving fiber reinforced laminates. The model can be used to determine the failure loads and failure modes of laminates containing a single pin-loaded hole, two pin-loaded holes in parallel, and two pin-loaded holes in series.

b)  Experimental procedures were developed to determine the characteristic lengths.

c)  Tests were performed to determine the values of the rail-shear strength and the characteristic lengths of Fiberite T300/1034-C composites, and to evaluate the effects of geometry and laminate lay up on these parameters.

d)  A series of tests was performed measuring the failure strengths and failure modes of Fiberite T300/1034-C laminates containing a single-pin loaded hole, two pin-loaded holes in parallel, and two pin-loaded holes in series.

e) Comparisons were made between the data and the results of
   the model. Good agreements were found between the
   analytical and the experimental results.

f) Procedures were developed for the design of composite
   laminates containing one, two, or more pin-loaded holes.

   The model was developed on the basis of the following
assumptions: a) classical, two-dimensional laminate plate
theory, and b) linear relationship between the stresses and
strains. Good agreements between the results of the model
and the data suggest that these assumptions are reasonable
for a wide range of problems. Three dimensional stress
distributions and nonlinear stress-strain relationships
could be incorporated into the model in the future.

# REFERENCES

1. J.P. Waszczak and T.A. Cruse, "Failure Mode and Strength Predictions of Anisotropic Bolt Bearing Specimens," J. of Composite Materials, Vol. 5, 1971, pp. 421-425.

2. D.W. Oplinger and D.R. Gandhi, "Stresses in Mechanically Fastened Orthotropic Laminates," Proceedings of the 2nd Conference on Fibrous Composites in Flight Vehicle Design, May 1974, pp.813-834.

3. D.W. Oplinger and D.R. Gandhi, "Analytical Studies of Structural Performance in Mechanically Fastened Fiber-Reinforced Plates," in Proceedings of the Army Symposium on Solid Mechanics, 1974: The Role of Mechanics in Design-Structural Joints, Army Materials and Mechanics Research Center, 1974, AMMRC MS 74-8, pp.211-242.

4. B.L. Agarwal, "Static Strength Prediction of Bolted Joint in Composite Material," AIAA Journal, Vol. 18, 1980, pp.1345-1375.

5. S.R. Soni, "Failure Analysis of Composite Laminates with a Fastener Hole,"J. of Composite Materials, 1981, pp. 145-164.

6. S.P. Garbo and J.M. Ogonowski, "Effect of Variances and Manufacturing Tolerances on the Design Strength and Life of Mechanically Fastened Composite Joints," Flight Dynamics Laboratory, Air Force Wright Aeronautical Laboratories, Technical Report AFWAL-TR-81-3041, April, 1981.

7. J.L. York, D.W. Wilson, and R.B. Pipes,"Analysis of Tension Failure Mode in Composite Bolted Joints," J. of Reinforced Plastics and Composites, Vol. 1, 1982, pp. 141-153.

8. D.W. Wilson and R.B. Pipes, "Analysis of the Shearout Failure Mode in Composite Bolted Joints," Proceedings of the 1st International Conference on Composite Structure, Paisley College of Technology, Scotland, 1981, pp. 34-49.

9. T.A. Collings, "On the Bearing Strengths of CFRP Laminates," Composites, Vol. 13, 1982, pp. 242-252.

REFERENCES (Cont'd)

10. C.M.S. Wong and F.L. Matthews, " A Finite Element
    Analysis of Single and Two-Hole Bolted Joints in Fibre
    Reinforced Plastic," J. of Composite Materials,
    Vol. 16, 1982, pp.481-491.

11. N,J. Pagano, R.B. Pipes, "The Influence of Stacking
    Sequence on Laminate Strength," J. of Composite
    Materials, 1971, pp.50-57.

12. W.J. Quinn and F.L. Matthews, "The Effect of Stacking
    Sequence on the Pin-Bearing Strength in Glass Fibre
    Reinforced Plastic," J. of Composite Materials,
    Vol. 11, 1977, pp. 139-145.

13. J.M. Whitney and R.Y. Kim, "Effect of Stacking Sequence
    on the Notched Strength of Laminated Composites,"
    Composite Materials: Testing and Design (Fourth
    Conference), ASTM STP 617, 1977, pp 229-242.

14. I.M. Daniel, R.E. Rowlands, and J.B. Whiteside,
    "Effects of Material and Stacking Sequence on the
    Behavior of Composite Plates With Holes," Experimental
    Mechanics, 1974. pp. 1-9.

15. E.F. Rybicke and D.W. Schmueser, "Effect of Stacking
    and Lay-Up Angle on Free Edge Stresses Around a Hole in
    a Laminated Plate Under Tension," J. of Composite
    Materials, Vol. 12, 1978, pp. 300-313.

16. T.A. Collings,"The Strength of Bolted Joints in
    Multi-Directional CFRP Laminates," British Royal
    Aircraft Establishment, TR 75127, 1975.

17. J.H. Stockdale and F.L. Matthews,"The Effect of
    Clamping Pressure on Bolt  Bearing Loads in Glass
    Fibre Reinforced Plastics," Composites, Vol. 7, 1976,
    pp.34-38.

18. Y.C. Fung, Foundations of Solid Mechanics, Prentice-
    Hall, Inc. Englewood Cliffs, New Jersey, 1965.

19. R.M. Jones, Mechanics of Composite Materials, Scripta
    Book Company, Washington, D.C. 1975.

20. T.L. Wilkinson, R.E. Rowlands and R.D. Cook, "An
    Incremental Finite Element Determination of Stresses
    Around Loaded Holes in Wood Plates," J. of Composites
    and Structures, 1981, Vol. 14, pp. 123-128.

21. C.-S. Hong, "Stresses Around Pin-Loaded Hole in Finite
    Orthotropic Laminates," Transactions of the Japan
    Society for Composite Materials, Trans. JSCM, Vol. 6,
    1980, pp. 50-55.

REFERENCES (Concluded)

22. R.E. Rowlands, M. U. Rahman, T.L. Wilkinson and Y.I. Chiang, "Single- and Multiple- Bolted Joints in Orthotropic Materials," Composites, Vol. 13, 1982, pp. 273-279.

23. W. Bickley, "The Distribution of Stress Round a Circular Hole in a Plate," Phil. Trans. Roy. Soc., A(London), Vol. 227, 1982, pp. 383-415.

24. T. De Jong, "Stress Around Pin-Loaded Holes in Elastically Orthotropic or Isotropic Plates," J. of Composite Materials, Vol. 11, 1977, pp.313-331.

25. O.C. Zienkiewicz, The Finite Element Method, McGraw-Hill Book Co., New York, 1977.

26. C.S. Tsai and J.F. Abel, Introduction to the Finite Element Method, Litton Educational Publishing, Inc., 1972.

27. P. Tong and J.N. Rossettos, Finite Element Method-Basic Technique and Implementation, The MIT Press, 1972.

28. S.E. Yamada and C.T. Sun,"Analysis of Laminate Strength and Its Distribution," J. of Composite Materials, Vol. 12, 1978, pp.275-284.

29. S.W. Tsai, "Strength Theories of Filamentary Structures," in Fundamental Aspects of Fiber Reinforced Plastic Composites, R.T. Schwartz and H.S. Schwartz (eds.), Wiley Interscience, New York, 1968, pp. 3-11.

30. S.W. Tsai and E.M. Wu, "A General Theory of Strength for Anisotropic Materials," J. of Composite Materials, Vol. 5, 1971, pp. 58-80.

31. S.W. Tsai, "Mechanics of Composite Materials, Part II-Theoretical Aspects," Air Force Material Laboratory. Technical Report, AFML-TR-66-149, 1966.

32. O. Hoffman, "The Brittle Strength of Orthotropic Materials", J. of Composite Materials, Vol. 1, 1967, pp.200-206.

33. A Rotem and Z. Hashin, "Failure Modes of Angle Ply Laminates," J. of composite Materials, Vol. 19, 1975, pp.191-206.

34. J.M. Whitney and R.J. Nuismer, "Stress Fracture Criteria for Laminated Composite Containing Stress Concentrations," J. of Composite Materials, Vol. 8, 1974, pp.253-265.

35. R.J. Nuismer and J.M. Whitney, "Uniaxial Failure of Composite Laminates Containing Stress Concentrations," Fracture Mechanics of Composites, ASTM STP 593, 1975, pp. 117-142.

36. R.J. Nuismer and J.D. Labor, "Applications of the Average Stress Failure Criterion:  Part I-Tension," J. of Composite Materials, Vol. 12, 1978, pp.238-249.

37. R.J. Nuismer and J.D. Labor, "Applications of the Average Stress Failure Criterion:  Part II-Compression," J. of Composite Materials, Vol. 13, 1979, pp. 49-60.

38. S. Timoshenko, and S. Woinowsky-Krieger, Theory of Plates and Shells, McGraw-Hill, New York, 1940.

39. S.G. Lekhnitskii, Anisotropic Plates, (translated from the second Russian Edition by S.W. Tsai and T. Cheron), Gordon and Breach Science Publisher, Inc., New York, 1968.

40. J.M. Whitney, D.L. Stansbarger and H.B. Howell, " Analysis of the Rail Shear Test- Applications and Limitations," J. of Composite Materials, Vol.5, 1971, pp.24-34.

41. R. Garcia, T.A. Weisshaar and R.R. McWithey, "An Experimental and Analytical Investigation of the Rail-test Method as Applied to Composite Materials," Experimental Mechanics, Vol. 20, pp. 273-279.

42. L.T. Hart-Smith, "Bolted Joints in Graphite-Epoxy Composites," NASA-CR-144899.

43. Private Communication, Fiberite Company, Winona, Minnesota 55987.

# APPENDIX A

## The Transformed Reduced Stiffness Matrix $\bar{Q}_{ij}^p$
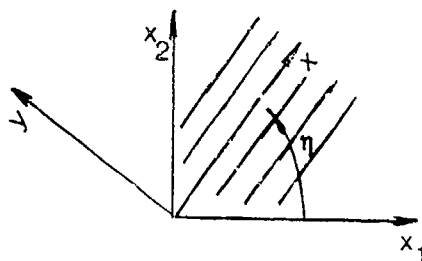


The components of the matrix $\bar{Q}_{ij}^P$ appearing in Eq. (12) are

$$\bar{Q}_{11}^P = Q_{11}^P \cos^4\eta + 2(Q_{12}^P + 2Q_{66}^P)\sin^2\eta + Q_{22}^P \sin^4\eta$$

$$\bar{Q}_{12}^P = (Q_{11}^P + Q_{22}^P - 4Q_{66}^P)\sin^2\eta\cos^2\eta + Q_{12}^P(\sin^4\eta + \cos^4\eta)$$

$$\bar{Q}_{22}^P = Q_{11}^P \sin^4\eta + 2(Q_{12}^P + 2Q_{66}^P)\sin^2\eta\cos^2\eta + Q_{22}^P \cos^4\eta$$

$$\bar{Q}_{13}^P = (Q_{11}^P - Q_{12}^P - 2Q_{33}^P)\sin\eta\cos^3\eta + (Q_{12}^P - Q_{22}^P + 2Q_{33}^P)\sin^3\eta\cos\eta$$

$$\bar{Q}_{23}^P = (Q_{11}^P - Q_{12}^P - 2Q_{33}^P)\sin^3\eta\cos\eta + (Q_{12}^P - Q_{22}^P + 2Q_{33}^P)\sin\eta\cos^3\eta$$

$$\bar{Q}_{33}^P = (Q_{11}^P + Q_{22}^P - 2Q_{12}^P - 2Q_{33}^P)\sin^2\eta\cos^2\eta + Q_{33}^P(\sin^4\eta + \cos^4\eta)$$

in which

$$Q_{11}^P = E_1^P/(1 - \mu_{12}^P\mu_{21}^P)$$

$$Q_{12}^P = (\mu_{12}^P E_2^P)/(1 - \mu_{12}^P\mu_{21}^P) = \mu_{21}^P E_1^P/(1 - \mu_{12}^P\mu_{21}^P)$$

$$Q_{22}^P = E_2^P/(1 - \mu_{12}^P\mu_{21}^P)$$

$$Q_{33}^P = G_{12}^P$$

The superscript p denotes the material properties of the p-th ply, and the angle $\eta$ is measured from the $x_1$-axis to the x-axis. $E^P_1$, $E^P_2$ and $G^P_{12}$ are the longitudinal, transverse, and shear moduli of the p-th ply, respectively. $\mu^P_{12}$ and $\mu^P_{21}$ are Poisson's ratios for the p-th ply and satisfy the relation

$$\mu^P_{12}/E^P_1 = \mu^P_{21}/E^P_2$$

# APPENDIX B

## The Coordinate Transformation matrix $T_{ij}$
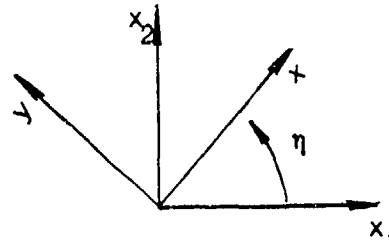


$$[T] = \begin{bmatrix} \cos^2\eta & \sin^2\eta & 2\sin\eta\cos\eta \\ \sin^2\eta & \cos^2\eta & -2\sin\eta\cos\eta \\ -\sin\eta\cos\eta & \sin\eta\cos\eta & \cos^2\eta-\sin^2\eta \end{bmatrix}$$

The angle $\eta$ is measured from the $x_1$-axis to the x axis.

APPENDIX C

The Finite Element Mesh Generator

The mesh generator generates 306 quadrilateral elements for a single hole, and 612 and 655 elements for two holes in parallel and two holes in series, respectively. To control costs, this number was held fixed (the reader should note that 612 elements involve a matrix of size 1400 x 300). The mesh is designed in such way that the characteristic curve can be encompassed by a square of size 2z x 2z, in which a fine mesh was generated and outside of which the calculated stresses are still reasonably accurate (see Figures 5, 6, 7). A suitable value of z for a given geometry has to be determined before calculating the stresses. Mathematically, this problem may be stated :

Optimize    z

subject to    $( R_c + D/2 ) \leq z \leq W/2$         (C.1)

$z \leq E$         (C.2)

Equation (C.1) can be rewritten as

$$0 \leq ( z - R_c - D/2 ) \leq ( W/2 - R_c - D/2 ) \qquad (C.3)$$

Assume that E is large enough that eq.(C.2) is always satisfied. Assume that $z/D$ is a function of $W/D$ and $R_c/D$,

and can be expressed by

$$z/D = f(\ W/2D - R_c/D - 1/2\ ) = f(\ \zeta/D\ ) \qquad (C.4)$$

where $\zeta/D = W/2D - R_c/D - 1/2$ and $f$ is some unknown function.

Assume that $z/D$ is a second order polynomial function of $\zeta/D$. Then eq.(C.4) can be written as

$$z/D = a(\zeta/D)^2 + b(\zeta/D) + c \qquad (C.5)$$

This equation reflects the general trend that as W, and hence $\zeta$, increases, z must be made bigger, since the total number of elements is constant. Three conditions are necessary to determine the constants, a, b, and c.

When $W/2 = R_c + D/2$ ( $\zeta = 0$ ), then the only choice of z is

$$z/D = R_c/D + 1/2 = W/2 \qquad (C.6)$$

Substituting eq.(C.6) into (C.5), gives
v 2300

$$c = R_c/D + 1/2 \qquad (C.7)$$

When W changes from $W_1$ to $W_2$, say, $\zeta$ changes by the amount $\Delta\zeta = \zeta_1 - \zeta_2$. The writer has found from computational experience that the following changes in z

generated results close to known analytical solutions.

$$1 \leq \xi \leq 1.5 \qquad \Delta(z/D) \simeq (1/4) \, \Delta(\xi/D) \qquad \text{(C.8)}$$

$$\xi \geq 2 \qquad \Delta(z/D) \simeq 4 \, \Delta(\xi/D) \qquad \text{(C.9)}$$

Imposing these conditions, we have

at $\xi = 1$, $\Delta(z/D)/\Delta(\xi/D) \simeq d(z/D)/d(\xi/D) = 2a + b = 1/4$
(C.10)

at $\xi$  .5, $\Delta(z/D)/\Delta(\xi/D) \simeq d(z/D)/d(\xi/D) = 5a + b = 4$ (C.11)

From eqs (C.10) and (C.11), give

$$a = 0.05 \qquad \text{(C.12)}$$

$$b = 0.15 \qquad \text{(C.13)}$$

As a result, eq.(C.5) becomes

$$z = D \, [ \, 0.05 \, (W/2D - R_c/D - 1/2)^2 + 0.15 \, (W/2D - R_c/D - 1/2)$$
$$+ (R_c/D + 1/2) ] \qquad \text{(C.14)}$$

Using this result, excellent agreement between the
computational results, and Timoshenko's and De Jong's
solutions were obtained (Figures 13 and 14, Section V).

## Appendix D

### Shape Function Used in the Finite Element Code

In the isoparametric element, the geometry and the displacement of the element are described in terms of the shape function $N_\alpha$, by a transformation from a master element in the r-s coordinate system to the element in the $x_1$-$x_2$ coordinate system (Figure 40).

$$X_i = N_\alpha(\gamma, s)\, \bar{x}_{i\alpha} \qquad\qquad i = 1, 2$$

$$u_i = N_\alpha(\gamma, s)\, q_{i\alpha} \qquad\qquad \alpha = 1, 2, 3, \text{ or } 4$$

$$N_\alpha(r, s) = 1/4 (1 + rr_\alpha)(1 + ss_\alpha) \qquad -1 \le r, s \le 1$$

Here $x_{i\alpha}$ is the coordinate of node $\alpha$ in the i-direction, $q_{i\alpha}$ is the displacement of node $\alpha$ in the i-direction, and $r_\alpha$ and $s_\alpha$ are the coordinates of node $\alpha$ referred to the master element. Note the property

$$N_\alpha(r_\beta, s_\beta) = \begin{cases} 1, & \text{if } \alpha = \beta \\ \\ 0, & \text{if } \alpha \neq \beta \end{cases}$$

Element in $x_1 - x_2$ coordinates

Master element in local
r - s coordinates
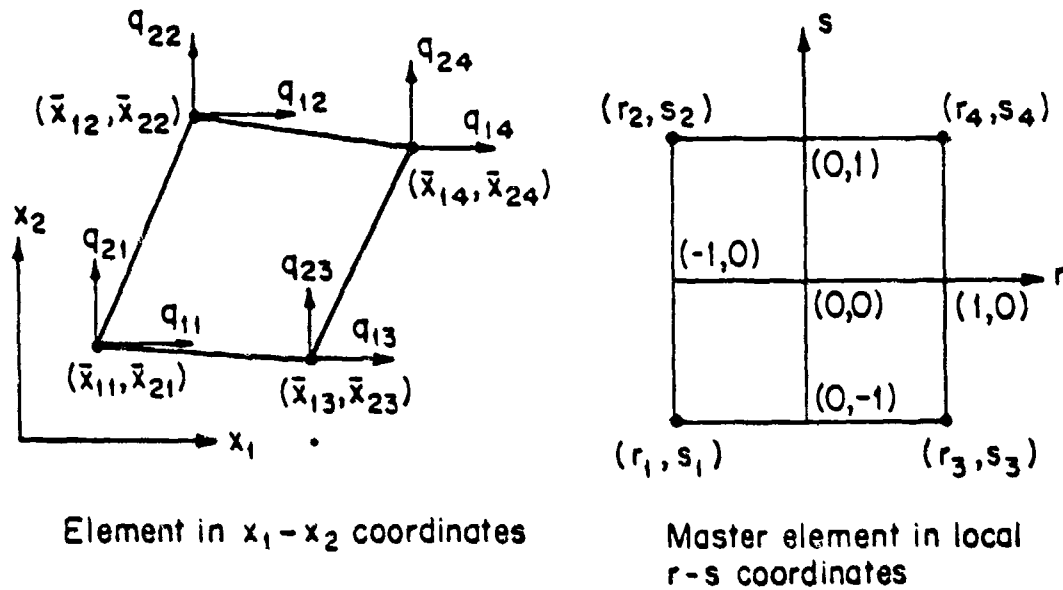
Figure 40    Geometry of an Element Used in the Finite Element
Calculations; Left: Element in the $x_1 - x_2$
Coordinate System. Right: Element (Master
Element) in the Local (r-s) Coordinate System.
$x_{i\alpha}$ is the Coordinate of Node $\alpha$ in the i
Direction, $q_{i\alpha}$ is the Displacement of Node
$\alpha$ in the i Direction and $(r_\alpha, s_\alpha)$ are the
Coordinates of Node $\alpha$ in the r-s Coordinate
System, i=1,2, $\alpha$=1,2,3, or 4.

## APPENDIX E

Listing of a Sample of Input-Output of the Computer Code

\*\*\*\*\*\*\*\*\*\*\*\*\*\*\*\*\*\*\*\*\*\*\*\*\*\*\*\*\*\*\*\*\*\*\*\*\*\*\*\*\*\*\*\*\*\*\*\*\*\*\*\*\*\*\*\*\*\*\*\*\*\*\*\*\*\*\*

--- << BOLTED JOINTS >> ---

THE PURPOSE OF THIS PROGRAM IS TO PREDICT
THE FAILURE LOAD AND THE FAILURE MODE OF
BOLTED COMPOSITE JOINTS.

FU-KUO CHANG, RICHARD A. SCOTT, GEORGE S. SPRINGER
MECHANICAL ENGINEERING AND APPLIED MECHANICS
THE UNIVERSITY OF MICHIGAN
ANN ARBOR, MI 48109
APRIL 30, 1983

\*\*\*\*\*\*\*\*\*\*\*\*\*\*\*\*\*\*\*\*\*\*\*\*\*\*\*\*\*\*\*\*\*\*\*\*\*\*\*\*\*\*\*\*\*\*\*\*\*\*\*\*\*\*\*\*\*\*\*\*\*\*\*\*\*\*\*

----- CAPABILITIES:

THIS PROGRAM HAS THE CAPABILITY TO DEAL WITH THREE
TYPES OF BOLTED COMPOSITE JOINTS DEFINED AS FOLLOWS:

    TYPE 1 --   JOINTS WITH A SINGLE HOLE
    TYPE 2 --   JOINTS WITH TWO IDENTICAL HOLES IN A ROW
    TYPE 3 --   JOINTS WITH TWO IDENTICAL HOLES IN TANDEM

SEE FIGURE BELOW:

```
 -------        ----------         ----------
|       |      |          |       |          |
|   •   |      |   •   •  |       |    •     |
|       |      |          |       |          |
|   .   |      |          |       |    •     |
|       |      |          |       |          |
|       |      |          |       |          |
|       |      |          |       |          |

  TYPE 1          TYPE 2              TYPE 3
```
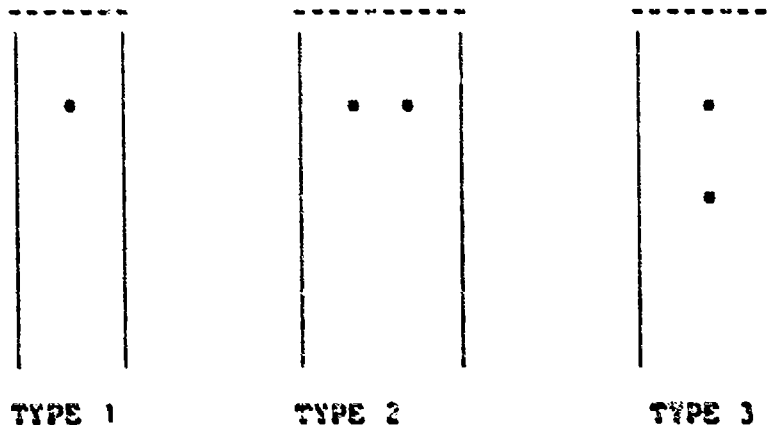
THIS PROGRAM CAN ALSO HANDLE THE FOLLOWING
LOADING CONDITIONS:
(A). PIN OR PINS CARRY ALL THE APPLIED LOAD.
(B). PIN OR PINS CARRY ONLY A FRACTION OF THE TOTAL
     LOAD APPLIED AT THE BOTTOM OF THE JOINT.  THE
     REST OF THE LOAD IS CARRIED BY THE UPPER END.

SEE FIGURE BELOW:
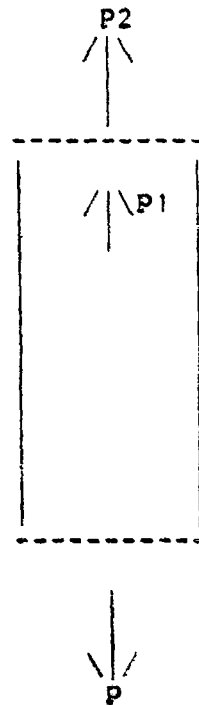
```
            P2
           /|\
            |
  ----------------
 |              |
 |   /|\P1      |
 |   /|\        |      P=P1+P2, P>P1 AND P>P2 OR P=P1
 |   |          |
 |   |          |      P: THE APPLIED LOAD
 |   |          |      P1:LOAD CARRIED BY THE PIN (PINS)
 |   |          |      P2:BY-PASSED LOAD
 |   |          |
 |   |          |
  ----------------
            |
           \|/
            P
```

FOR EACH TYPE OF JOINT, THIS PROGRAM CAN HANDLE

THE FOLLOWING SITUATIONS:


(A). DIFFERENT PLY ORIENTATIONS
(B). DIFFERENT MATERIAL PROPERTIES (SYMMETRIC LAMINATE)
(C). DIFFERENT GEOMETRICAL CONFIGURATIONS INCLUDING
     DIFFERENT HOLE SIZES, HOLE POSITIONS, JOINT
     THICKNESSES, AND JOINT LENGTHS.

-------    RESTRICTIONS:


THE PROGRAM IS BASED ON THE FOLLOWING ASSUMPTIONS:
(1). A UNIFORM TENSILE LOAD IS APPLIED SYMMETRICALLY
     WITH RESPECT TO THE CENTERLINE OF THE PLATE.
(2). THE LAMINATE IS SYMMETRIC.

(3). HOLE SIZES ARE EQUAL IN EACH JOINT WITH TWO HOLE
(4). PIN IS RIGID. THE PIN SUPPORT IS ALSO RIGID.


-------- ANALYSIS:


THE STRESSES ARE CALCULATED USING A FINITE ELEMENT METHOD
FORMULATED ON THE BASIS OF TWO DIMENSIONAL CLASSICAL
LAMINATION PLATE THEORY.  THE FAILURE LOAD AND FAILURE
MODE ARE CALCULATED USING THE CHANG-SCOTT-SPRINGER FAILURE
HYPOTHESIS TOGETHER WITH THE YAMADA-SUN FAILURE CRITERION



-------- INPUT INSTRUCTIONS

*****   ENTER MATERIAL PROPERTIES  ****

DO YOU WANT TO USE GRAPHITE/EPOXY T300/1034-C?
ENTER YES OR NO
yes

MATERIAL PROPERTIES OF T300/1034-C :

LONGITUDINAL YOUNGS MODULUS:            21300000.00000 PSI
TRANSVERSE YOUNGS MODULUS:               1700000.00000 PSI
SHEAR MODULUS:                            897000.00000 PSI
POISSON RATIO:                                 0.30000
LONGITUDINAL TENSILE STRENGTH:            251000.00000 PSI
LONGITUDINAL COMPRESSIVE STRENGTH:        200000.00000 PSI
LAMINATE SHEAR STRENGTH:                   19400.00000 PSI

CHARACTERISTIC LENGTH (TENSION):        0.0180 INCH
CHARACTERISTIC LENGTH(COMPRESSION):     0.0700 INCH


-----------------------------------------------------------


JOINT TYPE SELECTION


TYPE 1 : JOINT WITH A SINGLE HOLE
TYPE 2 : JOINT WITH TWO HOLES IN ROW
TYPE 3 : JOINT WITH TWO HOLES IN TANDEM


WHICH TYPE OF JOINT DO YOU WANT TO SELECT?

ENTER 1, 2, OR 3.

1

DO YOU CONSIDER A BY-PASS LOAD?
ENTER YES OR NO

no

THE FOLLOWING GEOMETRIC PARAMTERS MUST BE SPECIFIED:

(A) DIAMETER OF THE HOLE, D
    (D SHOULD BE LESS THAN 1 INCH FOR DEPENDABLE RESULTS)
(B) WIDTH OF THE JOINT, W
(C) LENGTH OF THE JOINT, L
(D) EDGE DISTANCE OF THE JOINT, E
(E) DISTANCE BETWEEN THE CENTERS OF
    TWO HOLES, S

SEE FIGURE BELOW:

```
        |-      W       -|
  -- -----------------  --
  |                       |       |
  |                       |       E
          |- S -|   |   | |       |
          *       *  -   |        --
                      S
  L.          *       -
                      |



  |   |                   |
  -- -----------------  --
```

THE DIAMETER MUST BE INPUTED IN INCHES, THE OTHER
GEOMETRIC PARAMETERS MAY BE EITHER IN INCHES
OR AS A RATIO TO DIAMETER (PARAMETER/ DIAMETER)


ENTER THE HOLE DIAMETER IN INCHES

0.25

DO YOU WISH TO ENTER ALL GEOMETRIC PARAMETERS
IN TERMS OF DIAMETER RATIO (PARAMETER/DIAMETER) ?
ENTER YES OR NO
y


ENTER THE WIDTH TO DIAMETER RATIO:

8

ENTER THE EDGE TO DIAMETER RATIO:

3

ENTER  THE LENGTH TO DIAMETER RATIO:

20

INPUT THE JOINT THICKNESS AND THE PLY ORIENTATIONS
(SYMMTRIC LAMINATE ONLY)
THE PLY ORIENTATION AND THE NUMBERS OF PLIES IN THE
PLY GROUP HAVE TO BE SPECIFIED.

*1. THE PLY GROUP IS DEFINED AS A GROUP OF PLIES
     HAVING THE SAME PLY ORIENTATION.
*2. EACH PLY ORIENTATION IS MEASURED FROM THE
     LOADING DIRECTION TO THE FIBER DIRECTION.
     THE ANGLE IS POSITIVE CLOCKWISE AND
     NEGATIVE COUNTERCLOCKWISE

    SEE FIGURE BELOW
    ----------------------

```
|                         |
|      |ANGLE/            |
|      |  ◆ /             |
|      |  /               |
|      | /                |
|      |/                 |
|                         |
|                         |
|       ◆ HOLE            |
|                         |
|                         |
|                         |
```
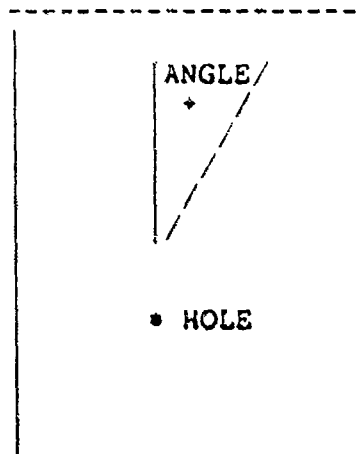
ENTER THE JOINT THICKNESS IN INCHES

0.125

ENTER THE TOTAL NUMBER OF PLY GROUPS.
*** THE MAXIMUM NUMBER OF THE PLY GROUPS < 100
INPUT AN INTEGER


4

ENTER THE PLY ORIENTATION OF EACH PLY GROUP

ENTER THE PLY ORIENTATION OF PLY GROUP    1

IN DEGREES

0

ENTER THE NUMBER OF PLIES IN PLY GROUP  1 IN INTEGER

6

ENTER THE PLY ORIENTATION OF PLY GROUP   2
IN DEGREES

45

ENTER THE NUMBER OF PLIES IN PLY GROUP  2 IN INTEGER

6

ENTER THE PLY ORIENTATION OF PLY GROUP   3
IN DEGREES

-45

ENTER THE NUMBER OF PLIES IN PLY GROUP  3 IN INTEGER

6

ENTER THE PLY ORIENTATION OF PLY GROUP   4
IN DEGREES

90

ENTER THE NUMBER OF PLIES IN PLY GROUP  4 IN INTEGER

6

DO YOU WANT TO HAVE A LIST OF THE INPUT DATA ?
ENTER YES OR NO

Y

--------    LIST OF DATA    -----------

JOINT TYPE SELECTION= 1
LOAD TYPE SELECTION:  0.0  % OF BY-PASSED LOAD

<    GEOMETRY  >: (INCHES)

| DIAMETER | WIDTH | EDGE | THICKNESS | LENGTH |
|----------|-------|------|-----------|--------|
| 0.2500 | 2.0000 | 0.7500 | 0.1250 | 5.0000 |

< GROUP ORIENTATION >:

TOTAL PLY GROUP NO.= 4

GROUP 1 ORIENTATION= 0.0 THICKNESS= 0.03125 INCH

GROUP 2 ORIENTATION= 45.000 THICKNESS= 0.03125 INCH

GROUP 3 ORIENTATION=-45.000 THICKNESS= 0.03125 INCH

GROUP 4 ORIENTATION= 90.000 THICKNESS= 0.03125 INCH

< MATERIAL PROPERTIES > :

```
LONGITUDINAL YOUNGS MODULUS   :        21300000.00000 PSI
TRANSVERSE YOUNGS MODULUS   :           1700000.00000 PSI
SHEAR MODULUS:                           897000.00000 PSI
POISSON RATIO:                                0.30000
LONGITUDINAL TENSILE STRENGTH:           251000.00000 PSI
LONGITUDINAL COMPRESSIVE STRENGTH:       200000.00000 PSI
LAMINATE SHEAR STRENGTH:                  19400.00000 PSI

CHARACTERISTIC LENGTH (TENSION):          0.0180 INCH
CHARACTERISTIC LENGTH(COMPRESSION):       0.0700 INCH
```

-------------------------------------------------------

DO YOU WANT TO MAKE ANY CHANGE IN YOUR DATA?
ENTER YES OR NO

no

-------------------------------------------------------

< THE STRENGTH PREDICTION OF FASTENED COMPOSITE JOINTS >

-------------------------------------------------------

--------- LIST OF INPUT ----------

JOINT TYPE SELECTION= 1
LOAD TYPE SELECTION: 0.0 % OF BY-PASSED LOAD

< GEOMETRY > : (INCHES)

| DIAMETER | WIDTH | EDGE | THICKNESS | LENGTH |
|----------|--------|--------|-----------|--------|
| 0.2500 | 2.0000 | 0.7500 | 0.1250 | 5.0000 |

```
<   GROUP ORIENTATION   > :
 TOTAL PLY GROUP NO. =   4

  GROUP  1  ORIENTATION=  0.0    THICKNESS= 0.03125 INCH

  GROUP  2  ORIENTATION= 45.000  THICKNESS= 0.03125 INCH

  GROUP  3  ORIENTATION=-45.000  THICKNESS= 0.03125 INCH

  GROUP  4  ORIENTATION= 90.000  THICKNESS= 0.03125 INCH


  MATERIAL PROPERTIES:

  LONGITUDINAL YOUNGS MODULUS:         21300000.00000 PSI
  TRANSVERSE YOUNGS MODULUS:            1700000.00000 PSI
  SHEAR MODULUS:                         897000.00000 PSI
  POISSON RATIO:                              0.30000
  LONGITUDINAL TENSILE STRENGTH:         251000.00000 PSI
  LONGITUDINAL COMPRESSIVE STRENGTH:     200000.00000 PSI
  LAMINATE SHEAR STRENGTH:                19400.00000 PSI

  CHARACTERISTIC LENGTH (TENSION):         0.0180 INCH
  CHARACTERISTIC LENGTH(COMPRESSION):      0.0700 INCH


  ----------------------------------------------------------

  --------       LIST OF OUTPUT       ---------


 <  FAILURE LOAD AND FAILURE MODE >


  THE MAXIMUM LOAD ( P )=                   3012.7  LB

  THE BEARING STRENGTH( P/(D*H) )=       96406.5  PSI
  (H : THE LAMINATE THICKNESS)


  THE FAILURE MODE : BEARING MODE, AT THE ANGLE  8.437 DEGREE




  THE FAILURE ANGLE IS DEFINED IN THE FOLLOWING FIGURE :
```
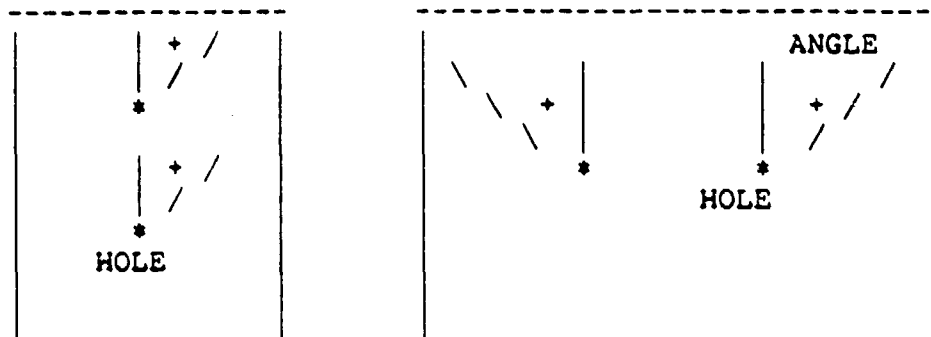
* THE INITIAL FAILED PLY GROUP (AT THE MAXIMUM LOAD) =    1
THE PLY ORIENTATION OF THIS PLY GROUP=   0.0

------------------------------------------------------


DO YOU WANT TO RUN THE PROGRAM AGAIN?
ENTER YES OR NO


y


DO YOU WANT TO MAKE ANY CHANGE IN YOUR DATA?
ENTER YES OR NO


y

WHICH PART OF THE DATA DO YOU WANT TO CHANGE ?
(1). JOINT TYPE AND GEOMETRY.
(2). PLY ORIENTATION.
(3). MATERIAL PROPERTIES.

ENTER 1,2,OR 3.


1

JOINT TYPE SELECTION


TYPE 1 : JOINT WITH A SINGLE HOLE
TYPE 2 : JOINT WITH TWO HOLES IN ROW
TYPE 3 : JOINT WITH TWO HOLES IN TANDEM


WHICH TYPE OF JOINT DO YOU WANT TO SELECT?

ENTER 1, 2, OR 3.

3

DO YOU CONSIDER A BY-PASS LOAD?
ENTER YES OR NO

n

THE FOLLOWING GEOMETRIC PARAMTERS MUST BE SPECIFIED:

(A) DIAMETER OF THE HOLE, D
    (D SHOULD BE LESS THAN 1 INCH FOR DEPENDABLE RESULTS)
(B) WIDTH OF THE JOINT, W
(C) LENGTH OF THE JOINT, L
(D) EDGE DISTANCE OF THE JOINT, E
(E) DISTANCE BETWEEN THE CENTERS OF
    TWO HOLES, S

SEE FIGURE BELOW:

```
    |-      W      -|
 --  ----------------  --
 |   |                |   |
 |   |                |   E
 |   |  |- S -|  |    |   |
 |   |  •     •  |    |  --
 |   |           -    
 |   |           S    
 |   |     •     -    
 L   |           |    
 |   |                
 |   |                
 |   |                
 |   |                
 --  ----------------
```

THE DIAMETER MUST BE INPUTED IN INCHES, THE OTHER
GEOMETRIC PARAMETERS MAY BE EITHER IN INCHES
OR AS A RATIO TO DIAMETER (PARAMETER/ DIAMETER)

ENTER THE HOLE DIAMETER IN INCHES

0.25

DO YOU WISH TO ENTER ALL GEOMETRIC PARAMETERS
IN TERMS OF DIAMETER RATIO (PARAMETER/DIAMETER) ?
ENTER YES OR NO

y

ENTER THE WIDTH TO DIAMETER RATIO:

8

ENTER THE EDGE TO DIAMETER RATIO:

3

ENTER  THE LENGTH TO DIAMETER RATIO:

20

ENTER THE TWO HOLE DISTANCE TO DIAMETER RATIO:

3

DO YOU WANT TO HAVE A LIST OF THE INPUT DATA ?
ENTER YES OR NO

n

------------------------------------------------------

<   THE STRENGTH PREDICTION OF FASTENED COMPOSITE JOINTS   >

------------------------------------------------------

--------       LIST OF INPUT      ----------


JOINT TYPE SELECTION= 3
LOAD TYPE SELECTION:  0.0  % OF BY-PASSED LOAD

<   GEOMETRY  > : (INCHES)
   DIAMETER      WIDTH     EDGE     THICKNESS     LENGTH

    0.2500     2.0000    0.7500     0.1250      5.0000


DISTANCE BETWEEN THE TWO HOLES (INCHES)

   0.7500


<   GROUP ORIENTATION  > :
 TOTAL PLY GROUP NO.=  4

 GROUP  1  ORIENTATION=  0.0     THICKNESS= 0.03125 INCH

 GROUP  2  ORIENTATION= 45.000   THICKNESS= 0.03125 INCH

 GROUP  3  ORIENTATION=-45.000   THICKNESS= 0.03125 INCH

GROUP 4 ORIENTATION= 90.000 THICKNESS= 0.03125 INCH

MATERIAL PROPERTIES:

| | |
|---|---|
| LONGITUDINAL YOUNGS MODULUS: | 21300000.00000 PSI |
| TRANSVERSE YOUNGS MODULUS: | 1700000.00000 PSI |
| SHEAR MODULUS: | 897000.00000 PSI |
| POISSON RATIO: | 0.30000 |
| LONGITUDINAL TENSILE STRENGTH: | 251000.00000 PSI |
| LONGITUDINAL COMPRESSIVE STRENGTH: | 200000.00000 PSI |
| LAMINATE SHEAR STRENGTH: | 19400.00000 PSI |
| CHARACTERISTIC LENGTH (TENSION): | 0.0180 INCH |
| CHARACTERISTIC LENGTH(COMPRESSION): | 0.0700 INCH |

-------------------------------------------------------

--------    LIST OF OUTPUT    ---------

< FAILURE LOAD AND FAILURE MODE >

THE MAXIMUM LOAD ( P )=                          5346.7  LB

THE BEARING STRENGTH( P/(D*H) )=       171093.2  PSI
(H : THE LAMINATE THICKNESS)

THE FAILURE MODE = SHEAROUT MODE, AT THE ANGLE 47.812
DEGREE

THE FAILURE ANGLE IS DEFINED IN THE FOLLOWING FIGURE :
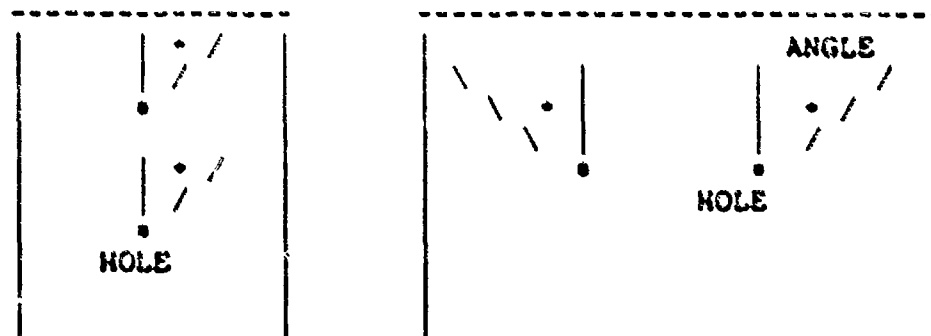
* THE INITIAL FAILED PLY GROUP (AT THE MAXIMUM LOAD) =    2
THE PLY ORIENTATION OF THIS PLY GROUP= 45.000

*** THE FAILURE INITIATED FROM THE BOTTOM HOLE


LOAD CARRIED BY THE TOP PIN =    2028.644466 LB
LOAD CARRIED BY THE BOTTOM PIN =    3318.018795 LB

----------------------------------------------------


DO YOU WANT TO RUN THE PROGRAM AGAIN?
ENTER YES OR NO

no
#Execution terminated

# APPENDIX F

## Summary of Data for Calculating $R_t$ and $R_c$

This Appendix contains the data which were generated to determine the rail shear strength S and the characteristic lengths $R_t$ and $R_c$ for Fiberite T300/1034-C graphite epoxy laminates.

Notations used in Tables 6-14

| | | |
|---|---|---|
| D | hole diameter | (in) |
| W | specimen width | (in) |
| L | specimen length | (in) |
| H | specimen thickness | (in) |
| E | edge distance | (in) |
| P | failure load under tension | (lbf) |
| $P_{avg}$ | average failure load under tension | (lbf) |
| S | rail shear strength | (psi) |
| $S_{avg}$ | average rail shear strength | (psi) |
| $R_t$ | characteristic length in tension | (in) |
| $R_c$ | characteristic length in compression | (in) |

Table 6 Rail Shear Strength S of Cross Ply $[0/90]_s$ Laminate
(all length units in inches)

| No. of Plies | Volume Fraction of $0°$ Plies (percent) | Stacking Sequence | W | L | H | S | $S_{avg}$ |
|---|---|---|---|---|---|---|---|
| 24 | 50 | $[(0/90)_6]_s$ | 1.5<br>1.5<br>1.75<br>2.00<br>2.00 | 7.75<br>7.75<br>8.00<br>8.00<br>8.00 | 0.125 | 19096<br>19870*<br>18320*<br>15250*<br>13500 | 19483 |
| 20 | 60 | $[0,0,90,0,0,90,0,90,0,90]_s$ | 2.00<br>1.75<br>1.75 | 8.00 | 0.103 | 12500<br>13350<br>12740 | 12863 |
| 20 | 70 | $[0,0,90,0,0,90,0,0,90,0]_s$ | 2.00<br>1.75<br>1.75 | 8.00 | 0.103 | 12740<br>13531<br>13350 | 13206 |

* excessive cracking of the specimens. Data not included in the average.

Table 7  Characteristic Length in Tension $R_t$
Ply Orientation $[(0/\pm45/90)_3]_s$

| D | W | L | H | P | $P_{avg}$ | $R_t$ |
|---|---|---|---|---|---|---|
| 0.145 | 0.507 | 7.00 | 0.125 | 2550 | 2792 | 0.010 |
|  | 0.502 |  |  | 2850 |  |  |
|  | 0.501 |  |  | 2900 |  |  |
|  | 0.501 |  |  | 2870 |  |  |
| 0.125 | 0.738 | 8.00 | 0.125 | 4460 | 4507 | 0.014 |
|  | 0.743 |  |  | 4300 |  |  |
|  | 0.738 |  |  | 4850 |  |  |
|  | 0.725 |  |  | 4620 |  |  |
| 0.250 | 1.015 | 8.00 | 0.125 | 5500 | 5280 | 0.019 |
|  | 1.010 |  |  | 5120 |  |  |
|  | 1.005 |  |  | 5200 |  |  |
|  | 1.010 |  |  | 5300 |  |  |
| 0.25 | 1.985 | 8.00 | 0.125 | 11200 | 11087 | 0.020 |
|  | 1.985 |  |  | 10850 |  |  |
|  | 1.987 |  |  | 11200 |  |  |
|  | 1.988 |  |  |  |  |  |

Table 8  Characteristic Length in Tension $R_t$
Ply Orientation $[(0/(\pm45)_3/90_3]_s$

| D | W | L | H | P | $P_{avg}$ | $R_t$ |
|---|---|---|---|---|---|---|
| 0.125 | 0.500 | 7.00 | 0.103 | 1600 | 1690 | 0.011 |
|  | 0.498 |  |  | 1600 |  |  |
|  | 0.500 |  |  | 1770 |  |  |
|  | 0.500 |  |  | 1790 |  |  |
| 0.125 | 0.755 | 8.00 | 0.103 | 3100 | 3122 | 0.020 |
|  | 0.755 |  |  | 2950 |  |  |
|  | 0.750 |  |  | 3270 |  |  |
|  | 0.753 |  |  | 3170 |  |  |
| 0.250 | 1.008 | 8.00 | 0.103 | 3750 | 3537 | 0.026 |
|  | 1.000 |  |  | 3400 |  |  |
|  | 1.005 |  |  | 3550 |  |  |
|  | 1.008 |  |  | 3450 |  |  |
| 0.250 | 1.500 | 8.00 | 0.103 | 5750 | 5750 | 0.032 |
|  | 1.497 |  |  | 6210 |  |  |
|  | 1.500 |  |  | 5400 |  |  |
|  | 1.501 |  |  | 5640 |  |  |

133

Table 9  Characteristic Length in Tension $R_t$
Ply Orientation $[0/(\pm45)_2/90_5]_s$

| D | W | L | H | P | $P_{avg}$ | $R_t$ |
|---|---|---|---|---|---|---|
| 0.125 | 0.493 | 7.00 | 0.103 | 1330 | 1315 | 0.007 |
|  | 0.495 |  |  | 1260 |  |  |
|  | 0.495 |  |  | 1320 |  |  |
|  | 0.500 |  |  | 1350 |  |  |
| 0.125 | 0.754 | 7.00 | 0.103 | 2600 | 2647 | 0.016 |
|  | 0.748 |  |  | 2720 |  |  |
|  | 0.750 |  |  | 2570 |  |  |
|  | 0.749 |  |  | 2700 |  |  |
| 0.250 | 1.065 | 8.00 | 0.103 | 2630 | 2780 | 0.013 |
|  | 1.000 |  |  | 2650 |  |  |
|  | 1.000 |  |  | 3200 |  |  |
|  | 1.001 |  |  | 2640 |  |  |
| 0.250 | 1.500 | 8.00 | 0.103 | 4700 | 4575 | 0.018 |
|  | 1.500 |  |  | 4620 |  |  |
|  | 1.500 |  |  | 4600 |  |  |
|  | 1.496 |  |  | 4380 |  |  |

Table 10  Characteristic Length in Tension $R_t$
Ply Orientation $[0/\pm45/90]_{7s}$

| D | W | L | H | P | $P_{avg}$ | $R_t$ |
|---|---|---|---|---|---|---|
| 0.125 | 0.498 | 7.00 | 0.103 | 950 | 1005 | 0.007 |
|  | 0.500 |  |  | 930 |  |  |
|  | 0.500 |  |  | 1090 |  |  |
|  | 0.500 |  |  | 1050 |  |  |
| 0.125 | 0.755 | 7.00 | 0.103 | 2030 | 2160 | 0.013 |
|  | 0.765 |  |  | 2270 |  |  |
|  | 0.753 |  |  | 2140 |  |  |
|  | 0.755 |  |  | 2200 |  |  |
| 0.250 | 1.009 | 8.00 | 0.103 | 2270 | 2407 | 0.015 |
|  | 1.006 |  |  | 2480 |  |  |
|  | 1.002 |  |  | 2450 |  |  |
|  | 1.005 |  |  | 2430 |  |  |
| 0.250 | 1.504 | 8.00 | 0.103 | 3770 | 3562 | 0.013 |
|  | 1.493 |  |  | 3180 |  |  |
|  | 1.500 |  |  | 3650 |  |  |
|  | 1.505 |  |  | 3650 |  |  |

135

Table 11 Characteristic Length in Tension $R_t$
Ply Orientation $[(90_2/\pm60/\pm30)_2]_s$

| D | W | L | H | P | P avg | $R_t$ |
|---|---|---|---|---|---|---|
| 0.125 | 0.504<br>0.504<br>0.506<br>0.500 | 7.00 | 0.125 | 1760<br>1930<br>2550<br>2025 | 2080 | 0.010 |
| 0.125 | 0.738<br>0.731<br>0.738<br>0.740 | 8.00 | 0.125 | 3250<br>3100<br>3300<br>3250 | 3225 | 0.011 |
| 0.250 | 1.015<br>1.005<br>1.013<br>1.015 | 8.00 | 0.125 | 3500<br>3300<br>3800<br>3700 | 3575 | 0.010 |
| 0.250 | 1.994<br>1.992<br>1.996<br>1.990 | 8.00 | 0.125 | 7910<br>8350<br>8150<br>8000 | 8202 | 0.016 |
| 0.500 | 1.970<br>1.955<br>1.965<br>1.965 | 8.00 | 0.125 | 6500<br>6150<br>6350<br>5900 | 6225 | 0.015 |

Table 12  Characteristic Length in Tension $R_t$
Ply Orientation $[(0/90)_6]_s$

| D | W | L | H | P | $P_{avg}$ | $R_t$ |
|---|---|---|---|---|---|---|
| 0.125 | 0.505 | 7.00 | 0.125 | 3690 | 3732 | 0.007 |
|  | 0.507 |  |  | 3270 |  |  |
|  | 0.505 |  |  | 4050 |  |  |
|  | 0.505 |  |  | 3900 |  |  |
| 0.125 | 0.725 | 8.00 | 0.125 | 5750 | 5629 | 0.010 |
|  | 0.732 |  |  | 5600 |  |  |
|  | 0.728 |  |  | 5550 |  |  |
|  | 0.732 |  |  | 5950 |  |  |
| 0.250 | 1.018 | 8.00 | 0.125 | 7000 | 6762 | 0.013 |
|  | 1.012 |  |  | 6700 |  |  |
|  | 1.012 |  |  | 6850 |  |  |
|  | 1.017 |  |  | 6500 |  |  |
| 0.250 | 1.498 | 8.00 | 0.125 | 10180 | 10120 | 0.014 |
|  | 1.497 |  |  | 9800 |  |  |
|  | 1.498 |  |  | 9950 |  |  |
|  | 1.497 |  |  | 10160 |  |  |
| 0.500 | 2.003 | 8.00 | 0.125 | 11600 | 11959 | 0.022 |
|  | 2.003 |  |  | 11950 |  |  |
|  | 2.000 |  |  | 12050 |  |  |
|  | 2.000 |  |  | 12200 |  |  |

Table 13 Characteristic Length in Tension $R_t$ Ply Orientation $[(\pm 45)_6]_s$

| D | W | L | H | P | $P_{avg}$ | $R_t$ |
|---|---|---|---|---|---|---|
| 0.125 | 0.519 | 7.00 | 0.125 | 1300 | 1280 | 0.010 |
|  | 0.503 |  |  | 1270 |  |  |
|  | 0.495 |  |  | 1250 |  |  |
|  | 0.505 |  |  | 1300 |  |  |
| 0.125 | 0.735 | 8.00 | 0.125 | 2120 | 2121 | 0.011 |
|  | 0.737 |  |  | 2125 |  |  |
|  | 0.735 |  |  | 2170 |  |  |
|  | 0.740 |  |  | 2070 |  |  |
| 0.250 | 1.015 | 8.00 | 0.125 | 2600 | 2610 | 0.018 |
|  | 1.007 |  |  | 2680 |  |  |
|  | 1.010 |  |  | 2600 |  |  |
|  | 1.009 |  |  | 2560 |  |  |
| 0.250 | 1.980 | 8.00 | 0.125 | 5400 | 6350 | 0.036 |
|  | 1.990 |  |  | 6200 |  |  |
|  | 1.990 |  |  | 6400 |  |  |
|  | 1.988 |  |  | 6300 |  |  |
| 0.500 | 2.000 | 3.00 | 0.125 | 5600 | 5444 | 0.045 |
|  | 1.943 |  |  | 5400 |  |  |
|  | 1.990 |  |  | 5500 |  |  |
|  | 1.984 |  |  | 5275 |  |  |

Table 14   Characteristic Length in Compression $R_c$

| Ply Orientation | D | W | L | H | P | $P_{avg}$ | $R_c$ |
|---|---|---|---|---|---|---|---|
| $[0/\pm45/90)_3]_s$ | 0.25 | 1.940<br>1.940<br>1.942<br>1.935 | 8.00 | 0.125 | 3500<br>3800<br>3650<br>3800 | 3687 | 0.07 |
| $[(90_2/\pm60/\pm30)_2]_s$ | 0.25 | 1.945<br>1.955<br>1.955<br>1.953 | 8.00 | 0.125 | 2900<br>3100<br>3200<br>3300 | 3125 | 0.08 |
| $[(0/90)_6]_s$ | 0.25 | 1.969<br>1.967<br>1.972<br>1.970 | 8.00 | 0.125 | 3300<br>3100<br>3150<br>3550 | 3275 | 0.09 |
| $[(\pm45)_6]_s$ | 0.25 | 1.970<br>1.945<br>1.930<br>1.940 | 8.00 | 0.125 | 3600<br>3640<br>3640<br>3450 | 3582 | 0.13 |

## APPENDIX G

### Summary of Data for Loaded Holes

This Appendix contains the data which were generated from Fiberite T300/1034-C graphite epoxy laminates containing loaded holes. The Tables in this Appendix also contain the failure strengths and failure modes calculated by the present model for the conditions of the tests.

Notations used in Tables 15-29

| | | |
|------|------------------------------------------|-------|
| D | hole diameter | (in) |
| W | specimen width | (in) |
| L | specimen length | (in) |
| H | specimen thickness | (in) |
| E | edge distance | (in) |
| $G_H$ | distance between two parallel holes | (in) |
| $G_V$ | distance between two series holes | (in) |
| P | failure load under tension | (lbf) |
| $P_{avg}$ | average failure load under tension | (lbf) |
| $P_c$ | calculated failure load | (lbf) |
| M | experimental failure mode | |
| $M_c$ | calculated failure mode | |
| T | tension failure mode | |
| B | bearing failure mode | |
| S | shearout failure mode | |
| $T^s$ | tearout along fiber direction at $\pm45^\circ$ | |

Table 15  Data and Calculated Values for Joints Containing a single Hole.
$[(0/\pm45/90)_3]_s$

| D | W | L | H | E | P | $P_{avg}$ | $P_c$ | $M_e$ | $M_c$ |
|---|---|---|---|---|---|---|---|---|---|
| 0.125 | 0.385 | 5.0 | 0.125 | 0.375 | 1600 | 1725 | 2154 | T | T |
|  | 0.383 |  |  |  | 1600 |  |  | T |  |
|  | 0.390 |  |  |  | 1850 |  |  | T |  |
|  | 0.387 |  |  |  | 1850 |  |  | T |  |
| 0.1875 | 0.708 | 7.0 | 0.125 | 0.375 | 2900 | 2890 | 2781 | T | T |
|  | 0.700 |  |  |  | 2900 |  |  | T |  |
|  | 0.703 |  |  |  | 2960 |  |  | T |  |
|  | 0.715 |  |  |  | 2800 |  |  | T |  |
| 0.1875 | 0.975 | 7.0 | 0.125 | 0.375 | 2620 | 2622 | 2974 | B | B/S |
|  | 0.968 |  |  |  | 2580 |  |  | B |  |
|  | 0.975 |  |  |  | 2570 |  |  | B |  |
|  | 0.985 |  |  |  | 2720 |  |  | B |  |
| 0.25 | 0.738 | 7.0 | 0.125 | 0.75 | 3100 | 3070 | 3130 | T | T |
|  | 0.740 |  |  |  | 2800 |  |  | T |  |
|  | 0.735 |  |  |  | 3000 |  |  | T |  |
|  | 0.740 |  |  |  | 3300 |  |  | T |  |

Table 15  (continued) Data and Calculated Values for Joints Containing a single Hole.
$[(0/\pm45/90)_3]_s$

| D | W | L | H | E | P | P_avg | P_c | M_e | M_c |
|---|---|---|---|---|---|---|---|---|---|
| 0.25 | 1.190 | 7.0 | 0.125 | 0.75 | 3700 | 3615 | 3477 | B | B/S |
|  | 1.205 |  |  |  | 3800 |  |  | B |  |
|  | 1.220 |  |  |  | 3400 |  |  | B |  |
|  | 1.218 |  |  |  | 3550 |  |  | B |  |
| 0.25 | 1.220 | 7.0 | 0.125 | 1.25 | 3500 | 3487 | 3439 | B | B |
|  | 1.210 |  |  |  | 3500 |  |  | B |  |
|  | 1.185 |  |  |  | 3500 |  |  | B |  |
|  | 1.205 |  |  |  | 3450 |  |  | B |  |
| 0.50 | 1.453 | 7.00 | 0.125 | 1.50 | 4980 | 4920 | 4940 | T | T |
|  | 1.493 |  |  |  | 5100 |  |  | T |  |
|  | 1.470 |  |  |  | 4700 |  |  | T |  |
|  | 1.475 |  |  |  | 4900 |  |  | T |  |
| 0.50 | 2.500 | 7.0 | 0.125 | 1.50 | 5500 | 4825 | 5343 | B | B |
|  | 2.455 |  |  |  | 4850 |  |  | B |  |
|  | 2.425 |  |  |  | 4600 |  |  | B |  |
|  | 2.495 |  |  |  | 4300 |  |  | B |  |

Table 16  Data and Calculated Values for Joints Containing a Single Hole.
$[0/(\pm45)_3/90_3]_s$

| D | W | L | H | E | P | $P_{avg}$ | $P_c$ | $M_e$ | $M_c$ |
|---|---|---|---|---|---|---|---|---|---|
| 0.125 | 0.387 | 5.0 | 0.125 | 0.375 | 1240 | 1197 | 975 | T | T |
|  | 0.385 |  |  |  | 1200 |  |  | T |  |
|  | 0.385 |  |  |  | 1150 |  |  | T |  |
|  | 0.372 |  |  |  | 1200 |  |  | T |  |
| 0.1875 | 0.629 | 5.0 | 0.125 | 0.375 | 1700 | 1790 | 1589 | T | T |
|  | 0.630 |  |  |  | 1760 |  |  | T |  |
|  | 0.625 |  |  |  | 1850 |  |  | T |  |
|  | 0.622 |  |  |  | 1850 |  |  | T |  |
| 0.25 | 0.753 | 7.0 | 0.125 | 0.75 | 2200 | 2212 | 1866 | T | T |
|  | 0.753 |  |  |  | 2300 |  |  | T |  |
|  | 0.755 |  |  |  | 2100 |  |  | T |  |
|  | 0.753 |  |  |  | 2250 |  |  | T |  |
| 0.25 | 1.255 | 7.0 | 0.125 | 0.75 | 2600 | 2720 | 2316 | B | B |
|  | 1.255 |  |  |  | 2803 |  |  | B |  |
|  | 1.256 |  |  |  | 2780 |  |  | B |  |
|  | 1.253 |  |  |  | 2700 |  |  | B |  |

Table 17  Data and Calculated Values for Joints Containing a Single Hole.
$[0/(\pm45)_2/90_5]_s$

| D | W | L | H | E | P | $P_{avg}$ | $P_c$ | $M_e$ | $M_c$ |
|---|---|---|---|---|---|---|---|---|---|
| 0.125 | 0.388 | 5.0 | 0.125 | 0.375 | 1150 | 1077 | 1112 | T | T |
|  | 0.385 |  |  |  | 1130 |  |  | T |  |
|  | 0.384 |  |  |  | 960 |  |  | T |  |
|  | 0.385 |  |  |  | 1060 |  |  |  |  |
| 0.1875 | 0.629 | 5.0 | 0.125 | 0.375 | 1500 | 1505 | 1461 | T | T |
|  | 0.630 |  |  |  | 1520 |  |  | T |  |
|  | 0.625 |  |  |  | 1500 |  |  | T |  |
|  | 0.622 |  |  |  | 1510 |  |  | T |  |
| 0.25 | 0.750 | 7.0 | 0.125 | 0.75 | 1820 | 1837 | 1691 | T | T |
|  | 0.750 |  |  |  | 1700 |  |  | T |  |
|  | 0.750 |  |  |  | 1950 |  |  | T |  |
|  | 0.745 |  |  |  | 1880 |  |  | T |  |
| 0.25 | 1.245 | 7.0 | 0.125 | 0.75 | 2300 | 2495 | 2055 | T/B | B |
|  | 1.255 |  |  |  | 2850 |  |  | T/B |  |
|  | 1.255 |  |  |  | 2480 |  |  | B |  |
|  | 1.255 |  |  |  | 2350 |  |  | T/B |  |

Table 18  Data and Calculated Values for Joints Containing a Single Hole.
$[0/\pm45/90_7]_s$

| D | W | L | H | E | F | $P_{avg}$ | $P_C$ | $M_e$ | $M_C$ |
|---|---|---|---|---|---|---|---|---|---|
| 0.125 | 0.385 | 5.0 | 0.125 | 0.375 | 875 | 826 | 947 | T | T |
| | 0.383 | | | | 830 | | | T | |
| | 0.380 | | | | 800 | | | T | |
| | 0.384 | | | | 800 | | | T | |
| 0.1875 | 0.626 | 5.0 | 0.125 | 0.375 | 1200 | 1196 | 1232 | T | T |
| | 0.623 | | | | 1220 | | | T | |
| | 0.629 | | | | 1170 | | | T | |
| 0.25 | 0.760 | 7.0 | 0.125 | 0.75 | 1600 | 1485 | 1431 | T | T |
| | 0.753 | | | | 1560 | | | T | |
| | 0.755 | | | | 1430 | | | T | |
| | 0.760 | | | | 1350 | | | T | |
| 0.25 | 1.250 | 7.0 | 0.125 | 0.75 | 2280 | 2120 | 1540 | B/T | B |
| | 1.255 | | | | 2130 | | | B/T | |
| | 1.257 | | | | 2100 | | | B | |
| | 1.255 | | | | 2100 | | | B | |

Table 19  Data and Calculated Values for Joints Containing a Single Hole.
$[(90_2/\pm 60/\pm 30)_2]_s$

| D | W | L | H | e | P | $P_{avg}$ | $P_c$ | $M_e$ | $M_c$ |
|---|---|---|---|---|---|---|---|---|---|
| 0.125 | 0.385 | 5.0 | 0.125 | 0.375 | 1200 | 1130 | 1493 | T | T |
|  | 0.392 |  |  |  | 1100 |  |  | T |  |
|  | 0.390 |  |  |  | 1100 |  |  | T |  |
|  | 0.380 |  |  |  | 1120 |  |  |  |  |
| 0.1875 | 0.625 | 5.0 | 0.125 | 0.375 | 2050 | 2012 | 1945 | T | T |
|  | 0.615 |  |  |  | 1900 |  |  | T |  |
|  | 0.620 |  |  |  | 2000 |  |  | T |  |
|  | 0.625 |  |  |  | 2100 |  |  | T |  |
| 0.1875 | 0.745 | 7.0 | 0.125 | 0.375 | 2200 | 2150 | 2108 | T | B |
|  | 0.736 |  |  |  | 2200 |  |  | T |  |
|  | 0.745 |  |  |  | 2170 |  |  | T |  |
|  | 0.753 |  |  |  | 2000 |  |  | T |  |
| 0.1875 | 0.965 | 7.0 | 0.125 | 0.375 | 2280 | 2317 | 2264 | T | T |
|  | 0.980 |  |  |  | 2450 |  |  | B/T |  |
|  | 0.968 |  |  |  | 2230 |  |  | T |  |
|  | 0.945 |  |  |  | 2310 |  |  | B/T |  |
| 0.25 | 0.745 | 7.0 | 0.125 | 0.75 | 2100 | 2187 | 2258 | T | T |
|  | 0.740 |  |  |  | 2200 |  |  | T |  |
|  | 0.735 |  |  |  | 2150 |  |  | T |  |
|  | 0.740 |  |  |  | 2300 |  |  | T |  |

Table 19 (continued) Data and Calculated Values for Joints Containing a Single Hole.
$[(90_2/\pm60/\pm30)_2]_s$

| D | W | L | H | e | P | $P_{avg}$ | $P_c$ | $M_e$ | $M_c$ |
|---|---|---|---|---|---|---|---|---|---|
| 0.25 | 1.215 | 7.0 | 0.125 | 0.75 | 3000 | 3100 | 2676 | B | B/S |
|  | 1.223 |  |  |  | 3100 |  |  | B |  |
|  | 1.200 |  |  |  | 3200 |  |  | B |  |
|  | 1.205 |  |  |  | 3100 |  |  | B |  |
| 0.25 | 1.228 | 7.0 | 0.125 | 1.25 | 2900 | 2892 | 2678 | B | B/S |
|  | 1.218 |  |  |  | 2900 |  |  | B |  |
|  | 1.213 |  |  |  | 2870 |  |  | B |  |
|  | 1.220 |  |  |  | 2910 |  |  | B |  |
| 0.50 | 1.458 | 7.0 | 0.125 | 1.50 | 3500 | 3575 | 3736 | T | B |
|  | 1.483 |  |  |  | 3800 |  |  | T |  |
|  | 1.445 |  |  |  | 3500 |  |  | T |  |
|  | 1.448 |  |  |  | 3500 |  |  | T |  |
| 0.50 | 2.450 | 7.0 | 0.125 | 1.50 | 5500 | 4981 | 3672 | B | B |
|  | 2.450 |  |  |  | 5150 |  |  | B |  |
|  | 2.440 |  |  |  | 4125 |  |  | B |  |
|  | 2.650 |  |  |  | 5150 |  |  | B |  |

Table 20   Data and Calculated Values for Joints Containing a Single Hole.
$[(0/90)_6]_s$

| D | W | L | H | E | P | $P_{avg}$ | $P_c$ | $M_e$ | $M_c$ |
|---|---|---|---|---|---|---|---|---|---|
| 0.125 | 0.385 | 5.0 | 0.125 | 0.375 | 1420 | 1392 | 1461 | S/T | B |
|  | 0.387 |  |  |  | 1370 |  |  | S/T |  |
|  | 0.387 |  |  |  | 1380 |  |  | S/T |  |
|  | 0.386 |  |  |  | 1400 |  |  | S/T |  |
| 0.1875 | 0.637 | 5.0 | 0.125 | 0.375 | 1400 | 1385 | 1433 | S/T | S/T |
|  | 0.638 |  |  |  | 1400 |  |  | S/T |  |
|  | 0.640 |  |  |  | 1340 |  |  | S/T |  |
|  | 0.640 |  |  |  | 1400 |  |  | S/T |  |
| 0.1875 | 0.751 | 7.0 | 0.125 | 0.375 | 2200 | 2150 | 1474 | S | S |
|  | 0.752 |  |  |  | 2200 |  |  | S/T |  |
|  | 0.747 |  |  |  | 2120 |  |  | S |  |
|  | 0.751 |  |  |  | 2080 |  |  | S/T |  |
| 0.1875 | 1.011 | 7.0 | 0.125 | 0.375 | 1350 | 1452 | 1456 | B/S | B/S |
|  | 1.014 |  |  |  | 1440 |  |  | B/S |  |
|  | 1.015 |  |  |  | 1520 |  |  | B/S |  |
|  | 1.016 |  |  |  | 1500 |  |  | B/S |  |
| 0.25 | 0.763 | 7.0 | 0.125 | 0.75 | 2608 | 2657 | 1756 | S | S |
|  | 0.760 |  |  |  | 2650 |  |  | S/T |  |
|  | 0.765 |  |  |  | 2700 |  |  | S/T |  |
|  | 0.765 |  |  |  | 2600 |  |  | S/T |  |

Table 20 (continued) Data and Calculated Values for Joints Containing a Single Hole. $[(0/90)_6]_s$

| D | W | L | H | e | P | $P_{avg}$ | $P_c$ | $M_e$ | $M_c$ |
|---|---|---|---|---|---|---|---|---|---|
| 0.25 | 1.270 | 7.0 | 0.125 | 0.75 | 2700 | 2637 | 1719 | B/S | S |
|  | 1.255 |  |  |  | 2600 |  |  | B/S |  |
|  | 1.265 |  |  |  | 2600 |  |  | S |  |
|  | 1.272 |  |  |  | 2650 |  |  | B/S |  |
| 0.25 | 1.255 | 7.0 | 0.125 | 1.25 | 3150 | 3270 | 1799 | B | S |
|  | 1.255 |  |  |  | 3300 |  |  | B |  |
|  | 1.258 |  |  |  | 3230 |  |  | B |  |
|  | 1.258 |  |  |  | 3400 |  |  | B |  |
| 0.50 | 1.498 | 7.0 | 0.125 | 1.50 | 5000 | 4875 | 2659 | S | S |
|  | 1.500 |  |  |  | 4800 |  |  | S/T |  |
|  | 1.502 |  |  |  | 4800 |  |  | S |  |
|  | 1.502 |  |  |  | 4900 |  |  | S/T |  |
| 0.50 | 2.501 | 7.0 | 0.125 | 1.50 | 4450 | 4700 | 2943 | B/S | S |
|  | 2.497 |  |  |  | 4950 |  |  | B/S |  |
|  | 2.490 |  |  |  | 4800 |  |  | B/S |  |
|  | 2.501 |  |  |  | 4600 |  |  | S |  |

Table 2) Data and Calculated Values for Joints Containing a Single Hole.
$[(\pm45)_6]_s$

| D | x | L | H | E | P | $P_{avg}$ | $P_c$ | $M_e$ | $M_c$ |
|---|---|---|---|---|---|---|---|---|---|
| 0.125 | 0.388 | 5.0 | 0.125 | 0.375 | 930 | 1009 | | * | T |
| | 0.387 | | | | 987 | | | T* | |
| | 0.387 | | | | 1030 | | | T* | |
| | 0.390 | | | | 1009 | | | T* | |
| 0.1875 | 0.630 | 5.0 | 0.125 | 0.375 | 1600 | 1620 | 1644 | T* | T |
| | 0.629 | | | | 1600 | | | T* | |
| | 0.638 | | | | 1620 | | | T* | |
| | 0.633 | | | | 1600 | | | T* | |
| 0.1875 | 0.735 | 7.0 | 0.125 | 0.375 | 1950 | 1950 | 1304 | T* | T |
| | 0.730 | | | | 1940 | | | T* | |
| | 0.743 | | | | 1910 | | | T* | |
| | 0.747 | | | | 2000 | | | T* | |
| 0.1875 | 0.954 | 7.0 | 0.125 | 0.375 | 1750 | 1822 | 1421 | T* | T |
| | 0.967 | | | | 1800 | | | B/T* | |
| | 0.955 | | | | 1800 | | | B/T* | |
| | 0.951 | | | | 1940 | | | T* | |
| 0.25 | 0.740 | 7.0 | 0.125 | 0.75 | 1740 | 1697 | 1468 | * | T |
| | 0.740 | | | | 1700 | | | T* | |
| | 0.745 | | | | 1650 | | | T* | |
| | 0.741 | | | | 1700 | | | T* | |

Table 21 (continued) Data and Calculated Values for Joints Containing a Single Hole.
$[(\pm45)_6]_s$

| D | W | L | H | E | P | $P_{avg}$ | $P_c$ | $M_e$ | $M_c$ |
|---|---|---|---|---|---|---|---|---|---|
| 0.25 | 1.193 | 7.0 | 0.125 | 0.75 | 3150 | 3087 | 2037 | B/T* | |
| | 1.195 | | | | 3000 | | | B/T* | T |
| | 1.200 | | | | 3000 | | | B/T* | |
| | 1.162 | | | | 3200 | | | T* | |
| 0.25 | 1.233 | 7.0 | 0.125 | 1.25 | 3400 | 3250 | 2156 | B/T* | |
| | 1.205 | | | | 3300 | | | B/T* | T |
| | 1.193 | | | | 3200 | | | B/T* | |
| | 1.200 | | | | 3100 | | | B/T | |
| 0.50 | 1.440 | 7.0 | 0.125 | 1.50 | 3150 | 3238 | 2667 | T* | |
| | 1.445 | | | | 3200 | | | T* | T |
| | 1.450 | | | | 3300 | | | T* | |
| | 1.450 | | | | 3300 | | | T* | |
| 0.50 | 2.450 | 7.0 | 0.125 | 1.50 | 4500 | 4943 | 2964 | B | |
| | 2.500 | | | | 5250 | | | B | B |
| | 2.483 | | | | 4800 | | | B | |
| | 2.455 | | | | 5275 | | | B | |

Table 22 Data and calculated values for Joints containing Two Holes in Parallel.
$[(0/\pm45/90)_3]_s$

| D | W | L | H | E | $G_H$ | P | $P_{avg}$ | $F_c$ | $M_e$ | $M_c$ |
|---|---|---|---|---|---|---|---|---|---|---|
| 0.250 | 1.440 | 7.0 | 0.125 | 0.75 | 0.75 | 6350 | | | T | |
| | 1.465 | | | | | 6100 | 6196 | 6304 | T | T |
| | 1.483 | | | | | 6140 | | | T | |
| 0.250 | 1.943 | 7.0 | 0.125 | 0.75 | 1.25 | 5940 | | | T/B | |
| | 1.943 | | | | | 5720 | 5586 | 6314 | T/B | B |
| | 1.960 | | | | | 5100 | | | T/B | |
| 0.25 | 1.927 | 7.0 | 0.125 | 0.75 | 0.75 | 5350 | | | B | |
| | 1.925 | | | | | 6800 | 5937 | 6443 | B/T | B |
| | 1.935 | | | | | 6500 | | | B | |
| | 1.937 | | | | | 5800 | | | B | |

Table 23    Data and Calculated Values for Joints Containing Two Holes in Parallel.
$$[(90_2/\pm60/\pm30)_2]_s$$

| D | W | L | H | E | $G_H$ | P | $P_{avg}$ | $P_c$ | $M_e$ | $M_c$ |
|---|---|---|---|---|-------|---|-----------|-------|-------|-------|
| 0.250 | 1.655 | 7.0 | 0.125 | 0.75 | 0.75 | 3840 | 4375 | 4583 |  | T |
|  | 1.475 |  |  |  |  | 4800 |  |  | T |  |
|  | 1.458 |  |  |  |  | 4340 |  |  | T |  |
|  | 1.440 |  |  |  |  | 4520 |  |  | T |  |
| 0.250 | 1.943 | 7.0 | 0.125 | 0.75 | 1.25 | 4400 | 4637 | 4726 | T | B |
|  | 1.943 |  |  |  |  | 4800 |  |  | T |  |
|  | 1.922 |  |  |  |  | 4650 |  |  | T |  |
|  | 1.944 |  |  |  |  | 4700 |  |  | T |  |
| 0.250 | 1.940 | 7.0 | 0.125 | 0.75 | 0.75 | 5600 | 5655 | 4920 | T | B |
|  | 1.923 |  |  |  |  | 5500 |  |  | T |  |
|  | 1.935 |  |  |  |  | 5700 |  |  | T/B |  |
|  | 1.933 |  |  |  |  | 5820 |  |  | T |  |

Table 24  Data and Calculated Values for Joints Containing Two Holes In Parallel.
$[(0/90)_6]_s$

| D | W | L | H | ε | $G_H$ | P | $P_{avg}$ | $P_c$ | $M_e$ | $M_c$ |
|---|---|---|---|---|---|---|---|---|---|---|
| 0.25 | 1.505 | 7.0 | 0.125 | 0.75 | 0.75 | 5340 | 5230 | 3525 | S/T | s |
|  | 1.503 |  |  |  |  | 5320 |  |  | S/T |  |
|  | 1.494 |  |  |  |  | 5300 |  |  | S |  |
|  | 1.494 |  |  |  |  | 4960 |  |  | S |  |
| 0.25 | 1.937 | 7.0 | 0.125 | 0.75 | 1.25 | 4900 | 5175 | 3569 | S/T | s |
|  | 1.938 |  |  |  |  | 5300 |  |  | S/T |  |
|  | 1.938 |  |  |  |  | 5350 |  |  | S/T |  |
|  | 1.938 |  |  |  |  | 5150 |  |  | S/T |  |
| 0.25 | 1.936 | 7.0 | 0.125 | 0.75 | 0.75 | 5100 | 4950 | 3596 | S/T | s |
|  | 1.939 |  |  |  |  | 4500 |  |  | S/T |  |
|  | 1.938 |  |  |  |  | 5100 |  |  | S/T |  |
|  | 1.938 |  |  |  |  | 5100 |  |  | S/T |  |

Table 25  Data and Calculated Values for Joints Containing Two Holes in Parallel. $[(\pm45)_6]_s$

| D | W | L | H | E | $G_H$ | P | $P_{avg}$ | $P_c$ | $M_e$ | $M_c$ |
|---|---|---|---|---|---|---|---|---|---|---|
| 0.250 | 1.445 | 7.0 | 0.125 | 0.75 | 0.75 | 4200 | | | T* | |
| | 1.475 | | | | | 4300 | 4233 | 2958 | T* | T |
| | 1.450 | | | | | 4200 | | | T* | |
| | | | | | | | | | T | |
| 0.250 | 1.945 | 7.0 | 0.125 | 0.75 | 1.25 | 4900 | | | T* | |
| | 1.937 | | | | | 4650 | 4735 | 3325 | T* | T |
| | 1.945 | | | | | 4670 | | | T* | |
| | 1.945 | | | | | 4720 | | | T | |
| 0.250 | 1.913 | 7.0 | 0.125 | 0.75 | 0.75 | 5600 | | | T* | |
| | 1.935 | | | | | 5780 | 5692 | 3377 | B | T |
| | 1.937 | | | | | 5830 | | | B* | |
| | 1.934 | | | | | 5560 | | | T | |

Table 26  Data and Calculated Values for Joints Containing Two Holes in Series.
$[(0/\pm45/90)_3]_s$

| D | W | L | H | E | $G_V$ | P | $P_{avg}$ | $P_c$ | $M_e$ | $M_c$ |
|---|---|---|---|---|---|---|---|---|---|---|
| 0.125 | 0.518 | 7.0 | 0.125 | 0.375 | 0.375 | 2850 | 2730 | 2802 | T | T |
|  | 0.500 |  |  |  |  | 2700 |  |  | T |  |
|  | 0.515 |  |  |  |  | 2720 |  |  | T |  |
|  | 0.518 |  |  |  |  | 2650 |  |  |  |  |
| 0.1875 | 0.623 | 7.0 | 0.125 | 0.375 | 0.625 | 2930 | 2860 | 3057 | T | T |
|  | 0.632 |  |  |  |  | 2800 |  |  | T |  |
| 0.250 | 0.727 | 7.0 | 0.125 | 0.75 | 0.75 | 3050 | 3052 | 3254 | T | T |
|  | 0.730 |  |  |  |  | 3200 |  |  | T |  |
|  | 0.705 |  |  |  |  | 3106 |  |  | T |  |
|  | 0.680 |  |  |  |  | 2860 |  |  | T |  |
| 0.250 | 0.718 | 7.0 | 0.125 | 0.75 | 1.25 | 3200 | 3125 | 3231 | T | T |
|  | 0.705 |  |  |  |  | 3000 |  |  | T |  |
|  | 0.711 |  |  |  |  | 3500 |  |  | T |  |
|  | 0.720 |  |  |  |  | 3300 |  |  | T |  |
| 0.250 | 1.195 | 7.0 | 0.125 | 0.75 | 0.75 | 5300 | 5405 | 4732 | T | T |
|  | 1.210 |  |  |  |  | 4900 |  |  | T/B |  |
|  | 1.204 |  |  |  |  | 5720 |  |  | T |  |
|  | 1.213 |  |  |  |  | 5700 |  |  | T |  |
| 0.250 | 1.208 | 7.0 | 0.125 | 0.75 | 1.25 | 5750 | 5812 | 4642 | T | S |
|  | 1.204 |  |  |  |  | 5690 |  |  | T |  |
|  | 1.208 |  |  |  |  | 5900 |  |  | T |  |
|  | 1.225 |  |  |  |  | 5920 |  |  | T |  |

Table 27 Data and Calculated Values for Joints Containing Two Holes in series.
$[(90_2/\pm30/\pm60)_2]_s$

| D | W | L | H | E | $G_v$ | P | $P_{avg}$ | $P_c$ | $M_e$ | $M_c$ |
|---|---|---|---|---|---|---|---|---|---|---|
| 0.125 | 0.505 | 7.0 | 0.125 | 0.375 | 0.375 | 2050 | 2005 | 1881 | T | T |
| | 0.495 | | | | | 1890 | | | T | |
| | 0.520 | | | | | 1900 | | | T | |
| | 0.507 | | | | | 1970 | | | T | |
| 0.1875 | 0.627 | 7.0 | 0.125 | 0.375 | 0.625 | 2400 | 2355 | 2149 | T | T |
| | 0.630 | | | | | 2310 | | | T | |
| | 0.636 | | | | | 2300 | | | T | |
| | 0.625 | | | | | 2410 | | | T | |
| 0.250 | 0.625 | 7.0 | 0.125 | 0.75 | 0.75 | 2050 | 2135 | 2235 | T | T |
| | 0.680 | | | | | 2225 | | | T | |
| | 0.710 | | | | | 2130 | | | T | |
| 0.250 | 0.726 | 7.0 | 0.125 | 0.75 | 1.25 | 2330 | 2412 | 2335 | T | T |
| | 0.732 | | | | | 2350 | | | T | |
| | 0.720 | | | | | 2450 | | | T | |
| | 0.731 | | | | | 2520 | | | T | |
| 0.250 | 1.202 | 7.0 | 0.125 | 0.75 | 0.75 | 4100 | 3866 | 3387 | T | T |
| | 1.198 | | | | | 4000 | | | T | |
| | 1.223 | | | | | 3700 | | | T | |
| 0.250 | 1.222 | 7.0 | 0.125 | 0.75 | 1.25 | 3950 | 3887 | 3745 | T | T |
| | 1.223 | | | | | 4200 | | | T | |
| | 1.102 | | | | | 3600 | | | T | |
| | 1.097 | | | | | 3800 | | | T | |

Table 26  Data and Calculated Values for Joints Containing Two Holes in Series.
$[(0/90)_6]_s$

| D | W | L | H | E | $G_v$ | P | $P_{avg}$ | $P_c$ | $M_e$ | $M_c$ |
|---|---|---|---|---|---|---|---|---|---|---|
| 0.1875 | 0.641 | 7.0 | 0.125 | 0.375 | 0.375 | 2720 | | | S | |
| | 0.638 | | | | | 2520 | 2560 | 2136 | S | S |
| | 0.642 | | | | | 2500 | | | S/T | |
| | 0.629 | | | | | 2500 | | | S | |
| 0.1875 | 0.635 | 7.0 | 0.125 | 0.375 | 0.625 | 3225 | | | S | |
| | 0.642 | | | | | 3210 | 3191 | 2041 | S | S |
| | 0.639 | | | | | 3120 | | | S/T | |
| | 0.641 | | | | | 3210 | | | S | |
| 0.250 | 0.749 | 7.0 | 0.125 | 0.75 | 0.75 | 3800 | | | T | |
| | 0.751 | | | | | 4050 | 3725 | 2260 | T/S | S |
| | 0.749 | | | | | 3100 | | | T | |
| | 0.753 | | | | | 3950 | | | T | |
| 0.250 | 0.751 | 7.0 | 0.125 | 0.75 | 1.25 | 4150 | | | T | |
| | 0.752 | | | | | 4150 | 4145 | 2178 | T | S |
| | 0.746 | | | | | 3830 | | | T | |
| | 0.751 | | | | | 4450 | | | T | |
| 0.250 | 1.257 | 7.0 | 0.125 | 0.75 | 0.75 | 4800 | | | S/T | |
| | 1.257 | | | | | 4900 | 4862 | 2452 | S | S |
| | 1.256 | | | | | 4700 | | | S | |
| | 1.241 | | | | | 5050 | | | S/T | |
| 0.250 | 1.256 | 7.0 | 0.125 | 0.75 | 1.25 | 5750 | | | B/S | |
| | 1.258 | | | | | 5600 | 5616 | 2424 | B/S | S |
| | 1.256 | | | | | 5500 | | | B/S | |

Table 29 Data and Calculated Values for Joints Containing Two Holes in Series.
$[(\pm45)_6]$

| D | W | L | H | e | $G_v$ | P | $P_{avg}$ | $P_c$ | $M_e$ | $M_c$ |
|---|---|---|---|---|---|---|---|---|---|---|
| 0.125 | 0.515 | 7.0 | 0.125 | 0.375 | 0.375 | 1400 | 1380 | 1118 | T* | T |
|  | 0.516 |  |  |  |  | 1370 |  |  | T* |  |
|  | 0.518 |  |  |  |  | 1370 |  |  | T |  |
| 0.1875 | 0.611 | 7.0 | 0.125 | 0.375 | 0.625 | 1500 | 1522 | 1114 | T* | T |
|  | 0.620 |  |  |  |  | 1480 |  |  | T* |  |
|  | 0.613 |  |  |  |  | 1550 |  |  | T* |  |
|  | 0.623 |  |  |  |  | 1560 |  |  | T |  |
| 0.250 | 0.673 | 7.0 | 0.125 | 0.75 | 0.75 | 1400 | 1480 | 1181 | * | T |
|  | 0.680 |  |  |  |  | 1500 |  |  | T* |  |
|  | 0.708 |  |  |  |  | 1560 |  |  | T* |  |
|  | 0.675 |  |  |  |  | 1460 |  |  | T |  |
| 0.250 | 0.720 | 7.0 | 0.125 | 0.75 | 1.25 | 1500 | 1500 | 1221 | * | T |
|  | 0.715 |  |  |  |  | 1550 |  |  | T* |  |
|  | 0.690 |  |  |  |  | 1400 |  |  | T* |  |
|  | 0.704 |  |  |  |  | 1550 |  |  | T |  |
| 0.250 | 1.188 | 7.0 | 0.125 | 0.75 | 0.75 | 3300 | 3362 | 1878 | * | T |
|  | 1.209 |  |  |  |  | 3300 |  |  | T* |  |
|  | 1.208 |  |  |  |  | 3400 |  |  | T* |  |
|  | 1.183 |  |  |  |  | 3450 |  |  | T |  |
| 0.250 | 1.204 | 7.0 | 0.125 | 0.75 | 1.25 | 3350 | 3612 | 1917 | T* | T |
|  | 1.206 |  |  |  |  | 3450 |  |  | T* |  |
|  | 1.200 |  |  |  |  | 3350 |  |  | T* |  |
|  | 1.201 |  |  |  |  | 3500 |  |  | T |  |